Bacteria-Targeting Nanoparticles for Managing Infections

by

Aleksandar Filip Radovic-Moreno

B. S. Chemical Engineering
The Pennsylvania State University, 2005

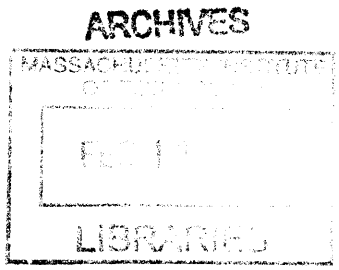

SUBMITTED TO THE HEALTH SCIENCES AND TECHNOLOGY PROGRAM IN PARTIAL FULFILLMENT OF THE REQUIREMENTS FOR THE DEGREE OF

DOCTOR OF PHILOSOPHY IN CHEMICAL AND BIOMEDICAL ENGINEERING
AT THE
MASSACHUSETTS INSTITUTE OF TECHNOLOGY

February 2013

Signature of Author .....
Health Sciences and Technology
November 9, 2012

Certified by .....
Robert Langer, Sc. D.
Institute Professor, MIT
Thesis Co-Supervisor

.....
Omid C. Farokhzad, M. D.
Associate Professor of Anesthesia, Harvard Medical School
Thesis Co-Supervisor

Accepted by .....
Arup Chakraborty, Ph. D.
Director, Institute for Medical Engineering and Sciences; Robert T. Haslam Professor of Chemical Engineering, Chemistry and Biological Engineering, MIT

Bacteria-Targeting Nanoparticles for Managing Infections

by

Aleksandar Filip Radovic-Moreno

Submitted to the Health Sciences and Technology Program on November 9, 2012 in Partial Fulfillment of the Requirements for the Degree of Doctor of Philosophy in Chemical and Biomedical Engineering

ABSTRACT

Bacterial infections continue to be a significant concern particularly in healthcare settings and in the developing world. Current challenges include the increasing spread of drug resistant (DR) organisms, the side effects of antibiotic therapy, the negative consequences of clearing the commensal bacterial flora, and difficulties in developing prophylactic vaccines. This thesis was an investigation of the potential of a class of polymeric nanoparticles (NP) to contribute to the management of bacterial infections. More specifically, steps were taken towards using these NPs (1) to achieve greater spatiotemporal control over drug therapy by more targeted antibiotic delivery to bacteria, and (2) to develop a prophylactic vaccine formulation against the common bacterial sexually transmitted disease (STD) caused by *Chlamydia trachomatis*.

In the first part, we synthesized polymeric NPs containing poly(lactic-co-glycolic acid)-*block*-poly(L-histidine)-*block*-poly(ethylene glycol) (PLGA-PLH-PEG). We show that these NPs are able to bind to bacteria under model acidic infection conditions and are able to encapsulate and deliver vancomycin to inhibit the growth of *Staphylococcus aureus* bacteria *in vitro*. Further work showed that the PLGA-PLH-PEG-based NPs demonstrated the potential for competition for binding bacteria at a site of infection from soluble protein and model phagocytic and tissue-resident cells in a NP composition dependent manner. The NPs demonstrated low toxicity *in vitro*, were well tolerated by mice *in vivo*, and circulated in the blood on timescales comparable to control PLGA-PEG NPs.

In the second part, we used PLGA-PLH-PEG-based NPs to design a prophylactic vaccine against the obligate intracellular bacterium *Chlamydia trachomatis*, the most common cause of bacterial STD in the world. Currently, no vaccines against this pathogen are approved for use in humans. We first formulated NPs encapsulating the TLR7 agonist R848 conjugated to poly(lactic acid) (R848-PLA) in PLGA-PLH-PEG-based NPs, then incubated these R848-NPs with UV-inactivated *C. trachomatis* bacteria in acidity, forming a construct. Mice immunized with this vaccine via genital or intranasal routes demonstrated protection from genital infection post immunization in a primarily $CD4^+$ T cell-dependent manner.

These results may suggest avenues for future work in designing and developing more targeted drug therapies or vaccine formulations for managing bacterial infections using polymeric nanoparticles.

Thesis Co-Supervisor: Robert Langer
Title: Institute Professor, MIT

Thesis Co-Supervisor: Omid C. Farokhzad
Title: Associate Professor of Anesthesia, Harvard Medical School

Para mi mami, mi hermana, y za moj tata.

Acknowledgments

First and foremost, I would like to thank my parents and sister for their unending love, support, inspirational words, kindness, courage, and patience. Without them, nothing would have been possible.

I would like to express my deepest gratitude to my advisors, Professor Robert Langer and Professor Omid Farokhzad, among other things, for being inspirational figures and for creating and maintaining a thoroughly stimulating research environment. I would also like to thank my thesis committee members, Professor Paula Hammond and Professor Alexander Klibanov.

I have had the privilege to work with many extremely talented and bright colleagues and collaborators during my PhD. Most directly, I would like to acknowledge the expert guidance of Professor Timothy Lu, who contributed insights and ideas that were invaluable in the development of concepts contained in this thesis, particularly as they related to antibacterial therapies. For the work towards a prophylactic *Chlamydia* vaccine, I am deeply indebted to Professor Uli von Andrian, Dr. Georg Stary, and Ms. Pamela Basto among others for collaborating to conceive the idea and executing the experiments. I would also like to acknowledge the many contributions of my highly diligent and talented UROPs, with a special mention of Mr. Vlad Puscasu. Over the years I have greatly enjoyed extended discussions, collaborations, and friendships with (now Dr.) Ben Teply, Dr. Frank Gu, Dr. Frank Alexis, Dr. Andrew Wang, Dr. Etgar Levy-Nissenbaum, Eric Pridgen, Pedro Valencia, Dr. Liangfang Zhang, as well as members of the Langer and Farokhzad labs since 2006.

I would also like to thank everyone close to me for their support and for making the last several years so much more enjoyable. I cannot go further without a special thanks to Sukant Mittal, Jay Komarneni, Div Bolar, Nick Blasioli, Kevin Fowler, Alexandra de Paz, Pamela Basto, Rumi Chunara, Jessie Bright, Arun Bhagat, Jeff Yang, Brian Werner, Said Bogatyrev, Ben Caplan, Kathleen Lambert, Mara Macdonald, Yoni Goldwasser, Jack Milwid, David Nguyen, Manny Simons, and Jason Fuller, among many others.

Table of Contents

List of Figures

List of Tables

Chapter 1

Introductory Remarks and Overview

1. 1. Introductory Remarks

Bacterial infections have been a scourge to mankind since the dawn of our species c.200,000 years ago. Exploring methods to improve treatment and prevention has been a continuing endeavor, albeit one characterized by a lack of clear vision or targeted methodology until perhaps the late 19th century, when Robert Koch published a set of postulates which could be used to precisely determine if a microorganism was causing a disease. This seminal contribution was a capstone to centuries of observations including Anton van Leeuwenhoek's first visualization of a bacterium in the 17th century to Louis Pasteur's seminal studies in the 19th century disproving the theory of spontaneous generation. These and many other examples together unambiguously made clear that bacteria can cause illness.[1] Alongside these key advances in microbiology were the seminal contributions by Paul Ehrlich, who in the early 20th century famously conceived of a "magic bullet" that could seek out and attack agents of disease with minimal collateral effects.[2] The stage had now been set for the fortuitous discovery of penicillin by Alexander Fleming in 1928, which was later developed into a drug by scaled production techniques in the 1940s. The use of penicillin in humans was truly landmark because of its remarkably fast and potent activity combined with few side effects, even when ingested in gram quantities per day.[3] This triggered a revolution known as the "golden era" of antibiotic discovery, a period of tremendous productivity from c.1940-1980, in which many of the major classes of antibiotics still in use today were

discovered.[4] Particularly in these years, a host of drugs were developed, bringing unprecedented success against a wide variety of bacterial infections, leading to important insights into bacterial physiology, and most importantly, saving the lives of many.

However, the story does not end there. Bacteria are among the oldest living organisms on planet Earth and in the approximately 2 billion years of their existence, have evolved tools and strategies that make them highly adaptable to extreme environments or chemical attacks. Bacteria can be found at extremes of temperature and pressure, have survived cataclysmic events, withstood variations in atmospheric composition and surface temperature over the evolution of planet Earth, encountered chemical attacks from sources like the environment, competing microorganisms, and faced sophisticated assaults by the immune systems of multicellular organisms. In addition, bacteria have extremely short generation times – on the order of only a few minutes in some cases – which allows them to rapidly iterate their genetic material across generations, and can readily transfer genes to each other using mobile genetic elements.[5] These tools acquired over billions of years of harsh survival positioned them quite favorably to counter antibiotics. In fact, antibiotics provided a relatively straightforward target because of their high specificity. Bacteria were able to respond almost immediately, with the phenomenon of drug resistance (DR) being broadly recognized as a major challenge already in the 1940s. Perhaps even more remarkably, it appears that bacteria had already developed (cross) resistance to antibiotics – *before* we even developed them, as suggested by the discovery of multi drug resistant bacteria in a deep cavern that had been isolated from all human intervention.[6] DR is just one of several strategies used by bacteria. Bacteria are able to evade therapy by building, inducing, or finding microenvironmental niches, such

as biofilms, abscesses, or by intracellular localization.[7, 8] These niches provide a protective barrier from many elements of humoral immunity and chemical intervention. Bacteria are also capable of entering into states of hibernation, in which very low metabolic activity reduces their susceptibility to antibiotics to almost zero, and can form extremely resilient endospores (for further discussion see Chapter 2).[9]

We cannot avoid bacteria – they are nearly omnipresent. Bacteria can be found in the air we breathe, on nearly all types of surfaces, in the food we eat, and perhaps most notably – in all of us. Bacteria outnumber us in our own bodies approximately 10:1 (bacteria:human cells), living in commensal status on our skin, in our intestinal tracts, and on our mucosal surfaces.[10] For the most part this is an indifferent or mutualist interaction. However, even commensal organisms can cause deadly infections under inauspicious conditions, such as trauma, interruptions in the normal flora (such as by antibiotic therapy), or in cases of weakened immune systems due to age or comorbidities. Today we live in an increasingly interconnected world, where humans may come into contact with a wider diversity of bacteria more than ever before. This puts us not only at greater risk of infection, but allows for bacteria from different parts of the world to come together to "share" genetic information, perhaps leading to bacterial "superbugs" that are resistant to all known antibiotics.[2] A historical perspective suggests that our species will likely be in a constant battle with bacteria. In fact, some believe that resistance is inevitable.[2, 11] To remain one step ahead, it will be necessary to continuously develop novel tools and approaches based on an increasingly deeper understanding not only of bacterial (patho)physiology, but also how bacteria interact with humans in ways that reduce the effectiveness of therapeutic strategies. These insights will allow us to create more tailored

approaches that can not only adapt to bacterial adaptations, but also to anticipate and perhaps neutralize future moves. Our existing primary tools to treat infections, antibiotics, can be highly effective, but years of (mis)use are putting them at serious threat for obsolescence due to DR in many cases. Multi-drug resistance is on the rise, and agents of last resort are usually less effective, more toxic, and their increasing use is likely to lead to more widespread resistance (see Chapter 2 for thorough discussion). In addition, drug therapy of bacterial infections is affected by a variety of other factors, including microenvironmental conditions, biofilms, and drug pharmacokinetic challenges, all of which can significantly impact the outcome of therapy. These factors suggest that novel tools and approaches are needed to improve antibacterial drug therapy.[12]

A complementary strategy to seeking new therapeutics is the search for novel methods of prevention. One part of a prevention strategy is proper sanitation, a concept pioneered by Ignaz Semmelweis and Joseph Lister in the 19^{th}-20^{th} centuries among many others, but major effects can also be obtained by safe and effective prophylactic vaccination. Vaccines have been credited with the eradication of smallpox (a viral illness) and have also made significant impacts on a host of bacterial illnesses including those caused by *Bacillus anthracis*, *Streptococcus pneumoniae*, *Haemophilus influenzae* type B, *Clostridium tetani*, and *Mycobacterium tuberculosis*, among others. These successes, while modest in some cases (such as for TB), nevertheless have protected many from infection, saved lives, and reduced healthcare expenditures for decades. Despite these successes, many bacterial infections remain without a safe and effective prophylactic vaccine. It appears that traditional tools and approaches are insufficient to yield immunity

in several important examples, creating a clear and pressing need for the development of more advanced tools and platforms to yield safe and effective vaccines.

This thesis is a contribution to the ongoing work to improve the treatment and prevention of bacterial infections. In one succinct phrase, this thesis was motivated primarily by (1) a need to continue exploring new methods for enhancing the effectiveness of drug therapy, and (2) the need to identify new platforms for achieving safe and effective vaccination.

1. 2. Thesis Overview

My main interest in this thesis was to make a contribution towards developing technologies that might improve the management of bacterial infectious disease. Within this broad goal, I focused on two major activities: (1) treatment of bacterial infections, and (2) prevention of infection by prophylactic vaccination. To begin taking steps towards these aims, in collaboration with others I developed and tested a novel polymeric nanoparticle (NP) platform that could be used to encapsulate and deliver active agents. The precise method of using the NPs varies depending on the application – this is discussed at length in the appropriate research chapters.

To begin, I discuss the rationale for NP-based approaches to treatment of bacterial infections in Chapter 2. This chapter is also a literature review, focusing on the different NP-based technologies that have been used to deliver drugs, particularly within the context of antibacterial therapy. I also include a discussion of why a polymeric NP platform is suitable for the work that follows. From there, I review some of the general principles that apply across NP platforms, including such concepts as passive targeting to inflammation by certain types of nanomaterials as well as methods to achieve binding to

bacteria, often termed "active" targeting. I emphasize the use of charge-charge interactions as a widely used basis for targeting bacteria with NPs, which also forms the basis for the work contained herein.

In Chapter 3, I delve into the synthesis and characterization of the polymeric NP platform that is used (albeit with some modification over the years) throughout this thesis. This chapter also documents the first steps we took to explore the applicability of our NP system for treating bacterial infections, beginning with the synthesis of the polymer, continuing with basic characterization, drug loading/release, confocal microscopy of interactions with bacteria, then culminating with *in vitro* studies of bacterial growth inhibition using *Staphylococcus aureus* as a model pathogen.

Chapter 4 is a continuation of the work done in Chapter 3, focused on complementary studies that can potentially better predict the outcome of using this NP platform to treat infections *in vivo*. We achieve this by first exploring how the NPs interact with model biological components present at sites of infection (other than bacteria) – namely proteins and host cells. Based on these studies, we devised and explored a method that might improve the specificity of NP binding to bacteria in more complex environments, such as those containing proteins and mammalian cells. The chapter concludes with an *in vivo* assessment of relevant NP properties that might inform future studies in this area.

Chapter 5 documents efforts to improve the potency of the antibacterial NP formulation by co-delivering drugs that work synergistically together. We describe the rationale for selecting silver(I) and vancomycin, describe the formation and characterization of these co-delivering NPs, then test them for their ability to inhibit bacterial growth.

Chapter 6 describes our efforts in applying our NP platform to yield a prophylactic vaccine against *Chlamydia trachomatis*. We begin the chapter with a short review of the pertinent literature, highlighting examples of how NPs can broadly be used as vaccines as well as explaining the continuing need for a vaccine against this disease. From there, we discuss the design and characterization of the vaccine formulation that was tested, leading to demonstrations of the ability to prevent infections in vaccinated mice.

Chapter 7 summarizes the highlights and conclusions of this thesis, as well as providing suggestions for future work in this area.

1. 3. References

1. Madigan, M. T.; Martinko, J. M.; Stahl, D. A.; Clark, D. P., *Brock Biology of Microorganisms*. 13 ed.; Pearson Education, Inc: San Francisco, CA, 2012.

2. Wright, G. D., The antibiotic resistome: the nexus of chemical and genetic diversity. *Nat Rev Microbiol* 2007, 5, 175-86.

3. Fleming, A., Nobel Lecture: Penicillin. In *Nobelprize.org*, 2012 ed.; 2012.

4. Overbye, K.; Barrett, J., Antibiotics: where did we go wrong. *Drug Discovery Today* 2005, 10, 45-52.

5. Levy, S. B.; Marshall, B., Antibacterial Resistance Worldwide: Causes, Challenges and Responses. *Nat Med* 2004, 10, S122-S129.

6. Bhullar, K.; Waglechner, N.; Pawlowski, A.; Koteva, K.; Banks, E. D.; Johnston, M. D.; Barton, H. A.; Wright, G. D., Antibiotic Resistance Is Prevalent in an Isolated Cave Microbiome. *Plos One* 2012, 7.

7. Costerton, J. W.; Stewart, P. S.; Greenberg, E. P., Bacterial biofilms: a common cause of persistent infections. *Science* 1999, 284, 1318-22.

8. Donlan, R., Biofilms: Microbial life on surfaces. *Emerging Infectious Diseases* 2002, 8, 881-890.

9. Lewis, K., Persister cells, dormancy and infectious disease. *Nat Rev Microbiol* 2007, 5, 48-56.

10. Ackerman, J. How bacteria in our bodies protect our health *Scientific American* [Online], 2012.

11. D'Costa, V. M.; King, C. E.; Kalan, L.; Morar, M.; Sung, W. W.; Schwarz, C.; Froese, D.; Zazula, G.; Calmels, F.; Debruyne, R.; Golding, G. B.; Poinar, H. N.; Wright, G. D., Antibiotic resistance is ancient. *Nature* 477, 457-61.

12. Bush, K.; Courvalin, P.; Dantas, G.; Davies, J.; Eisenstein, B.; Huovinen, P.; Jacoby, G. A.; Kishony, R.; Kreiswirth, B. N.; Kutter, E.; Lerner, S. A.; Levy, S.; Lewis, K.; Lomovskaya, O.; Miller, J. H.; Mobashery, S.; Piddock, L. J.; Projan, S.; Thomas, C. M.; Tomasz, A.; Tulkens, P. M.; Walsh, T. R.; Watson, J. D.; Witkowski, J.; Witte, W.; Wright, G.; Yeh, P.; Zgurskaya, H. I., Tackling antibiotic resistance. *Nat Rev Microbiol* 2011, 9, 894-896.

Chapter 2

Background: Nanoparticles for Treating Bacterial Infectious Diseases

This chapter acknowledges contributions from: Radovic-Moreno A. F., Lu T. K., Langer R., Farokhzad O. C. *Review in preparation.*

2. 1. Introduction

The clinical impact of drug resistant (DR) bacterial infections is unprecedented and growing. Currently, the majority of hospital-acquired infections involve microbes with resistance to at least one antibiotic and multidrug resistance is spreading.[1] It is estimated that the economic costs of treating resistant infections are as high as USD $30 billion annually.[2] Drugs used to treat these resistant organisms are generally less effective, more toxic, can have solubility problems, and are susceptible to resistance. Furthermore, the pipeline for new drugs is thin. There is a limited number of recently approved or investigational new drugs in clinical trials, with many of these belonging to existing drug classes and few providing obvious advantages over existing therapies.[3]

Complicating matters is the observation that drug resistance is only one of a host of strategies that bacteria use to evade therapy. Bacteria thrive in niches in host organisms that reduce the effectiveness of therapeutics and the immune system. Bacteria can cooperate with each other to form large, difficult to permeate colonies called biofilms that are extremely difficult to remove and very difficult to penetrate.[4] Inside these colonies may reside persister cells – bacteria that have such low level metabolic activity as to be largely unaffected by the presence of antibiotics.[5] In addition, bacteria have developed the ability to escape phagocytosis and can reside intracellularly, using the host cell

membrane as protection from both the immune system and from chemical attacks.[6] Infection sites can also have a nefarious combination of conditions that can affect the outcome of therapy, with abscesses, localized acidity, and hyperviscous mucus barriers all potentially affecting the efficacy of therapeutics. These conditions can prolong duration of therapy, increase morbidity and mortality, or increase the likelihood of treatment failure.

In light of these urgent challenges, there is a pressing need to explore new strategies that might improve the treatment of infections. Currently, a variety of approaches are being evaluated including small molecule antibiotics,[3, 7] bacteriophages,[8] antimicrobial peptides,[9] antivirulence or drug potentiators,[10, 11] and nanoparticles (NP). Here, we focus on NP-based approaches. The potential of NPs stem from their small size, unique chemical, physical, electrical, or magnetic properties, ability to encapsulate and deliver drugs, and large surface area-to-volume ratio, among others. These properties can potentially be used to reduce the impact of delivery barriers, achieve improved efficacy, and reduce toxicity. Furthermore, now that the clinical evaluation of NPs for cancer therapy is well underway,[12, 13] the relative safety and potential for efficacy of nanomedicine is becoming increasingly validated.

In this review, we highlight examples where NPs might enable improvements in the treatment of bacterial infections. We stress a deep understanding of the barriers to drug efficacy or delivery, showing how NP technology can potentially be engineered to help overcome these. Most examples will focus on bacterial infections, though applicable examples in treating fungi, protozoans, and cancer are included. Finally, we highlight a

sampling of the taxonomy of materials that have high potential, focusing on systemically deliverable formulations.

2. 2. Challenges to Effective Bacterial Clearance

2. 2. 1 Drug Resistance

Bacterial drug resistance (DR) to antibiotics is one of the major challenges facing modern medicine.[14] DR can be defined as the acquisition of gene(s) which act to reduce the effectiveness of a drug. This reduced drug activity can occur through several mechanisms, including reduced drug penetration into bacteria, increased drug efflux, drug modification or degradation, or drug target modification (Figure 1).[5] DR can be observed in the laboratory as an increase in the minimum inhibitory concentration (MIC) of a drug. Multidrug resistance (MDR), that is, resistance to multiple antibiotics, is also on the rise, with as many as 16% of healthcare associated infections involving MDR pathogens in one report.[15]

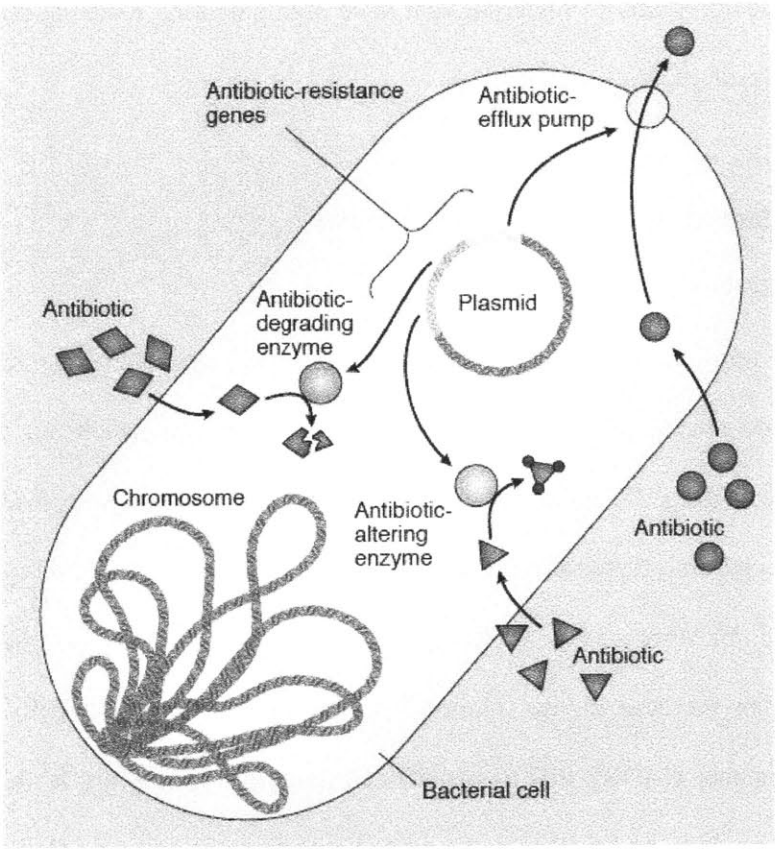

Figure 2. 1. Drug Resistance Mechanisms. Common mechanisms of resistance to antibiotics include reduced drug penetration (not shown), increased drug efflux, antibiotic alteration by enzymes, antibiotic degradation, or drug target modification (not shown). Reprinted by permission from Macmillan Publishers Ltd: *Nature Medicine* Levy and Marshall,[2] copyright 2004.

Traditional antibiotics typically act on a narrow target and have a specific mechanism of action. While this specificity has obvious advantages, it also creates a selection environment favoring expansion of DR organisms. It is currently believed that subtherapeutic drug exposure is a mechanism driving DR.[16] Theoretically, reasons why antibiotics may fall below a therapeutic level *in vivo* include insufficient dose (caused by patient non-compliance, incorrect dosing, or dose-limiting toxicity), rapid elimination

from the site of infection, inactivation or loss of activity, or poor delivery to the infection site due to high barriers to diffusion or low tissue partition coefficients.

Nanomedicine is potentially well-suited to both improve traditional antibiotic formulations and contribute to overcoming the DR challenge. NPs have been shown to improve antibiotic drug efficacy or delivery,[17, 18] directly kill bacteria,[19-21] or enable novel treatment paradigms such as targeted photothermal-mediated bacterial killing.[22, 23] In addition, NPs can be used to reduce drug toxicity, potentially reduce clearance of beneficial bacteria, achieve drug concentrations high enough to overwhelm resistance mechanisms,[24, 25] protect various antibiotics from degradative enzymes,[26] or co-deliver multiple antibacterial agents. Further, because of the nature of NP-mediated killing or because of improvements in delivery, it may be intrinsically more difficult for bacteria to develop resistance to NP therapeutics. The sections below will further explore the potential of NPs to improve treatment of infections, which is likely to simultaneously reduce the likelihood of DR emerging.

2. 2. 2. Infection Microenvironment

The microenvironment of an infection presents significant challenges for proper drug delivery and effective killing of bacteria. Infection sites are complex and dynamic entities, whose delivery challenges may vary as a function of the causative organism(s), the immune status of the patient, as well as the anatomic location. Infection sites can have intra- or extracellular bacteria, neutrophils, macrophages, lymphocytes, dendritic cells, host tissue cells, inflammatory mediators, bacterial toxins, and plasma proteins, among many others (Figure 2A). Other obstacles to delivery include aberrant tissue architecture

from chronic disease, hyperviscous mucus secretions, abscesses, acidity, and biofilms. Here we will highlight some examples of challenges to proper delivery together with nanomedicine approaches towards their resolution.

Chronic diseases can result in aberrations of the normal tissue architecture, which can impact the efficacy of therapy. For example, delivery of drugs to lung infections in patients with cystic fibrosis (CF), chronic obstructive pulmonary disease, or advanced asthma is complicated by severe mucus plugging, areas of reduced ventilation, and significant tissue remodeling and fibrosis. In a step towards improving delivery to these regions, NPs have been developed which can penetrate mucus barriers. Tang *et al* formulated NPs using a diblock copolymer of poly(sebacic acid)-*block*-poly(ethylene glycol) (PSA-PEG) designed to penetrate the hyperviscous mucus secretions of patients with cystic fibrosis.[27] The authors densely coated the surface of the NPs with PEG to reduce interactions between the NPs and mucins, leading to more rapid and effective penetration rates. Using 173 nm PSA-PEG NPs, at a time scale of 1 second they demonstrated a 50-fold greater mean square displacement diffusion distance of the NPs than control latex NPs in mucus expectorated from CF patients. Further study showed that NP size is important, with NPs less than 200 nm in diameter moving more rapidly through low viscosity pores.[28]

Abscesses are collections of bacteria, white blood cells, and associated cell debris that are known to prevent effective antibiotic delivery. They are a significant clinical problem, with skin or subcutaneous abscesses alone accounting for ~2% of emergency room visits.[29] Current clinical practice involves surgical drainage of the abscess with antibiotic therapy not practiced unless there are signs of systemic infection. Non-surgical methods

of therapy may help to reduce morbidity and tissue damage, leading to more rapid and satisfactory resolution. Nitric oxide-releasing NPs made from a hydrogel/glass composite have demonstrated activity against methicillin-resistant *Staphylococcus aureus* (MRSA) subcutaneous abscesses.[30] These NPs were shown to not only inhibit MRSA growth and reduce abscess area in mice, but to also stimulate healing by promoting fibroblast migration and inducing collagen deposition.

Another factor that can reduce drug activity is the formation of localized acidity at a site of infection. Acidity has been documented across a range of different infections involving single and multiple organisms and at different anatomic locations. The mechanism of acidity is still incompletely understood but may involve a switch to anaerobic fermentation by bacteria under settings of low oxygen tension, leading to the production of organic acids.[31] In addition, recruitment of acid-producing neutrophils and release of products of inflammatory processes exacerbate the localized acidity, which can reach as low as pH ~5.5.[32, 33] Superficial skin infections, where the normal tissue pH is already acidic, can be as low as pH 4.0.[34] Localized acidity is significant in that the activity of several antibiotics is known to be affected by changes in pH. Selman Waksman, accepting the Nobel prize in 1952 for his discovery of streptomycin, noted the loss in bactericidal potency of this antibiotic in acidity. Loss of activity has been noted in amikacin,[35] the fluoroquinolones ciprofloxacin and sparfloxacin,[36] and vancomycin.[37] Interestingly, certain β-lactams demonstrate increased potency in slight acidity.[38] These observations suggest that there is a need to develop systems that may help to optimize antibiotic activity in different pH environments. In a step in this direction, Pornpattananangkul *et al* designed an acid-sensitive drug targeting system.[34] The authors

developed cationic liposomes that remain stable at neutral pH due to surface-bound anionic gold NPs. As the local pH declines to below 5.0, the gold NPs dissociate, allowing the cationic liposomes to regain their ability to fuse with bacteria and deliver high doses of drugs.

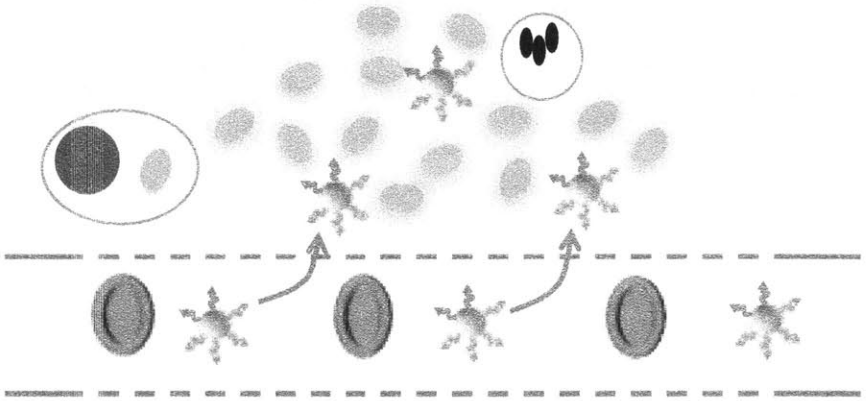

Figure 2. 2. Infection Microenvironments. The microenvironment of an infection can have far-reaching implications in achieving proper drug delivery and bacterial killing. Schematic of a typical infection site. Nanoparticles (NP) circulate in the blood until they encounter a site of increased vascular permeability (dashed lines). NPs of appropriate size are able to extravasate and come into contact with the infectious process.

2. 2. 3. Biofilms

Discovering methods for clearing bacteria residing in biofilms is one of the most demanding challenges in bacterial infectious disease research today. Biofilms are a set of structurally diverse matrix-enclosed bacterial communities that adhere to surfaces and are remarkably resistant to antibiotic therapy. They form in a regulated developmental sequence, beginning with the adhesion of an active bacterium and production of an extracellular polymeric substance (EPS) matrix, often a polysaccharide, and have sophisticated architectures, growing flat or mushroom-shaped and with internal aqueous channels for diffusion of nutrients. The lack of efficacy of antibiotics against biofilms is believed to occur through three main mechanisms: (1) hindered diffusion rates inside of

biofilms, (2) existence of bacteria in semi-starved states, leading to slower growth and subsequent reduced antibiotic susceptibility, and (3) existence of subpopulation of cells known as "persisters", which do not respond to antibiotics.[5, 40] Biofilms are especially important in various chronic infections, including device-related infections, CF pneumonias, wounds, and periodontal disease.[4] Nanoparticles have been hypothesized to be able to contribute to clearing biofilms through several mechanisms, including improved drug targeting, enhancing drug penetration into the biofilm, and reducing bacterial adhesion, the first step in biofilm formation.[41] Efficacy against biofilms formed by clinically significant pathogens including *Pseudomonas aeruginosa* and *Staphylococcus aureus* have been reported using nitric oxide-releasing silica NPs.[42] In addition, magnetic silver ring-coated NPs ~30-40 nm in diameter have been developed that can penetrate deep into biofilms after application of an external magnetic field.[43] Similarly, carboxyl-grafted superparamagnetic iron oxide NPs (SPIONs) were magnetically concentrated deep in biofilms, demonstrating ~8-fold higher percentage bacterial kill than gentamicin in a gentamicin-resistant strain of *Staphylococci.*[44] Nanoparticles have also been used to prevent the formation of biofilms. A glycopeptide dendrimer was used to inhibit the formation of *P. aeruginosa* biofilms[45] and silver bromide NP/polymer composites, when used as a coating, demonstrated the ability to resist biofilm formation.[46] Despite these promising advances, much more work is needed to investigate methods of completely eradicating bacteria in these colonies, including dormant persister cells.

2. 2. 4. Intracellular Organisms

Microorganisms have evolved the ability to evade the immune system by entering host cells, where intracellular conditions enable their continued survival. These organisms, broadly classified as "intracellular" can be very difficult to treat, have high mortality rates, and generally represent some of the most formidable challenges for designing therapeutics. Intracellular organisms inhibit the normal cellular digestive process in phagolysosomal compartments and reside there or escape into the cytoplasm.[47] By residing intracellularly, bacteria are protected from attacks by antibodies, complement, and certain antibiotics.

A variety of intracellular organisms remain without a truly robust therapy, with rampant drug resistance, complex or lengthy regimens, lack of efficacy, and possible drug interactions in patients with comorbidities. Perhaps the most notorious is *Mycobacterium tuberculosis*, the causative agent of tuberculosis (TB). TB is one of the most common and dangerous diseases in the world and is highly multidrug resistant, with estimates by the World Health Organization suggesting that one third of the entire world population has latent TB. Other clinically significant intracellular pathogens include *Listeria monocytogenes*, the causative organism of the highly fatal food-borne illness listeriosis, *Salmonella typhi*, the bacterium that causes typhoid fever, *Legionella pneumophila*, the etiology of Legionnaires' disease, a dangerous infection of the respiratory tract, and *Chlamydia trachomatis* among many others.[48]

The extent to which intracellular habitat affects antibiotic therapy depends on the drug and targeted cell type. Certain antibiotics, such clarithromycin, are actively transported into eukaryotic cells. Others, such as some β-lactams, vancomycin, or gentamicin, have relatively poor intracellular-to-extracellular ratios.[6] Enhanced delivery precisely to the

subcellular site of bacterial habitat using NPs could potentially improve drug efficacy. Macrophages are a common target for intracellular bacteria due to this cell type's role in clearing pathogens. NPs can be engineered to target subcellular compartments in a wide variety of eukaryotic cells, including macrophages, using appropriate surface modifications. Consequently, several different NPs have been explored for their potential to treat intracellular infections.

Several NPs have been explored to treat TB. Poly(N-butylcyanoacrylate) and poly(isobutylcyanoacrylate) NPs encapsulating the often-used drugs isoniazid, rifampin, and streptomycin have been evaluated in terms of their uptake by human blood monocytes and their activity against TB.[49] The NP-encapsulated drugs showed higher intracellular accumulation than free drugs and more potent antibacterial effect for isoniazid and streptomycin but not rifampin. In addition, PLGA particles have been used as an inhalable delivery system for rifampicin, isoniazid, and pyrazinamide, showing enhanced bioavailability and improved efficacy in a guinea pig model.[50] In this study, only 5 doses of PLGA-formulated drugs led to complete clearance of bacteria – the equivalent of 46 daily doses of free drugs. This is particularly remarkable since complex dosing regimens lead to high patient non-compliance – a major contributing factor to the widespread multidrug resistant nature of TB.

Polyalkylcyanoacrylate (PACA) NPs are a class of materials that have been explored extensively for treating intracellular infections. Polyisohexylcyanoacrylate NPs with bound ampicillin were shown to have significantly improved efficacy as compared to free drug in a mouse model of listeriosis.[51] The mechanism behind this improved activity *in vivo* was suggested to be improved activity of the NP-bound drug.[52]

Polyethylbutylcyanoacrylate NPs were developed which incorporated ciprofloxacin, a drug with a broader spectrum of action.[53] Polyacrylate NPs have also been explored as delivery systems for *N*-thiolated β-lactams.[17] These modified β-lactams are believed to act via a different mechanism of action than the conventional parent β-lactams, potentially making them suitable for use against drug resistant organisms. However, their low water solubility is a challenge for effective clinical translation. Polyacrylate NPs prepared with modified β-lactam monomers via emulsion polymerization in water demonstrated good drug encapsulation, small size (~40 nm), good stability, and low toxicity. Remarkably, the MIC of the NPs were 4-8x lower than the free drug monomer, suggesting significant enhancement of drug function by the NPs. Given the lack of antibacterial activity of empty NPs, it is believed that the lower MIC was due to either enhanced membrane permeability or higher local concentration of drug. Further, polyacrylate NPs formed containing acrylated penicillin G were evaluated *in vivo* by topical or intraperitoneal administration, demonstrating no obvious toxicity and promising activity, particularly in a model of an infected wound.[54] Nevertheless, the potential for cytotoxicity of these and any other type of materials should be considered in further development, noting that PACA NPs may be cytotoxic at high concentrations.[55]

Notable improvement in efficacy was found by encapsulating azithromycin in PLGA NPs. The PLGA NP formulation was shown to have an 8-fold lower MIC than free drug in treating *S. typhi*.[18] These NPs may potentially be well-suited to target azithromycin to macrophages in the spleen or liver to treat typhoid fever. PLGA NPs have also been used to deliver the antibiotic combination of rifampin and azithromycin to *Chlamydia*-infected

cells, showing efficient targeting of the inclusion body and better efficacy than free drug.[56]

2. 3. Nanoparticles Creating Opportunities for Improved Therapy

2. 3. 1. Potential Advantages of Targeting Pathogenic Bacteria

One of the main advantages of using nanomaterials for treating bacterial infections is the potential to achieve more targeted effects. Possible advantages of targeting include improved drug efficacy, reduced side effects, reduced clearance of mutualist bacteria – which might impact a variety of diseases ranging from antibiotic-associated *Clostridium difficile* diarrhea to immune diseases including asthma, eczema, and diabetes[57] – reduced potential for emergence of drug resistance, and ability to overcome drug resistance with drug concentrations not achievable using traditional antibiotic formulations due to toxicity. Nanomaterials have shown the ability to target bacteria through a number of different mechanisms, which generally fall under passive targeting or active targeting.

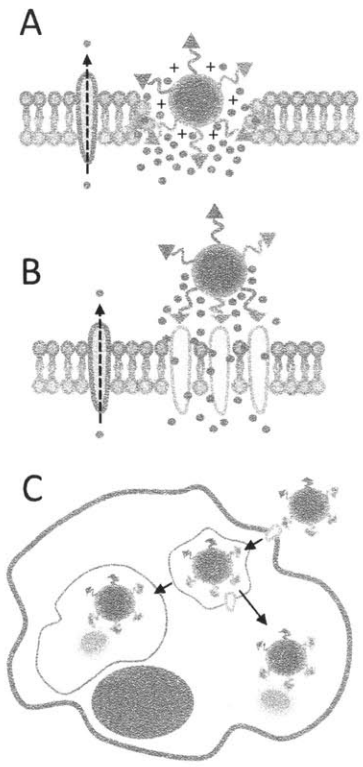

Figure 2. 3. Targeting Bacteria with Nanoparticles. Examples of different methods by which nanoparticles (NP) can target bacteria to clear infections. A) A combination of surface moieties (purple triangles) and cationic surface charge disrupting the outer membrane (in green) of a Gram-negative bacterium. The large quantities of drug (in red) delivered in this manner can overwhelm drug efflux pumps (in blue). B) An approach where a targeting ligand (purple triangle) enables NP binding to the surface of a model protein (in orange), leading to more specific drug delivery and high local drug concentration. C) NPs targeting intracellular bacteria. A NP binds to a model membrane protein leading to internalization, where either fusion with bacteria-containing endosomes/phagolysosomes or endosome escape can lead to bacterial targeting. Note: NP not drawn to scale.

2. 3. 2 Passive Targeting

"Passive" targeting is the selective accumulation of nanomaterials at a site of disease by virtue of convection (primarily in the blood) and diffusion. This is contrast to "active" targeting, which includes specific interactions that occur between the nanomaterial and components of the targeted site that lead to accumulation, binding, or eukaryotic cell

internalization. Passive targeting of infections is initiated by the accumulation and release of bacterial components at the infection site, particularly pathogen-associated molecular patterns (PAMPs). These components activate immune cells, leading to generation of bradykinin, nitric oxide, prostaglandins, and other vascular mediators. Bacterial proteases, lipopolysaccharide, and lipoteichoic acids are also known to trigger production of bradykinin independent of immune cell action. This process can occur within minutes, lasting for hours to days following bacterial transmission and is characterized by vasodilation and increased vascular permeability locally in the vicinity of the infection. The vascular mediators trigger a widening of interendothelial gaps, allowing for extravasation of plasma components into the site of infection.[58]

Selective NP accumulation due to passive targeting can be modulated by physicochemical properties, including size, zeta potential, shape, rigidity, roughness, surface hydrophilicity, density of poly(ethylene glycol) (PEG), and others (for a more thorough treatment, see reviews[59, 60]). Significant effort has gone towards understanding the impact of these parameters on passive targeting. Much of this literature comes from studies of NP accumulation in tumors, which are similar to infections in that they exhibit local increases in vascular permeability. Important differences to consider include the aberrant vascular architecture, impaired lymphatic drainage, and reduced vascular density in tumors.[61] Data that clearly and directly address the impact of NP properties on residence time at an infection are generally lacking. However, existing results suggest that NP infection residence time is significantly shorter than in tumors and is on the order of days vs. weeks.[58] This suggests that a strategy that facilitates NP binding to the infection site may be preferable to one that relies on passive targeting alone.

Optimization of passive targeting is achieved by extending NP stability and circulation time in the blood, since NPs must circulate until they encounter the site of "leaky" vasculature. NP size is one of the principal factors governing passive targeting, with nanomaterials as small as 40 kDa and objects as large as bacteria (~1000 nm) being able to enter or leave the vascular space.[58] However, NPs in the range 10-400 nm are generally preferred for achieving extended circulation.[60] Strongly cationic surfaces are a common feature of several antibacterial NPs. While certain examples have shown promise both *in vitro* and *in vivo*, in general, cationic charge would be expected to have high levels of non-specific eukaryotic cell uptake, negatively charged protein binding, and shorter circulation time. A mitigation strategy is to PEGylate the NP surface. However, even a single terminal cationic charge (primary amine) on PEG was shown to markedly affect the biodistribution of ~8-11 nm PEG-coated gadolinium oxide NPs, with the amine terminal group PEG-modified NPs showing much greater accumulation in the spleen and liver than similar negatively charged or neutral NPs.[62] Consequently, efforts to design NPs with high surface charges should pay special attention to these considerations. The potential to target infections with nanoparticles is well-established.[63] Technetium-99m-labeled liposomes of different mean sizes between 90 and 220 nm were shown to accumulate selectively at sites of *S. aureus* infection in rats.[64] The biodistribution of these liposomes was shown to be dependent on size, with differences occurring mainly in rates of splenic uptake. The % injected dose per gram of tissue (% ID/g) at the infection was not statistically different for liposomes 90, 120, 160, and 220 nm in size, with between 1.37-1.72% ID/g reaching the infection site. The targeting mechanism was believed to be passive targeting, with minimal contribution from monocyte uptake. Superparamagnetic

iron oxide nanoparticles (SPIONs) have been shown to rapidly and selectively accumulate in the lungs of mice infected with *S. aureus*.[65] Accumulation could be observed as early as 24 hours postinfection – considerably before structural changes or edema could be appreciated using conventional T2* or T2-weighted imaging. SPIONs 18-30 nm have also been shown to accumulate in macrophages at sites of inflammation, including arthritic knees[66] and soft tissue infections.[67] The mechanism of selective accumulation in these examples is believed to be a combination of passive targeting followed by selective phagocyte uptake at the infection site.

2. 3. 3 Active Targeting

Active targeting involves the engineering of the nanomaterial to specifically interact with an infection site. Three general strategies have been explored to achieve active targeting: (1) cationic surface charge, which interacts with the negative surface charge of bacteria, (2) specific binding to the bacterial surface using targeting ligands, such as antimicrobial peptides or peptidomimetics, lectins, cell wall-targeting antibiotics, inflammation targeting, antibodies, or aptamers, and (3) targeting internalization inside of phagocytic cells for reaching intracellular organisms.

2. 3. 3. 1. Cationic Materials

Engineering a cationic surface charge to bind to the negative surface charge of bacteria is the most widely used mechanism to achieve active targeting. Components of the bacterial cell wall that contribute to a negative charge include (lipo)teichoic acids, peptidoglycan, negatively charged phospholipids and the lipid A/acidic phospholipids of the Gram-negative outer membrane. A wide variety of bacteria are negatively charged under physiologic conditions, making this approach suitable for different types of infections or

for infections that are polymicrobial. In addition, multivalent effects and the variety of chemical structures that can be engineered to produce a cationic charge make this an attractive method for targeting bacteria. Cationic bacteria-targeting materials generally fall under two major categories: (1) synthetic antimicrobial polycations and (2) natural peptide or peptidomimetic structures. The majority of interest in developing these materials has been to yield surfaces with contact-killing properties. Such surfaces are particularly well-suited to prevent bacterial colonization and have been explored principally as coatings for medical devices or other objects one might find in healthcare settings.

Synthetic antimicrobial polycations include materials such as quaternary ammonium[68] or phosphonium[69] compounds, or alkyl pyridiniums.[70] Many more synthetic antimicrobial polymers have been explored for their antimicrobial effects (for review, see Kenawy et al[71]). These polymers could potentially be grafted onto the surfaces of nanomaterials and used for their bacteria-targeting and/or contact-killing properties, or be engineered to self-assemble into nanoscale structures. In general, accumulated studies have shown that high charge density, particularly zeta potential above +40 mV, and chain mobility are important for achieving a bactericidal surface.[72] However, a challenge with these types of materials is their lack of specificity for bacterial membranes. High charge density is known to correlate with toxicity to human cells, and many of the reported polymers are not biodegradable. In addition, the antimicrobial efficacy of these materials is typically reported at concentrations in the mg/mL range, which is too high for systemic application in many cases. Furthermore, there is risk with the mode of action of some of these polymers – bacteriolysis can lead to endotoxin release and fatal anaphylactic shock.

Despite these challenges, there have been notable successes. Cationic amphiphilic biodegradable polycarbonates that self-assembled into ~40-200 nm NPs with low polydispersity were developed, demonstrating low micromolar MICs against *Bacillus subtilis*, MRSA, and *Enterococcus faecalis*, among others.[20] These NPs did not show evidence of damaging red blood cell membranes even at concentrations much greater than their MIC, and were well tolerated in mice. The selective targeting appears to be a result of the highly cationic surface charge (+47 to +65 mV) interacting with the more negative microbial membranes. The biodegradable nature of these NPs, their excellent efficacy, and their broad spectrum activity make these synthetic structures very promising antimicrobial NPs.

Synthetic NPs that use cationic charge-based targeting have shown excellent potential *in vivo*. A NP composed of a linear structure of TAT peptide (sequence YGRKKRRQRRR), hexarginine (R_6), triglycine (G_3), and cholesterol (C) (combined = CG_3R_6TAT) was designed to target drug-resistant infections in the central nervous system.[21] The hydrophobic cholesterol region triggered self-assembly of NPs 177 nm in diameter with a zeta potential of +55 mV. *In vitro* studies demonstrated low MIC across a range of pathogens, including MRSA and vancomycin resistant *Enterococcus*. Further, the NPs were shown to have an MIC six times lower than the soluble G_3R_6TAT peptide, suggesting that the high positive charge density of the NP was important for the high potency of the antimicrobial effects. The NPs appeared to have selectivity for bacterial membranes, demonstrating relatively low rates of hemolysis and good tolerability *in vivo*. PLGA NPs have been given a cationic surface charge by incorporating Eudragit RL100 into the NP formulation step.[73] The cationic NPs were shown to bind avidly to both *S.*

aureus and *P. aeruginosa*, with potential application in the targeted and sustained delivery of ciprofloxacin to the eye.

2. 3. 3. 2. Antimicrobial Peptides or Peptidomimetics

Antimicrobial peptide (AMP) or peptidomimetic structures can be used to target bacteria. Currently, more than 1000 AMPs have been described, with a large diversity of structures and subclassifications.[9] In general, AMPs are peptides of ~10-50 residues composed of both cationic and hydrophobic regions with secondary structures such as α-helices or β-sheet-like tubes. Above certain critical concentrations, AMPs lead to increases in membrane permeability, resulting in loss of membrane function and ultimately bacterial death. It is believed that the cationic regions of AMPs mediate the initial attraction step to negatively charged regions of the bacterial membrane. Following this initial interaction, hydrophobic regions adhere to the hydrophobic portion of the lipid membrane, leading to the formation of pores.[74] Advantages of antimicrobial peptides as either targeting moieties or as drugs to be delivered include a binding mechanism of action that cannot easily be invalidated by microbial evolution, wide variety of structures and functionalities, relatively small size, and selectivity for bacterial membranes. However, certain AMPs only function under a defined set of conditions. Consequently, special care should be taken to ensure that AMPs will function under local pathologic conditions. In addition, the orientation of the AMPs on the NP surface may also play a role in their proper function. Finally, one should note that the site of interaction of many AMPs, the cytosolic membrane, may lie underneath one or more outer layers, making it difficult for the AMP to reach cytosolic membrane. Despite this, there is evidence to suggest NP-conjugated

AMPs may still be able to reach the cytoplasmic membrane, even in Gram-negative organisms that have an outer membrane. 10 nm gold NPs conjugated to the AMP Sushi 1 (S1) were shown to be able to target the Gram-negative *E. coli*, with NP penetration across all layers, though the majority (~77%) associated with the outer membrane.[75] Further, the potential to target *E. coli* with ~20 nm quantum dots conjugated to S1 was demonstrated using fluorescence microscopy. These concerns are likely to be less significant in Gram-positive organisms, where the lack of an outer membrane allows for easier access to the cytoplasmic membrane. In fact, molecules of molecular weight up to 90 kDa are known to be able to diffuse across the peptidoglycan layer of the Gram-positive organism *S. aureus*.[71] Potential challenges to AMP use include toxicity at high concentrations, lack of efficacy, enzymatic degradation, or negative effects on NP pharmacokinetics, particularly for highly cationic charged AMPs. Some of these challenges may be mitigated using peptidomimetics.[76]

2. 3. 3. 3. Lectins

The sugars of the bacterial membrane represent a potential binding site for targeted NPs. A gliadin NP containing acetohydroxamic acid was targeted to *Helicobacter pylori* using the lectins Ulex Europeaus Agglutinin I (UEA I) or Conconavalin A (Con A).[77] The lectin-targeted NPs demonstrated greater growth inhibition of *H. pylori in vitro* than both untargeted NPs and free drug. The lectin-targeted NPs also reduced the binding of *H. pylori* to samples of the human gastric mucosa *ex vivo*. A potential mechanism for the enhanced efficacy of the targeted NPs was a higher local concentration of drug in the vicinity of the bacteria.

2. 3. 3. 4. Antibiotics

Antibiotics that interact with accessible extracellular targets may be used to target NPs. The glycopeptide vancomycin binds to the D-alanyl-D-alanine dipeptide in the peptidoglycan layer of the cell wall of Gram-positive organisms with high affinity (K_d in the 1-4 uM range). Vancomycin was conjugated to the surface of magnetic beads and used to capture different types of bacteria from samples, demonstrating that proper orientation and a long tether both contributed to improved capture efficiency.[78] Vancomycin-modified gold NPs demonstrated improved killing efficacy as compared to vancomycin alone against vancomycin-resistant *Enterococci in vitro*.[79] This was attributed to the higher vancomycin density achievable on a NP surface as compared to soluble form.

2. 3. 3. 5. Inflammation Targeting: E-selectin

E-selectin is a cell adhesion molecule that is expressed on the surface of endothelial cells adjacent to sites of inflammation. Since infections trigger inflammation in immunocompetent patients, it may be possible to target infections by targeting this molecule. Nanomaterials have been designed to target E-selectin using carbohydrate motifs including Sialyl Lewis A or X (SLE^a or SLE^x) or monoclonal antibodies or their fragments.[80] An advantage of this approach is that by not interacting with bacteria directly, it may be possible to avoid DR completely. However, success of this approach would depend on whether the drug can cross the endothelial layer and permeate the targeted tissue to reach the bacteria at sustained therapeutic levels.

2. 3. 3. 6. Antibodies

A silica NP was modified with a monoclonal antibody against *E. coli* O157, demonstrating the ability to target this bacterium for detection at trace quantities – on the

order of 1-400 cells in a 1 gram sample of ground beef.[81] Similarly, polystyrene NPs were targeted to *L. monocytogenes* using a monoclonal antibody against N-acetylmuramidase.[82] Parenthetically, these NP-bacterium conjugates were applied as a novel platform for DNA delivery by utilizing the endosome-escaping ability of this intracellular pathogen. In addition, various antibodies are being evaluated for their therapeutic potential in treating infections.[10] These antibodies generally function by facilitating phagocytosis or by inactivating bacterial toxins.

2. 3. 3. 7. Aptamers

Aptamers have been used to target bacteria. An aptamer targeting a virulent strain of *M. tuberculosis* was identified using whole-bacterium SELEX (Systematic Evolution of Ligands by Exponential Enrichment), using the non-virulent bacillus Calmette-Guérin (BCG) for counter-selection. This aptamer was shown to potentiate CD4+ T cell immune responses, leading to efficacy *in vivo*.[83]

2. 3. 4. Drug Co-Delivery

The potential advantages of antibiotic combinations are well-documented but several challenges to their widespread use remain, particularly side effects, toxicity, and lack of or declining efficacy in some cases. NP formulations offer the potential to more effectively and safely co-deliver multiple agents. These benefits can be attained by using NPs to exert greater control over drug ratios and concentrations spatiotemporally, enable co-delivery of drugs that have synergistic effects but different physicochemical properties that would normally preclude their effective co-administration, the potential to optimize synergy ratios, reduce toxicity through targeting, and achieve anti-DR benefits due to multiple mechanisms of action. These benefits might arise because NPs offer multiple

possibilities for drug loading and release, which enable combination and release optimization. In one example of the potential of co-delivery, the combination of chitosan-silver NPs with molecular iodine was shown to be more effective than just chitosan-silver NPs or each type of NP in isolation.[84] Amoxicillin chelated onto silver NPs showed synergistic effects against *E. coli in vitro*.[85] Certain infections, such as multiple drug-resistant TB, require many drugs to be delivered, which could be targeted more effectively together in a single NP delivery system. In addition, co-delivery can be a strategy to overcome persister cells' lack of response to antibiotic therapy. Treating these dormant bacteria with glucose, fructose, or mannitol together with the aminoglycoside gentamicin was shown to induce rapid killing.[86] Other potential strategies involve delivering drug potentiators together with drugs, such as β-lactams with β-lactamase inhibitors.

2. 4. Nanoparticle Platforms

This section will highlight characteristics of some widely used materials and structures for treating bacterial infections (Figure 4). For continued discussions and other examples, the reader is referred to other excellent reviews.[1, 63, 87-90]

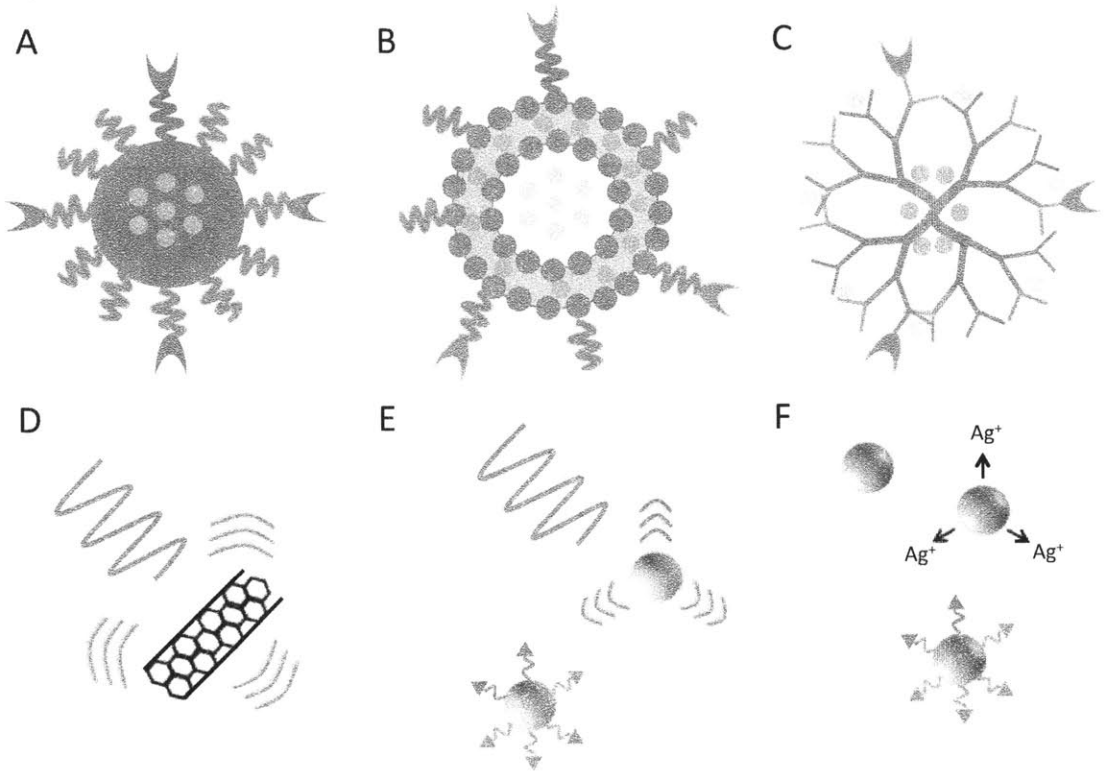

Figure 2. 4. Antibacterial Nanoparticle Platforms. A) A polymeric nanoparticle (NP) with drug encapsulated in the interior (green) protected with a layer of poly(ethylene glycol) (PEG). At the distal end of the PEG is a targeting ligand (purple) to trigger bacteria-specific interactions. B) A unilamellar liposome with a hydrophilic drug encapsulated in the aqueous core and hydrophobic drug (green) intercalated in the lipid bilayer (blue). C) A dendrimer with drugs adsorbed in the hydrophobic interior (green) or in the hydrophilic exterior (orange). A near infrared (NIR)-absorbing D) carbon nanotube or E) gold NP (with or without targeting ligand) producing targeted hyperthermia. F) Examples of antibacterial silver NPs.

2. 4. 1. Liposomes

Liposome drug delivery systems have been in development since at least the 1960s and benefit from extensive preclinical and clinical data validating their potential.[59] Liposomes are spherical lipid bilayer vesicles composed primarily of phospholipids and cholesterol. Liposomes can be uni- or multi-lamellar with the bilayer(s) delimiting a hollow aqueous core. The outer membrane phospholipids can be modified with PEG to enhance the

circulation half-life, with targeting ligands to trigger eukaryotic cell internalization, or with stimuli-responsive elements such as pH-sensitivity to increase eukaryotic cell uptake.[91] PEGylated liposomes have been shown to circulate for long periods in the body, allowing for passive accumulation at infection sites.[64] Loading of drug is possible either in the aqueous core (hydrophilic drugs) or in the lipid bilayer(s) (hydrophobic drugs). Drug combinations, including the difficult loading combination of hydrophobic and hydrophilic drugs, are possible. Several studies have illustrated their potential advantages, including extended drug pharmacokinetics, reduced toxicity, enhanced targeting, ability to fuse with the bacterial membrane to deliver high quantities of drug, and increased therapeutic efficacy.[1]

Antimicrobial liposome formulations have been evaluated and used clinically for years. A liposome formulation of amphotericin B (AmBisome) was approved in Europe in 1990 and by the US FDA in 1997 and has seen extensive clinical use not only for treating fungal infections including Cryptococcal meningitis, general invasive Candidal disease, and osteoarticular candidiasis but also for treating infections involving *Leishmania* protozoans. A randomized, double-blind, multicenter trial involving 687 patients demonstrated improved efficacy with fewer side effects of liposomal amphotericin B as compared to conventional formulation in treating occult invasive fungal infections.[92] Liposomal amphotericin B and conventional formulation had a similar effect on survival (93% survival vs. 90%, respectively) but liposomal formulation was associated with fewer breakthrough infections (3.2% vs. 7.8%) and less toxicity (fever 17% vs. 44%; chills or rigors 18% vs. 54%).

MiKasome, a unilamellar liposomal formulation of the aminoglycoside antibiotic amikacin, demonstrated prolonged drug residence time and sustained efficacy in rats,[93] but this did not appear to be effective in treating patients with pulmonary tuberculosis.[94] The authors postulated that this low efficacy was due to liposome targeting of macrophages and limited drug delivery to bacteria. Devising methods of increasing drug release from liposomes in the vicinity of bacteria may therefore improve the efficacy of this delivery approach. Other challenges to liposome use include burst release on liposome destabilization, difficulty in encapsulating neutral hydrophobic or agents with intermediate solubility, and problems encapsulating larger hydrophilic agents, such as proteins.[95]

2. 4. 2. Inorganic Materials and Carbon Nanotubes

A variety of inorganic materials, including metal or metal oxide NPs and carbon nanotubes have been explored for their antibacterial activity. The most commonly used metal/metal oxide NPs include silver,[96] zinc oxide,[97] and titanium dioxide.[98] Common mechanisms of action for these types of materials include production of reactive oxygen species, interactions with the bacterial membrane leading to disrupted energy production, and inhibition of enzyme activity.[87] In addition, carbon nanotubes[99] and gold[23] have been used for targeted photothermal therapy due to their ability to absorb near infrared radiation, killing bacteria by localized hyperthermia. Further, carbon nanotubes have also been shown to have direct killing ability, due to their ability to disrupt the bacterial membrane.[100]

Silver compounds are known to have potent and broad spectrum antibacterial activity. Multiple mechanisms have been elucidated, including destabilization of the bacterial

membrane and reduction of intracellular ATP levels.[101] These multiple mechanism of action makes it more difficult for bacteria to develop resistance, though resistance to silver compounds has been documented.[102] Size and shape play a role in the efficacy of silver-containing systems, with truncated triangular NPs demonstrating potent activity against *E. coli*.[103] Use of silver NPs should continue to be evaluated together with its potential toxicity and side effects, including argyria and cytotoxicity.[104]

2. 4. 3. Polymeric Nanoparticles

Polymeric NPs are supramolecular structures formed by the self-assembly of previously made polymers or emulsion polymerization of monomers into NPs. These NPs can have antibacterial activity either by encapsulating and delivering drugs, directly killing bacteria, or both. Advantages of polymeric NPs include the ability to optimize their properties (such as tuning size, zeta potential, targeting ligand density, and drug release for example), the abilities to encapsulate a wide variety of drugs or drug combinations, control drug release, and target infections by active or passive means, good shelf life and stability *in vivo*, as well as clinical validation of safety in some cases. Drug-loaded polymeric NPs are typically synthesized through either chemical conjugation of the drug to the polymer followed by NP formulation, free drug encapsulation using emulsion/solvent evaporation, nanoprecipitation, salting out, or emulsion polymerization in the presence of free or polymer-conjugated drug.[59] A variety of different types of drugs can be loaded in polymeric NPs, though higher loading efficiencies are typically reported using hydrophobic drugs.

The potential for both improved drug targeting and extended drug release achievable using polymeric NPs aligns well with the delivery needs of an antibiotic. Greater drug

targeting can lead to higher local drug concentration at the site of infection, which can improve drug efficacy or reduce the likelihood of subtherapeutic dose. Extended release of an agent following selective accumulation can lead to sustained drug levels above the MIC locally, which might not only improve therapy, but also reduce the potential for the emergence of drug resistance and facilitate dosing. For example, achieving high and sustained levels of vancomycin with an $AUC_{24}/MIC > 400$ is recommended for improved treatment efficacy.[105] Release rates that are too slow will result in subtherapeutic drug exposure, leading to potential antibiotic drug resistance emerging, as an inverted U-shaped curve has been reported for the number of resistant mutants as a function of AUC/MIC.[106] In addition, controlling drug release is important for treating biofilms. Using levofloxacin-loaded PLGA or PCL NPs, it was concluded that a more rapid antibiotic release initially followed by slower extended release will more successfully inhibit biofilm growth.[107] Further, polymeric NPs can be used in innovative ways, such as forming films using PEO-*b*-PCL triclosan-encapsulating NPs to control drug release from surfaces, yielding potent bacterial killing efficacy.[108]

2. 4. 4. Dendrimers

Dendrimers are small (3-7 nm), highly monodisperse macromolecules synthesized via convergent or divergent methods to yield a core with multiple branches with defined structures.[109] Dendrimers are typically defined by their generation number. Higher generations imply larger molecular weights and hydrodynamic diameters and exponential increases in the number of terminal surface groups, though it is challenging to achieve a higher generation number than 6 or 7.[110] Drugs can be loaded onto dendrimers by

chemical or physical (charge-based) conjugation to the surface, or by loading in the more hydrophobic interior. Dendrimers can be used to co-deliver multiple agents.[111] Because of their functionalizability, intrinsic bactericidal activity, and drug loading capabilities, dendrimers have been explored for treating bacterial infections. In general, these types of dendrimers primarily fall into a few categories[88]: glycodendrimers to block bacterial and bacterial toxin adhesion to human cells,[112] cationic dendrimers to disrupt bacterial membranes[19] or deliver drugs such as silver,[113] and peptide-based dendrimers that incorporate peptide sequences that have antibacterial activity[114]. These dendrimers generally show low MICs comparable to traditional antibiotics, which together with their functionalizability and drug delivery capability, make them attractive for further development in antibacterial therapy.

Table 2. 1. Methods for Targeting Bacteria

Targeting Method	**Target**	**Potential Advantages**	**Potential Challenges**	**References**
Cationic charge	Anionic charges on bacterial surface	Broad spectrum, less DR, potential for direct antibacterial effects	Lower specificity, toxicity, shorter NP PK, DR	[20,21,115,116]
Antibody	Various possible	High affinity, specificity	NP manufacturing complexity, Denaturation,	[81,82]

			DR	
Antibiotic	Various possible, cell wall targeting antibiotics preferred	High affinity, specificity, potential for antibacterial effects	May be ineffective against established DR, Path to DR emergence exists	[78,79]
Aptamer	Various possible	High affinity, specificity, powerful selection strategy (SELEX)	Degradation, DR	[83]
Lectin	Surface polysaccharides	Broadly applicable	Denaturation, DR	[77]
Antimicrobial peptide	Cell membrane	Broadly applicable, less DR	Shorter PK (if cationic), toxicity, DR	[9,75]
Sialyl Lewis A or X	E-selectin on inflamed endothelium adjacent to infection	Less DR (does not act on bacteria)	Drug diffusion into infection necessary	[80]
Macrophage-assisted	Interior of macrophages	Targets precise location, good for	More limited applicability,	[52,65,67]

		intracellular organisms	More complex design	

Table 2. 2. Example of Nanoparticles Overcoming Challenges

Challenge	**Approach**	**References**
Drug resistance	Enhancing drug function	[17, 79]
	Membrane targeting	[20, 21]
	Drug co-delivery	[49, 50, 84]
	Targeted hyperthermia	[22, 23]
Biofilms	Nitric oxide release	[42]
	Magnetic penetration	[43, 44]
Hyperviscous mucus	Enhanced penetration	[27]
Acidity	pH-sensitive increases in activity	[34]
Intracellular organisms	Intracellular targeting	[51, 52]
Abscesses	Nitric oxide release with improved wound resolution rate	[30]

2. 5. Future Perspective

There is an acute need to develop new methods for treating bacterial infections. Drug resistance has reached unprecedented levels, and existing drugs are inadequately or suboptimally treating biofilms, intracellular organisms, or infections that have significant microenvironmental obstacles, leading to continued morbidity and mortality. Nanomedicine is increasingly showing its potential to yield more effective and less toxic therapeutics in various fields. Early efforts at applying nanomedicine to develop novel antibacterials have shown great promise, but still there is much more work to be done.

NPs have the potential to contribute to new therapeutic development as drug delivery vehicles, intrinsically bactericidal materials, or both. NPs can be engineered to overcome obstacles and specifically target bacteria. Improved targeting and delivery can reinvigorate old drugs or facilitate new drug development, especially in the case of toxic or poorly soluble drugs. Key to improved design is an intimate understanding of the delivery challenges. In the most generic sense, delivery vehicles are needed that can (1) encapsulate a drug or drug combination at a precisely optimized quantity or ratio, (2) protect the drugs while in transit to the bacteria, (3) accumulate specifically at sites where pathogenic bacteria reside, overcoming delivery challenges like thick mucus, fibrosis, abscesses, clearance by the immune system or acidity, while simultaneously avoiding mutualist bacteria or sites susceptible to side effects, (4) release the drugs in a manner that yields the most effective bactericidal effect, taking care to avoid sustained sublethal drug levels, (5) be non-toxic and biocompatible, and (6) demonstrate improvement in efficacy or susceptibility to DR as compared to free drug formulations, particularly *in vivo*. In addition to passive delivery vehicles, nanoparticles that are intrinsically

bactericidal, act synergistically with the drugs they deliver, or potentiate drug function are needed. Greater diversity in mechanism of action correlates with reduced susceptibility to drug resistance, so a variety of mechanisms and approaches may need to be explored in combination to develop highly robust new therapeutics. Some of these may not be chemically based, such as using targeted hyperthermia.

The remaining challenges in bacterial infectious disease are immense and it is likely that a combination of drug optimization and delivery vehicle optimization will need to occur in tandem to yield the most robust therapeutics possible. To achieve this, it will be necessary to continue exploring molecular mechanisms of drug resistance, microbial drug susceptibility, biofilm formation, and bacterial persister biology, among others, to determine the optimal pathways or combinations of pathways that can be targeted with drugs or NPs. Simultaneously, delivery vehicles that can overcome the challenges of the physiologic environment to properly present the optimized drugs to bacteria are needed, particularly if they can also improve drug function or have intrinsic bactericidal activity. In addition, one must remember that antibiotics are typically delivered at high doses, on the order of a few grams per dose per day. Consequently, materials used for antibiotic delivery must be nontoxic, even at very high concentrations.

We believe steps will be taken in each of these directions over the coming years. In addition, greater interactions between microbiologists, immunologists, clinicians, material scientists, engineers, and other experts in nanomedicine will yield novel insights into how the intersection of these fields can enable new therapeutics. In developing new antibacterial therapies, there is a great need but also great potential. In the next decade,

we expect to see significant strides taken towards realizing the promise of NP antibacterials.

2. 6. Summary

Introduction

- There is an urgent need to develop novel therapeutics for treating bacterial infections because existing drugs are at risk of resistance, because delivery hurdles and infection microenvironments can impair drug therapy, and because the pipeline for new antibiotics is thin.
- Among the various investigational new methods for treating infections, NPs have several potential advantages including the ability to overcome delivery barriers, improve drug efficacy, achieve targeted effects, reduce toxicity, and be less susceptible to drug resistance (DR).

Challenges to effective therapy

- DR is one of the major challenges in modern medicine. NPs have the potential to contribute to overcoming DR by: improving drug potency, delivering drugs at more optimal rates and concentrations, killing bacteria through mechanisms that are recalcitrant to DR, or by establishing novel DR-resistant treatment paradigms such as targeted hyperthermia.
- NPs can be designed to overcome delivery hurdles to potentially kill bacteria in complex environments such as hyperviscous mucus, abscesses, acidity, and biofilms.
- NPs have been explored extensively for their ability to target intracellular infections because they can be engineered to target subcellular compartments such as phagolysosomes or the cytoplasm *in vitro* and *in vivo*.

Nanoparticles creating opportunities for improved therapy

- Targeting NPs to infections can potentially improve drug efficacy, reduce side effects, reduce clearance of commensal flora, and reduce the risk of DR emerging.
- NPs can be targeted to infection sites through a variety of mechanisms, typically described as "passive" or "active" targeting.
- "Passive" targeting in this context refers to the selective accumulation of NPs (~40 kDa-1000 nm in size) at infection sites due to convective and diffusive transport. It can occur when bacterial components cause the release of vascular mediators at the infection site. Passive targeting has been observed in various animal models of infection using various different types of NPs.
- "Active" targeting refers to specific interactions between NPs and the infection site that lead to selective accumulation. Examples of active targeting include a cationic NP surface charge designed to interact with the anionic bacterial membrane, or NP surface modification with targeting ligands. Potential targeting ligands include antimicrobial peptides or peptidomimetics, lectins, antibiotics, antibodies, or aptamers.

Nanoparticle platforms

- Various NP platforms have been used in antibacterial therapy. In general, mechanisms of action include antibiotic drug delivery, direct bacterial toxicity, or both.
- Liposomes are spherical lipid bilayer vesicles that can deliver hydrophobic or hydrophilic drugs. They have led to clinically approved antimicrobial drug formulations, making them well-suited for continued development. Challenges that remain to be overcome include drug release that is too slow or too fast and difficulties encapsulating certain types of drugs.
- Metal or metal oxide NPs and carbon nanotubes have been explored for their potential to treat DR infections. Generally, these materials utilize mechanisms of action that target the bacterial membrane, making DR more difficult to emerge. A major challenge to *in vivo* use is toxicity.
- Polymeric NPs are capable of improving drug targeting and achieving sustained drug release – a combination that aligns well with the delivery needs of an antibiotic. A challenge that remains includes boosting the encapsulation efficiency and loading of hydrophilic agents.
- Dendrimers are macromolecules (3-7 nm) with a core surrounded by multiple branches. They have shown promise in antibacterial therapy due to intrinsic bactericidal activity and ability to deliver multiple types of drugs.

2. 7. Acknowledgments

This research was supported by National Institutes of Health Grants CA151884 and EB003647, the David Koch—Prostate Cancer Foundation Award in Nanotherapeutics, and the USA Department of Defense Prostate Cancer Research Program PC 051156. A.F.R.-M. thanks the MIT Portugal and NSF GRFP programs for funding support. T.K.L. was supported by Grant Number DP2OD008435 from the Office of the Director, National Institutes Of Health. The content is solely the responsibility of the authors and does not necessarily represent the official views of the Office of the Director, National Institutes Of Health or the National Institutes of Health.

R.L. and O.C.F. disclose their financial interest in BIND Biosciences, Selecta Biosciences, and Blend Therapeutics, three biotechnology companies developing nanoparticle technologies for medical applications.

2. 8. Reference Annotations

Papers of special note have been highlighted as:

* of interest

** of considerable interest

**Nederberg et al., 2011[20] – Illustrates exciting potential of NP antibacterials. Describes a NP that selectively disrupts the membranes of Gram-positive bacteria, MRSA, and fungi with low toxicity.

**Liu et al., 2009[21] – Remarkable results with a cationic peptide NP that can cross the blood-brain barrier and suppress *S. aureus*-induced meningitis in rabbits.

*Huh et al., 2011[87] – Recent and comprehensive review of the field with many excellent insights and examples.

*Zhang et al., 2010[1] – Insightful review of the various NP types used in antimicrobial drug delivery.

*Schroeder et al., 2010[63] – Penetrating and thorough review of the potential to target infections using liposomes.

*Kaim et al., 2002[67] – MR imaging of superparamagnetic iron oxide NPs accumulating in acute soft-tissue infections in rats.

*Gu et al., 2003[79] – Illustrates potential of NPs to reinvigorate old drugs. Vancomycin-capped gold NPs show enhanced activity against vancomycin-resistant *Enterococci* and Gram-negative bacteria.

2. 9. References

1. Zhang, L.; Pornpattananangku, D.; Hu, C. M.; Huang, C. M., Development of nanoparticles for antimicrobial drug delivery. *Curr Med Chem* 2010, 17, 585-94.

2. Levy, S. B.; Marshall, B., Antibacterial Resistance Worldwide: Causes, Challenges and Responses. *Nat Med* 2004, 10, S122-S129.

3. Butler, M.; Cooper, M., Antibiotics in the clinical pipeline in 2011. *Journal of Antibiotics* 2011, 64, 413-425.

4. Costerton, J. W.; Stewart, P. S.; Greenberg, E. P., Bacterial biofilms: a common cause of persistent infections. *Science* 1999, 284, 1318-22.

5. Lewis, K., Persister cells, dormancy and infectious disease. *Nat Rev Microbiol* 2007, 5, 48-56.

6. Hof, H., Intracellular microorganisms: a particular problem for chemotherapy. Introduction. *Infection* 1991, 19 Suppl 4, S193-4.

7. Payne, D.; Gwynn, M.; Holmes, D.; Pompliano, D., Drugs for bad bugs: confronting the challenges of antibacterial discovery. *Nature Reviews Drug Discovery* 2007, 6, 29-40.

8. Lu, T. K.; Koeris, M. S., The next generation of bacteriophage therapy. *Current Opinion in Microbiology* 2011, 14, 524-531.

9. Zasloff, M., Antimicrobial peptides of multicellular organisms. *Nature* 2002, 415, 389-95.

10. Fernebro, J., Fighting bacterial infections-Future treatment options. *Drug Resistance Updates* 2011, 14, 125-139.

11. Park, B.; Liu, G. Y., Targeting the host-pathogen interface for treatment of Staphylococcus aureus infection. *Seminars in Immunopathology* 2012, 34, 299-315.

12. Hrkach, J.; Von Hoff, D.; Mukkaram Ali, M.; Andrianova, E.; Auer, J.; Campbell, T.; De Witt, D.; Figa, M.; Figueiredo, M.; Horhota, A.; Low, S.; McDonnell, K.; Peeke, E.; Retnarajan, B.; Sabnis, A.; Schnipper, E.; Song, J. J.; Song, Y. H.; Summa, J.; Tompsett, D.; Troiano, G.; Van Geen Hoven, T.; Wright, J.; LoRusso, P.; Kantoff, P. W.; Bander, N. H.; Sweeney, C.; Farokhzad, O. C.; Langer, R.; Zale, S., Preclinical development and clinical translation of a PSMA-targeted docetaxel nanoparticle with a differentiated pharmacological profile. *Sci Transl Med* 2012, 4, 128ra39.

13. Heidel, J.; Davis, M., Clinical Developments in Nanotechnology for Cancer Therapy. *Pharmaceutical Research* 2011, 28, 187-199.

14. Levy, S. B.; Marshall, B., Antibacterial resistance worldwide: causes, challenges and responses. *Nat Med* 2004, 10, S122-9.

15. Hidron, A. I.; Edwards, J. R.; Patel, J.; Horan, T. C.; Sievert, D. M.; Pollock, D. A.; Fridkin, S. K.; Natl Healthcare Safety Network, T.; Participating Natl Healthcare, S., Antimicrobial-Resistant Pathogens Associated With Healthcare-Associated Infections: Annual Summary of Data Reported to the National Healthcare Safety Network at the Centers for Disease Control and Prevention, 2006-2007. *Infection Control and Hospital Epidemiology* 2008, 29, 996-1011.

16. Kohanski, M. A.; DePristo, M. A.; Collins, J. J., Sublethal antibiotic treatment leads to multidrug resistance via radical-induced mutagenesis. *Mol Cell* 2010, 37, 311-20.

17. Turos, E.; Shim, J. Y.; Wang, Y.; Greenhalgh, K.; Reddy, G. S. K.; Dickey, S.; Lim, D. V., Antibiotic-conjugated polyacrylate nanoparticles: New opportunities for development of anti-MRSA agents. *Bioorganic & Medicinal Chemistry Letters* 2007, 17, 53-56.

18. Mohammadi, G.; Valizadeh, H.; Barzegar-Jalali, M.; Lotfipour, F.; Adibkia, K.; Milani, M.; Azhdarzadeh, M.; Kiafar, F.; Nokhodchi, A., Development of Azithromycin-PLGA Nanoparticles: Physicochemical Characterization and Antibacterial Effect Against *Salmonella typhi*. *Colloids Surf B Biointerfaces* 2010, 80, 34-39.

19. Tulu, M.; Aghatabay, N. M.; Senel, M.; Dizman, C.; Parali, T.; Dulger, B., Synthesis, characterization and antimicrobial activity of water soluble dendritic macromolecules. *Eur J Med Chem* 2009, 44, 1093-9.

20. Nederberg, F.; Zhang, Y.; Tan, J. P.; Xu, K.; Wang, H.; Yang, C.; Gao, S.; Guo, X. D.; Fukushima, K.; Li, L.; Hedrick, J. L.; Yang, Y. Y., Biodegradable nanostructures with selective lysis of microbial membranes. *Nat Chem* 2011, 3, 409-14.

21. Liu, L. H.; Xu, K. J.; Wang, H. Y.; Tan, P. K. J.; Fan, W. M.; Venkatraman, S. S.; Li, L. J.; Yang, Y. Y., Self-assembled cationic peptide nanoparticles as an efficient antimicrobial agent. *Nature Nanotechnology* 2009, 4, 457-463.

22. Khan, S. A.; Singh, A. K.; Senapati, D.; Fan, Z.; Ray, P. C., Bio-conjugated popcorn shaped gold nanoparticles for targeted photothermal killing of multiple drug resistant Salmonella DT104. *Journal of Materials Chemistry* 2011, 21, 17705-17709.

23. Zharov, V. P.; Mercer, K. E.; Galitovskaya, E. N.; Smeltzer, M. S., Photothermal nanotherapeutics and nanodiagnostics for selective killing of bacteria targeted with gold nanoparticles. *Biophys J* 2006, 90, 619-27.

24. Gold, H. S.; Moellering, R. C., Jr., Antimicrobial-drug resistance. *N Engl J Med* 1996, 335, 1445-53.

25. Jumbe, N.; Louie, A.; Leary, R.; Liu, W. G.; Deziel, M. R.; Tam, V. H.; Bachhawat, R.; Freeman, C.; Kahn, J. B.; Bush, K.; Dudley, M. N.; Miller, M. H.; Drusano, G. L., Application of a mathematical model to prevent in vivo amplification of antibiotic-resistant bacterial populations during therapy. *Journal of Clinical Investigation* 2003, 112, 275-285.

26. Turos, E.; Reddy, G. S. K.; Greenhalgh, K.; Ramaraju, P.; Abeylath, S. C.; Jang, S.; Dickey, S.; Lim, D. V., Penicillin-bound polyacrylate nanoparticles: Restoring the activity of beta-lactam antibiotics against MRSA. *Bioorganic & Medicinal Chemistry Letters* 2007, 17, 3468-3472.

27. Tang, B. C.; Dawson, M.; Lai, S. K.; Wang, Y. Y.; Suk, J. S.; Yang, M.; Zeitlin, P.; Boyle, M. P.; Fu, J.; Hanes, J., Biodegradable polymer nanoparticles that rapidly penetrate the human mucus barrier. *Proc Natl Acad Sci U S A* 2009, 106, 19268-73.

28. Suk, J. S.; Lai, S. K.; Wang, Y. Y.; Ensign, L. M.; Zeitlin, P. L.; Boyle, M. P.; Hanes, J., The penetration of fresh undiluted sputum expectorated by cystic fibrosis patients by non-adhesive polymer nanoparticles. *Biomaterials* 2009, 30, 2591-7.

29. Kronfol, R.; Downey, K. A., *Technique of incision and drainage for skin abscess*. UpToDate: Waltham, MA, 2012.

30. Han, G.; Martinez, L. R.; Mihu, M. R.; Friedman, A. J.; Friedman, J. M.; Nosanchuk, J. D., Nitric Oxide Releasing Nanoparticles Are Therapeutic for Staphylococcus aureus Abscesses in a Murine Model of Infection. *Plos One* 2009, 4.

31. Fuchs, S.; Pane-Farre, J.; Kohler, C.; Hecker, M.; Engelmann, S., Anaerobic Gene Expression in *Staphylococcus aureus*. *J Bacteriol* 2007, 189, 4275-4289.

32. Simmen, H. P.; Blaser, J., Analysis of pH and pO2 in Abscesses, Peritoneal Fluid, and Drainage Fluid in the Presence or Absence of Bacterial Infection During and After Abdominal Surgery. *Am J Surg* 1993, 166, 24-27.

33. Vermeulen, M.; Giordano, M.; Trevani, A. S.; Sedlik, C.; Gamberale, R.; Fernandez-Calotti, P.; Salamone, G.; Raiden, S.; Sanjurjo, J.; Geffner, J. R., Acidosis Improves Uptake of Antigens and MHC Class I-Restricted Presentation by Dendritic Cells. *J Immunol* 2004, 172, 3196-3204.

34. Pornpattananangkul, D.; Olson, S.; Aryal, S.; Sartor, M.; Huang, C. M.; Vecchio, K.; Zhang, L., Stimuli-responsive liposome fusion mediated by gold nanoparticles. *ACS Nano* 2010, 4, 1935-42.

35. Maurin, M.; Raoult, D., Phagolysosomal alkalinization and intracellular killing of Staphylococcus aureus by amikacin. *J Infect Dis* 1994, 169, 330-6.

36. Kamberi, M.; Tsutsumi, K.; Kotegawa, T.; Kawano, K.; Nakamura, K.; Niki, Y.; Nakano, S., Influences of urinary pH on ciprofloxacin pharmacokinetics in humans and antimicrobial activity in vitro versus those of sparfloxacin. *Antimicrob Agents Chemother* 1999, 43, 525-9.

37. Radovic-Moreno, A. F.; Lu, T. K.; Puscasu, V. A.; Yoon, C. J.; Langer, R.; Farokhzad, O. C., Surface charge-switching polymeric nanoparticles for bacterial cell wall-targeted delivery of antibiotics. *ACS Nano* 2012, 6, 4279-87.

38. Lemaire, S.; Glupczynski, Y.; Duval, V.; Joris, B.; Tulkens, P. M.; Van Bambeke, F., Activities of ceftobiprole and other cephalosporins against extracellular and intracellular (THP-1 macrophages and keratinocytes) forms of methicillin-susceptible and methicillin-resistant Staphylococcus aureus. *Antimicrob Agents Chemother* 2009, 53, 2289-97.

39. Donlan, R., Biofilms: Microbial life on surfaces. *Emerging Infectious Diseases* 2002, 8, 881-890.

40. Hall-Stoodley, L.; Costerton, J. W.; Stoodley, P., Bacterial biofilms: from the natural environment to infectious diseases. *Nat Rev Microbiol* 2004, 2, 95-108.

41. Smith, A. W., Biofilms and antibiotic therapy: Is there a role for combating bacterial resistance by the use of novel drug delivery systems? *Advanced Drug Delivery Reviews* 2005, 57, 1539-1550.

42. Hetrick, E. M.; Shin, J. H.; Paul, H. S.; Schoenfisch, M. H., Anti-biofilm efficacy of nitric oxide-releasing silica nanoparticles. *Biomaterials* 2009, 30, 2782-9.

43. Mahmoudi, M.; Serpooshan, V., Silver-coated engineered magnetic nanoparticles are promising for the success in the fight against antibacterial resistance threat. *ACS Nano* 2012, 6, 2656-64.

44. Subbiandoss, G.; Sharifi, S.; Grijpma, D. W.; Laurent, S.; van der Mei, H. C.; Mahmoudi, M.; Busscher, H. J., Magnetic targeting of surface-modified superparamagnetic iron oxide nanoparticles yields antibacterial efficacy against biofilms of gentamicin-resistant staphylococci. *Acta Biomaterialia* 2012, 8, 2047-2055.

45. Kadam, R. U.; Bergmann, M.; Hurley, M.; Garg, D.; Cacciarini, M.; Swiderska, M. A.; Nativi, C.; Sattler, M.; Smyth, A. R.; Williams, P.; Camara, M.; Stocker, A.; Darbre, T.; Reymond, J. L., A glycopeptide dendrimer inhibitor of the galactose-specific lectin LecA and of Pseudomonas aeruginosa biofilms. *Angew Chem Int Ed Engl* 2011, 50, 10631-5.

46. Sambhy, V.; MacBride, M. M.; Peterson, B. R.; Sen, A., Silver bromide nanoparticle/polymer composites: dual action tunable antimicrobial materials. *J Am Chem Soc* 2006, 128, 9798-808.

47. Paumet, F.; Wesolowski, J.; Garcia-Diaz, A.; Delevoye, C.; Aulner, N.; Shuman, H. A.; Subtil, A.; Rothman, J. E., Intracellular Bacteria Encode Inhibitory SNARE-Like Proteins. *Plos One* 2009, 4.

48. Kaufmann, S. H. E., IMMUNITY TO INTRACELLULAR BACTERIA. *Annual Review of Immunology* 1993, 11, 129-163.

49. Anisimova, Y. V.; Gelperina, S. I.; Peloquin, C. A.; Heifets, L. B., Nanoparticles as antituberculosis drugs carriers: effect on activity against Mycobacterium tuberculosis in human monocyte-derived macrophages. *Journal of Nanoparticle Research* 2000, 2, 165-171.

50. Pandey, R.; Sharma, A.; Zahoor, A.; Sharma, S.; Khuller, G. K.; Prasad, B., Poly (DL-lactide-co-glycolide) nanoparticle-based inhalable sustained drug delivery system for experimental tuberculosis. *J Antimicrob Chemother* 2003, 52, 981-6.

51. Youssef, M.; Fattal, E.; Alonso, M. J.; Roblot-Treupel, L.; Sauzieres, J.; Tancrede, C.; Omnes, A.; Couvreur, P.; Andremont, A., Effectiveness of nanoparticle-bound

ampicillin in the treatment of Listeria monocytogenes infection in athymic nude mice. *Antimicrob Agents Chemother* 1988, 32, 1204-7.

52. Forestier, F.; Gerrier, P.; Chaumard, C.; Quero, A. M.; Couvreur, P.; Labarre, C., Effect of nanoparticle-bound ampicillin on the survival of Listeria monocytogenes in mouse peritoneal macrophages. *J Antimicrob Chemother* 1992, 30, 173-9.

53. Page-Clisson, M. E.; Pinto-Alphandary, H.; Ourevitch, M.; Andremont, A.; Couvreur, P., Development of ciprofloxacin-loaded nanoparticles: physicochemical study of the drug carrier. *J Control Release* 1998, 56, 23-32.

54. Greenhalgh, K.; Turos, E., In vivo studies of polyacrylate nanoparticle emulsions for topical and systemic applications. *Nanomedicine-Nanotechnology Biology and Medicine* 2009, 5, 46-54.

55. Lherm, C.; Muller, R. H.; Puisieux, F.; Couvreur, P., Alkylcyanoacrylate Drug Carriers .2. Cytotoxicity of Cyanoacrylate Nanoparticles with Different Alkyl Chain-Length. *International Journal of Pharmaceutics* 1992, 84, 13-22.

56. Toti, U. S.; Guru, B. R.; Hali, M.; McPharlin, C. M.; Wykes, S. M.; Panyam, J.; Whittum-Hudson, J. A., Targeted delivery of antibiotics to intracellular chlamydial infections using PLGA nanoparticles. *Biomaterials* 2011, 32, 6606-6613.

57. Willing, B. P.; Russell, S. L.; Finlay, B. B., Shifting the balance: antibiotic effects on host-microbiota mutualism. *Nat Rev Microbiol* 2011, 9, 233-43.

58. Maeda, H., Tumor-Selective Delivery of Macromolecular Drugs Via the EPR Effect: Background and Future Prospects. *Bioconjug Chem* 2010, 21, 797-802.

59. Kamaly, N.; Xiao, Z.; Valencia, P. M.; Radovic-Moreno, A. F.; Farokhzad, O. C., Targeted polymeric therapeutic nanoparticles: design, development and clinical translation. *Chem Soc Rev* 2012, 41, 2971-3010.

60. Alexis, F.; Pridgen, E.; Molnar, L. K.; Farokhzad, O. C., Factors affecting the clearance and biodistribution of polymeric nanoparticles. *Molecular Pharmaceutics* 2008, 5, 505-515.

61. Cairns, R.; Papandreou, I.; Denko, N., Overcoming physiologic barriers to cancer treatment by molecularly targeting the tumor microenvironment. *Molecular Cancer Research* 2006, 4, 61-70.

62. Faure, A. C.; Dufort, S.; Josserand, V.; Perriat, P.; Coll, J. L.; Roux, S.; Tillement, O., Control of the in vivo biodistribution of hybrid nanoparticles with different poly(ethylene glycol) coatings. *Small* 2009, 5, 2565-75.

63. Schroeder, A.; Turjeman, K.; Schroeder, J. E.; Leibergall, M.; Barenholz, Y., Using liposomes to target infection and inflammation induced by foreign body injuries or medical implants. *Expert Opin Drug Deliv* 2010, 7, 1175-89.

64. Boerman, O. C.; Oyen, W. J.; van Bloois, L.; Koenders, E. B.; van der Meer, J. W.; Corstens, F. H.; Storm, G., Optimization of technetium-99m-labeled PEG liposomes to image focal infection: effects of particle size and circulation time. *J Nucl Med* 1997, 38, 489-93.

65. Strobel, K.; Hoerr, V.; Schmid, F.; Wachsmuth, L.; Loffler, B.; Faber, C., Early detection of lung inflammation: Exploiting T(1) -effects of iron oxide particles using UTE MRI. *Magn Reson Med* 2012.

66. Lutz, A. M.; Seemayer, C.; Corot, C.; Gay, R. E.; Goepfert, K.; Michel, B. A.; Marincek, B.; Gay, S.; Weishaupt, D., Detection of synovial macrophages in an experimental rabbit model of antigen-induced arthritis: ultrasmall superparamagnetic iron oxide-enhanced MR imaging. *Radiology* 2004, 233, 149-57.

67. Kaim, A. H.; Wischer, T.; O'Reilly, T.; Jundt, G.; Frohlich, J.; von Schulthess, G. K.; Allegrini, P. R., MR imaging with ultrasmall superparamagnetic iron oxide particles in experimental soft-tissue infections in rats. *Radiology* 2002, 225, 808-14.

68. Li, Z.; Lee, D.; Sheng, X. X.; Cohen, R. E.; Rubner, M. F., Two-level antibacterial coating with both release-killing and contact-killing capabilities. *Langmuir* 2006, 22, 9820-9823.

69. Popa, A.; Davidescu, C. M.; Trif, R.; Ilia, G.; Iliescu, S.; Dehelean, G., Study of quaternary 'onium' salts grafted on polymers: antibacterial activity of quaternary phosphonium salts grafted on 4 gel-type' styrene-divinylbenzene copolymers. *Reactive & Functional Polymers* 2003, 55, 151-158.

70. Cen, L.; Neoh, K. G.; Kang, E. T., Surface functionalization technique for conferring antibacterial properties to polymeric and cellulosic surfaces. *Langmuir* 2003, 19, 10295-10303.

71. Kenawy el, R.; Worley, S. D.; Broughton, R., The chemistry and applications of antimicrobial polymers: a state-of-the-art review. *Biomacromolecules* 2007, 8, 1359-84.

72. Lichter, J. A.; Rubner, M. F., Polyelectrolyte multilayers with intrinsic antimicrobial functionality: the importance of mobile polycations. *Langmuir* 2009, 25, 7686-94.

73. Dillen, K.; Bridts, C.; Van der Veken, P.; Cos, P.; Vandervoort, J.; Augustyns, K.; Stevens, W.; Ludwig, A., Adhesion of PLGA or Eudragit/PLGA nanoparticles to Staphylococcus and Pseudomonas. *Int J Pharm* 2008, 349, 234-40.

74. Shai, Y., Mechanism of the binding, insertion and destabilization of phospholipid bilayer membranes by alpha-helical antimicrobial and cell non-selective membrane-lytic peptides. *Biochim Biophys Acta* 1999, 1462, 55-70.

75. Leptihn, S.; Har, J. Y.; Chen, J.; Ho, B.; Wohland, T.; Ding, J. L., Single molecule resolution of the antimicrobial action of quantum dot-labeled sushi peptide on live bacteria. *BMC Biol* 2009, 7, 22.

76. Rotem, S.; Mor, A., Antimicrobial peptide mimics for improved therapeutic properties. *Biochimica Et Biophysica Acta-Biomembranes* 2009, 1788, 1582-1592.

77. Umamaheshwari, R. B.; Jain, N. K., Receptor mediated targeting of lectin conjugated gliadin nanoparticles in the treatment of Helicobacter pylori. *J Drug Target* 2003, 11, 415-23; discussion 423-4.

78. Kell, A. J.; Stewart, G.; Ryan, S.; Peytavi, R.; Boissinot, M.; Huletsky, A.; Bergeron, M. G.; Simard, B., Vancomycin-modified nanoparticles for efficient targeting and preconcentration of Gram-positive and Gram-negative bacteria. *ACS Nano* 2008, 2, 1777-88.

79. Gu, H. W.; Ho, P. L.; Tong, E.; Wang, L.; Xu, B., Presenting vancomycin on nanoparticles to enhance antimicrobial activities. *Nano Letters* 2003, 3, 1261-1263.

80. Jubeli, E.; Moine, L.; Vergnaud-Gauduchon, J.; Barratt, G., E-selectin as a target for drug delivery and molecular imaging. *Journal of Controlled Release* 2012, 158, 194-206.

81. Zhao, X. J.; Hilliard, L. R.; Mechery, S. J.; Wang, Y. P.; Bagwe, R. P.; Jin, S. G.; Tan, W. H., A rapid bioassay for single bacterial cell quantitation using bioconjugated nanoparticles. *Proc Natl Acad Sci U S A* 2004, 101, 15027-15032.

82. Akin, D.; Sturgis, J.; Ragheb, K.; Sherman, D.; Burkholder, K.; Robinson, J. P.; Bhunia, A. K.; Mohammed, S.; Bashir, R., Bacteria-mediated delivery of nanoparticles and cargo into cells. *Nature Nanotechnology* 2007, 2, 441-449.

83. Chen, F.; Zhou, J.; Luo, F. L.; Mohammed, A. B.; Zhang, X. L., Aptamer from whole-bacterium SELEX as new therapeutic reagent against virulent Mycobacterium tuberculosis. *Biochemical and Biophysical Research Communications* 2007, 357, 743-748.

84. Banerjee, M.; Mallick, S.; Paul, A.; Chattopadhyay, A.; Ghosh, S. S., Heightened reactive oxygen species generation in the antimicrobial activity of a three component iodinated chitosan-silver nanoparticle composite. *Langmuir* 2010, 26, 5901-8.

85. Li, P.; Li, J.; Wu, C. Z.; Wu, Q. S., Synergistic antibacterial effects of beta-lactam antibiotic combined with silver nanoparticles. *Nanotechnology* 2005, 16, 1912-1917.

86. Allison, K. R.; Brynildsen, M. P.; Collins, J. J., Metabolite-enabled eradication of bacterial persisters by aminoglycosides. *Nature* 2011, 473, 216-20.

87. Huh, A. J.; Kwon, Y. J., "Nanoantibiotics": A New Paradigm for Treating Infectious Diseases Using Nanomaterials in the Antibiotics Resistant Era. *J Control Release* 2011, 156, 128-145.

88. Mintzer, M. A.; Dane, E. L.; O'Toole, G. A.; Grinstaff, M. W., Exploiting Dendrimer Multivalency To Combat Emerging and Re-Emerging Infectious Diseases. *Molecular Pharmaceutics* 2012, 9, 342-354.

89. Pinto-Alphandary, H.; Andremont, A.; Couvreur, P., Targeted delivery of antibiotics using liposomes and nanoparticles: research and applications. *Int J Antimicrob Agents* 2000, 13, 155-68.

90. Abeylath, S. C.; Turos, E., Nanobiotics to combat bacterial drug resistance. In *Antibiotic resistance: causes and risk factors, mechanisms and alternatives*, Bonilla, A. R.; Muniz, K. P., Eds. Nova Science Publishers: New York, 2009; pp 425-465.

91. Sawant, R. M.; Hurley, J. P.; Salmaso, S.; Kale, A.; Tolcheva, E.; Levchenko, T. S.; Torchilin, V. P., "SMART" drug delivery systems: double-targeted pH-responsive pharmaceutical nanocarriers. *Bioconjug Chem* 2006, 17, 943-9.

92. Walsh, T. J.; Finberg, R. W.; Arndt, C.; Hiemenz, J.; Schwartz, C.; Bodensteiner, D.; Pappas, P.; Seibel, N.; Greenberg, R. N.; Dummer, S.; Schuster, M.; Holcenberg, J. S., Liposomal amphotericin B for empirical therapy in patients with persistent fever and neutropenia. National Institute of Allergy and Infectious Diseases Mycoses Study Group. *N Engl J Med* 1999, 340, 764-71.

93. Fielding, R. M.; Lewis, R. O.; Moon-McDermott, L., Altered tissue distribution and elimination of amikacin encapsulated in unilamellar, low-clearance liposomes (MiKasome (R)). *Pharmaceutical Research* 1998, 15, 1775-1781.

94. Donald, P. R.; Sirgel, F. A.; Venter, A.; Smit, E.; Parkin, D. P.; Van de Wal, B. W.; Mitchison, D. A., The early bactericidal activity of a low-clearance liposomal amikacin in pulmonary tuberculosis. *Journal of Antimicrobial Chemotherapy* 2001, 48, 877-880.

95. Allen, T. M.; Cullis, P. R., Drug delivery systems: entering the mainstream. *Science* 2004, 303, 1818-22.

96. Marambio-Jones, C.; Hoek, E. M. V., A review of the antibacterial effects of silver nanomaterials and potential implications for human health and the environment. *Journal of Nanoparticle Research* 2010, 12, 1531-1551.

97. Raghupathi, K. R.; Koodali, R. T.; Manna, A. C., Size-Dependent Bacterial Growth Inhibition and Mechanism of Antibacterial Activity of Zinc Oxide Nanoparticles. *Langmuir* 2011, 27, 4020-4028.

98. Tsuang, Y.-H.; Sun, J.-S.; Huang, Y.-C.; Lu, C.-H.; Chang, W. H.-S.; Wang, C.-C., Studies of photokilling of bacteria using titanium dioxide nanoparticles. *Artificial Organs* 2008, 32, 167-174.

99. Kim, J. W.; Shashkov, E. V.; Galanzha, E. I.; Kotagiri, N.; Zharov, V. P., Photothermal antimicrobial nanotherapy and nanodiagnostics with self-assembling carbon nanotube clusters. *Lasers Surg Med* 2007, 39, 622-34.

100. Kang, S.; Herzberg, M.; Rodrigues, D. F.; Elimelech, M., Antibacterial effects of carbon nanotubes: Size does matter. *Langmuir* 2008, 24, 6409-6413.

101. Lok, C. N.; Ho, C. M.; Chen, R.; He, Q. Y.; Yu, W. Y.; Sun, H. Z.; Tam, P. K. H.; Chiu, J. F.; Che, C. M., Proteomic analysis of the mode of antibacterial action of silver nanoparticles. *Journal of Proteome Research* 2006, 5, 916-924.

102. Silver, S., Bacterial silver resistance: molecular biology and uses and misuses of silver compounds. *Fems Microbiology Reviews* 2003, 27, 341-353.

103. Pal, S.; Tak, Y. K.; Song, J. M., Does the antibacterial activity of silver nanoparticles depend on the shape of the nanoparticle? A study of the gram-negative bacterium Escherichia coli. *Applied and Environmental Microbiology* 2007, 73, 1712-1720.

104. AshaRani, P. V.; Mun, G. L. K.; Hande, M. P.; Valiyaveettil, S., Cytotoxicity and Genotoxicity of Silver Nanoparticles in Human Cells. *ACS Nano* 2009, 3, 279-290.

105. Rybak, M. J.; Lomaestro, B. M.; Rotschafer, J. C.; Moellering, R. C.; Craig, W. A.; Billeter, M.; Dalovisio, J. R.; Levine, D. P., Vancomycin therapeutic guidelines: a summary of consensus recommendations from the infectious diseases Society of America, the American Society of Health-System Pharmacists, and the Society of Infectious Diseases Pharmacists. *Clin Infect Dis* 2009, 49, 325-7.

106. Mouton, J.; Ambrose, P.; Canton, R.; Drusano, G.; Harbarth, S.; MacGowan, A.; Theuretzbacher, U.; Turnidge, J., Conserving antibiotics for the future: New ways to use old and new drugs from a pharmacokinetic and pharmacodynamic perspective. *Drug Resistance Updates* 2011, 14, 107-117.

107. Cheow, W. S.; Chang, M. W.; Hadinoto, K., Antibacterial efficacy of inhalable levofloxacin-loaded polymeric nanoparticles against E. coli biofilm cells: the effect of antibiotic release profile. *Pharm Res* 2010, 27, 1597-609.

108. Kim, B. S.; Park, S. W.; Hammond, P. T., Hydrogen-bonding layer-by-layer assembled biodegradable polymeric micelles as drug delivery vehicles from surfaces. *ACS Nano* 2008, 2, 386-392.

109. Svenson, S.; Tomalia, D. A., Commentary - Dendrimers in biomedical applications - reflections on the field. *Advanced Drug Delivery Reviews* 2005, 57, 2106-2129.

110. Grayson, S. M.; Frechet, J. M., Convergent dendrons and dendrimers: from synthesis to applications. *Chem Rev* 2001, 101, 3819-68.

111. Kaneshiro, T. L.; Lu, Z.-R., Targeted intracellular codelivery of chemotherapeutics and nucleic acid with a well-defined dendrimer-based nanoglobular carrier. *Biomaterials* 2009, 30, 5660-5666.

112. Joosten, J. A.; Loimaranta, V.; Appeldoorn, C. C.; Haataja, S.; El Maate, F. A.; Liskamp, R. M.; Finne, J.; Pieters, R. J., Inhibition of Streptococcus suis adhesion by dendritic galabiose compounds at low nanomolar concentration. *J Med Chem* 2004, 47, 6499-508.

113. Balogh, L.; Swanson, D. R.; Tomalia, D. A.; Hagnauer, G. L.; McManus, A. T., Dendrimer-silver complexes and nanocomposites as antimicrobial agents. *Nano Letters* 2001, 1, 18-21.

114. Tam, J. P.; Lu, Y. A.; Yang, J. L., Antimicrobial dendrimeric peptides. *European Journal of Biochemistry* 2002, 269, 923-932.

115. Dillen, K.; Bridts, C.; Van der Veken, P.; Cos, P.; Vandervoort, J.; Augustyns, K.; Stevens, W.; Ludwig, A., Adhesion of PLGA or Eudragit/PLGA Nanoparticles to *Staphylococcus* and *Pseudomonas*. *Int J Pharm* 2008, 349, 234-240.

116. Chung, Y. C.; Wang, H. L.; Chen, Y. M.; Li, S. L., Effect of Abiotic Factors on the Antibacterial Activity of Chitosan Against Waterborne Pathogens. *Bioresour Technol* 2003, 88, 179-184.

Chapter 3

Bacteria-Targeting Nanoparticles for Antibiotic Delivery

This chapter has been reproduced in part from: Radovic-Moreno A. F., Lu T. K., Puscasu V. A., Yoon C. J., Langer R., Farokhzad O. C. *ACS Nano* **2012**, *6*, 4279-4287.

3. 1. Introduction

In recent years, advances in the design of nanoparticles (NPs) for drug delivery applications have enabled potential strategies for improving the treatment of a variety of diseases.[1-3] So far, success has been linked to the ability to precisely engineer interactions between NPs and the biologic milieu in ways that may lead to gains in drug potency or properties *in vivo*. Promising methods include: molecular targeting,[4, 5] environmental sensing leading to NP property switching or drug release,[6-8] optimizing NP physicochemical properties,[9, 10] and sustained drug release.[11, 12] Despite these advances, NPs have only really begun to demonstrate their potential in treating infections. Recent reports have demonstrated advances in selective targeting of bacterial membranes for lysis,[13] improved drug delivery,[14, 15] enhanced drug function,[16-18] and the potential for selective accumulation at sites of infection due to increased vascular permeability.[19] In particular, designing methods for improving antibiotic targeting and activity *in vivo*, such as through NP drug carrier design, are important efforts that may: 1) improve treatment outcomes with fewer side effects, 2) reduce the likelihood of drug resistance emerging given that ineffective drug dosing or targeting can lead to the rapid development of drug resistance under inauspicious conditions,[20] and 3) overwhelm drug resistance mechanisms with high sustained local drug concentrations.[3, 21, 22] However, a significant challenge has been designing antibacterial NPs that may be suitable for systemic

administration. A common feature of antibacterial NPs developed to date is a strong, relatively pH-insensitive cationic surface charge which, while demonstrating potent bactericidal activity *in vitro*,[23, 24] is not specific for bacteria and is known in some cases to adversely affect the blood circulation and biodistribution properties of NPs[25] and potentially demonstrating toxicity.[26] The ability to systemically administer antibacterial NP formulations may enable their use in a variety of applications, including examples where infections are disseminated, where local delivery would be overly complicated or impossible, or where other delivery routes or methods are either compromised by disease pathology or ineffective.

Bacteria are highly adaptive organisms that have evolved the ability to thrive in various types of environments. Of these environments, low pH is particularly significant both because of its association with serious infections and its implications for treatment. Certain antibiotics are known to demonstrate significant loss of activity in acidity,[27] and even more troubling, a reduction in localized pH is usually a sequela of worsening disease severity and prognosis – precisely when maximal efficacy is most needed.[28] Bacteria may habitat acidic environments in the body either because acidity is the naturally prevailing condition, such as the stomach (pH 1.0-2.0), intestines (pH 5.0-8.0), vagina (pH 4.0-5.0), bladder (pH 4.5-8.0), and skin (pH 4.0-5.5)[29, 30] or through a combination of bacterial activity and the resulting immune response. Acidity associated with infections occurs through a combination of low oxygen tension triggering anaerobic fermentation in certain bacteria, the products of which are organic acids including lactic, and acetic acids[31] and through inflammation, which is known to exacerbate acidity due to increased levels of acidic products through mechanisms including production of lactic

acid during phagocytosis.[32, 33] Together, these factors are associated with reducing the pH of a site of infection as far as pH 5.5.[34, 35] Examples of clinical indications where pH-dependent loss of drug activity may be relevant include pneumonias, especially in cystic fibrosis (CF) patients,[36, 37] abscesses,[34] and *H. pylori* infections, the major cause of peptic ulcers.[38] Developing systemically available NP drug carriers that can target and improve antibiotic properties in the setting of localized acidity may therefore be a method to improve treatment of these and potentially other infections.

In the present work, we sought to develop a polymeric NP antibiotic carrier that could target the cell walls of bacteria in acidity in order to potentially improve bacterial targeting and antibiotic properties at sites of infections. We chose to target the cell wall because its integrity is vital to bacterial survival, it is the outermost and therefore most accessible layer, and is the site of action of many antibiotics. Important design criteria to achieve effective cell wall targeting NPs are the following. First, a targeting strategy that applies across a range of bacterial classifications is important, since many serious infections are polymicrobial and acidity is not isolated to one particular type of bacterium. For example, 67% of CF patients test positive for *S. aureus* (Gram-positive), and 51% with *P. aeruginosa* (Gram-negative) in their sputum, with co-infection having an additive effect on disease pathology.[39] To achieve this broad NP bacterial targeting, we chose to exploit electrostatic attractions, since many different types of bacteria are known to be negatively charged due to the composition of their cell walls,[40] and this approach has been validated extensively on surfaces,[41] using cationic Eudragit/PLGA[42] or chitosan[23] NPs, as well as by noting that electrostatics, at least partially, underlie the binding mechanism of scores of antimicrobial peptides and cationic peptide-based NPs.[43, 44]

Second, selecting an encapsulation strategy that can be used with a diversity of agents is key, as bacterial drug susceptibility is constantly evolving and new agents are continuously being developed. We selected PLGA as the basis for an encapsulation matrix because it offers the advantages of low toxicity, flexibility in terms of drug payload, ease of synthesis, and the ability to fine tune surface properties through NP engineering.[3] In addition, PLGA has been validated as an effective antibiotic-laden implant or microparticle formulation for antibiotics, and, when formulated into NPs, has demonstrated extended[45, 46] and optimized[11] release kinetics or improved efficacy.[18] Third, the potential to achieve infection-specific targeting through a combination of extended circulation time and low non-specific binding in the blood but avid bacterial binding when located in acidity-associated infections was desirable to improve systemic administration potential. NPs have the potential to target areas of infection due to localized increases in vascular permeability mediated by both the cell-mediated inflammatory response as well as by direct activation of the kinin-kallikrein system by bacterial proteases, though this mechanism has not been deeply investigated in this context.[19] Nevertheless, it is clear that plain PLGA NPs would have a limited ability to exploit this potential targeting mechanism due to their rapid clearance (in seconds to minutes) by the mononuclear phagocytic system.[47] Surface modifying PLGA NPs with PEG is widely known to reduce non-specific interactions, leading to prolonged circulation, but PLGA-PEG NPs alone lack significant bacterial binding ability and therefore would be expected to drain through the (intact) lymphatics at infection sites. We sought to maximize the potential for infection-specific targeting by minimizing nontarget interactions at physiologic pH 7.4 and by using acidity as a trigger to selectively produce

a cationic NP surface for binding. To impart this pH functionality, we incorporated poly-L-histidine, a peptide containing imidazole groups that gain protons under acidic conditions (pKa ~6.0-6.5) into a triblock copolymer structure consisting of poly(D, L-lactic-co-glycolic acid)-*b*-poly(L-histidine)-*b*-poly(ethylene glycol) (PLGA-PLH-PEG), which could be formulated into NPs using emulsion/solvent evaporation techniques. Under acidic conditions, the PLH segment would become positively charged, yielding an overall positive zeta potential on the NP surface, facilitating interactions with the negatively charged elements of bacterial cell wall and producing strong multivalent electrostatic-mediated binding. Finally, it was important to be able to demonstrate efficacy with a clinically significant antibiotic. We chose the glycopeptide antibiotic vancomycin because of its established role in treating serious and life threatening infections, because it loses activity at low pH, because it has a low minimum inhibitory concentration (MIC), and because its targets are components of the cell wall. The results of our studies demonstrate that pH-sensitive, surface charge-switching PLGA-PLH-PEG NPs can be used to bind to bacteria under conditions of acidity. Further, when NPs are used to encapsulate vancomycin, vancomycin demonstrates a higher MIC than free drug but a partial reduction in its loss of activity in acidity as compared to free drug and non-pH sensitive PLGA-PEG delivery systems. This work is a first step towards developing systemically-delivered bacteria-targeting NP drug delivery systems and may have implications for designing improved treatment strategies for various acidity-associated infections.

3. 2. Results and Discussion

3. 2. 1. Design of Surface Charge-Switching PLGA-PLH-PEG NPs. A linear PLGA-PLH-PEG architecture was selected to provide NP characteristics compatible with extended circulation, charge-mediated targeting, and controlled drug release (Figure 3.1). PLGA was used to form the hydrophobic core and drug depot. To decide how to incorporate the PLH in the NPs, we reasoned that by placing the PLH between the PLGA and PEG blocks to yield the linear structure PLGA-PLH-PEG we could achieve the following: 1) the PLGA segment could form a solid core matrix without having the destabilizing force of PLH at acidic pH, since PLLA-PEG / PLH-PEG mixed micelles have been demonstrated to be effective pH-sensitive triggered-release systems.[48, 49] We wanted to retain the slow release characteristics of intact NPs in order to reduce complexity in processing and use, potentially achieve a larger area-under-the-curve (AUC) at the site of infection, and be able tailor drug-bacterium interactions using NPs. 2) PLH would be preferentially placed near the NP surface as the polymer self-assembled, due to its intrinsic hydrophilicity under typical formulation conditions as well as its close association with the PEG, which would preferentially rise to the surface due to its relative hydrophilicity. This is significant in that it would increase the magnitude of the surface charge switching capability, as the cationic charge of the PLH at acidic pH would be closer to the NP surface. 3) Having the PEG portion at the distal end of the polymer would facilitate NP colloidal stability and circulation time at physiologic pH, as has been reported in the literature.[47] The polymer was synthesized using an block end-grafting strategy (see Materials and Methods).

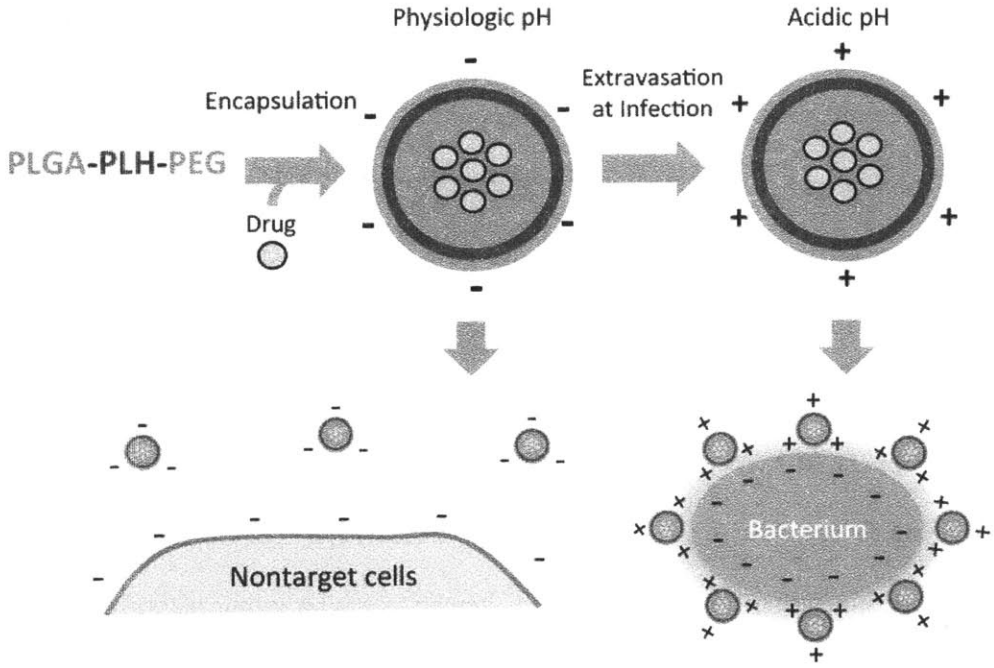

Figure 3. 1. Schematic representation of the designed nanoparticle (NP)-mediated drug targeting to bacterial cell walls. Drugs are encapsulated into NPs using a double emulsion/solvent evaporation process. The NPs avoid uptake or binding to nontarget cells or blood components at physiologic pH 7.4 due to a slight negative charge and surface PEGylation. Inflammation at a site of infection causes increased local vascular permeability, promoting NP extravasation. The weakly acidic conditions at sites of certain infections activate the surface charge-switching mechanism, resulting in NP binding to negatively charged bacteria. Finally, controlled release of the encapsulated drug leads to antibacterial effect.

3. 2. 2. NP Formulation and pH-Dependent Characterization. Understanding the physicochemical properties of PLGA-PLH-PEG NPs as a function of pH was key to tailoring NP-bacterium interactions. To evaluate these properties, we formulated PLGA-PLH-PEG and PLGA-PEG polymers into nanoparticles using a modified double emulsion/solvent evaporation method.[50] The NPs were purified by triple ultrafiltration, resuspended in appropriate pH-buffered PBS solutions ranging from pH 5.5 to pH 7.4, and characterized in terms of their physicochemical properties by quasi-elastic laser light scattering. The results show that the PLGA-PLH-PEG NPs switched their surface charge

from a negative zeta potential at pH 7.4 (ζ = -3.9±0.4 mV, N=3) to a positive one with reduction in pH, with the transition occurring as early as pH 7.0 (ζ = 2.3±1.0, N=3) (Figure 3.2A) and a linear slope of -8.6 mV/pH unit (R^2 = 0.951). In contrast, PLGA-PEG diblock copolymer had a negative zeta potential at every pH tested (At pH 7.4, PLGA-PEG ζ = -36.5±0.5 mV, N=3) and demonstrated little pH sensitivity, with a slope of -2.9 mV/pH unit (R^2 = 0.447). The lower R^2 reflects the observation that subtle changes only occurred at a very low pH of 5.5. The negative charge of both polymers at pH 7.4 is likely a result of residual negative charge from acid groups in the PLGA-COOH precursor, partially hydrolyzed PLGA chains, and from carbonyl groups in the PLGA block. The more positive zeta potential of the PLGA-PLH-PEG relative to PLGA-PEG is likely due to the presence of the neutrally charged PLH block near the surface. The gain in charge with reduction in pH is due to the exponentially increasing presence of positive charges from the imidazole group of the PLH with reductions in pH, as described by the Henderson-Hasselbalch equation. Both PLGA-PLH-PEG (mean size = 196.0±7.8 nm, N=3) and PLGA-PEG (mean size = 222.1±1.8 nm, N=3) NPs did not demonstrate large differences in size with decreasing pH (Figure 3.2B). In addition, transmission electron microscopy (TEM) suggests that the PLGA-PLH-PEG NPs retained their integrity at acidic pH values (Figure 3.2C), in contrast to reports of PLLA-PEG / PLH-PEG mixed micelles.[49]

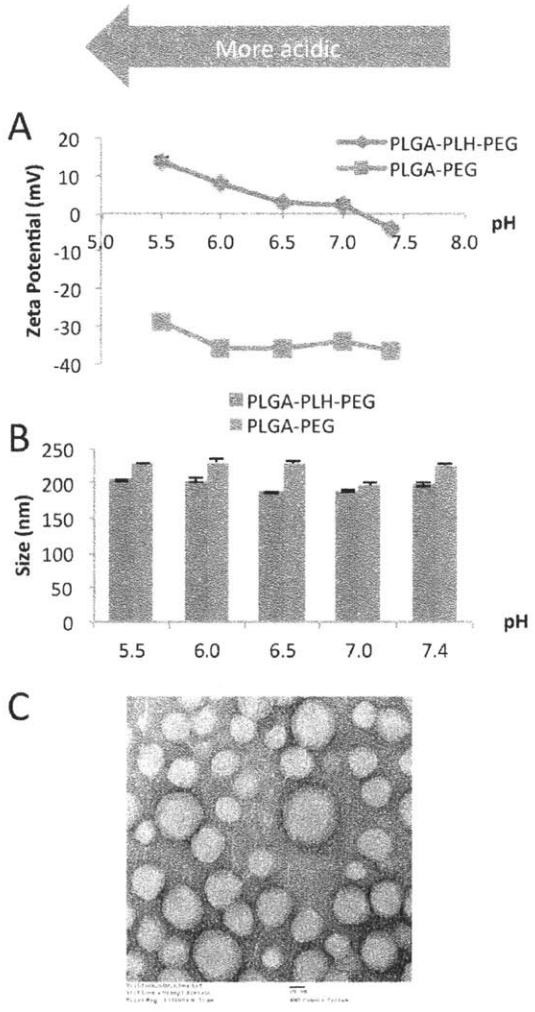

Figure 3. 2. Physicochemical characterization of NPs. (A) NP zeta potential vs. pH demonstrates notable switching from anionic to cationic with decreases in pH in PLGA-PLH-PEG but not PLGA-PEG NPs. (B) NP size vs. pH. (C) Transmission electron micrograph (TEM) of PLGA-PLH-PEG NPs. Scale bar 20 nm. N=3 for all observations.

3. 2. 3. pH-Dependent Binding of NPs to Bacteria. We then evaluated whether the observed changes in NP physicochemical properties with pH would enable binding to bacteria under acidic conditions. As model organisms of two major subtypes of bacteria, we selected the Gram-negative *Escherichia coli* (*E. coli*) and Gram-positive *Staphylococcus aureus* (*S. aureus*). We initially evaluated to what extent PLGA-PLH-

PEG NPs could bind to these bacteria as a function of pH by labeling NPs using Alexa-488 to form green fluorescent NP-488 (modified with Alexa-488 PLGA, see Materials and Methods section) and incubating them with the different bacteria for 30 min in pH-adjusted PBS solutions from pH 5.5 to 7.4 at 37°C. PLGA-PEG NP-488 were used as a non-pH-sensitive control. Following binding, the NP-488-bacteria aggregates and/or bacteria were centrifuged and washed, resuspended in PBS pH 7.4, and run on a flow cytometer to evaluate their fluorescence levels. In the case of both bacteria, a large and significant ($p < 0.05$) increase in binding was observed as pH was decreased < pH 6.5 (Figure 3.3A, 3.3B). The increase in binding to both *S. aureus* and *E. coli* became very pronounced at pH 6.0 (*S. aureus* PLGA-PLH-PEG 3.5±0.2; *E. coli* 5.8±0.1, all N=3) as compared to PLGA-PEG (*S. aureus* 1.0±0.1; *E. coli* 1.1±0.1, all N=3) and peaked at pH 5.5. Given that NP residence time at a site of infection may be limited, we wished to determine how quickly NPs bound to bacteria under acidic conditions. We performed a kinetic study of PLGA-PLH-PEG NPs to both types of bacteria at pH 6.0, selecting incubation time points between 10 min and 4 hours and measuring bacteria-associated fluorescence using flow cytometry. We observed rapid saturation of fluorescence, with ~80% of maximal binding occurring within 10 minutes for both *E. coli* (Figure 3.3C) and *S. aureus* (Figure 3.3D). This binding kinetics data suggests that even a relatively short residence time at an acidic site of infection might be sufficient to enable binding to bacteria using PLGA-PLH-PEG NPs. To provide visual confirmation of PLGA-PLH-PEG NP binding to bacteria, we used fluorescence confocal microscopy. PLGA-PLH-PEG NP-488 were freshly prepared, purified, and resuspended in pH 6.0 or pH 7.4 PBS solutions. *S. aureus* bacteria were prepared as before and inoculated into the PLGA-PLH-

PEG NP-488-containing solutions. We selected *S. aureus* as a model bacterium for the confocal studies due to our observation of the slightly more positive but still anionic charge of these bacteria as compared to *E. coli*, which would therefore yield a more conservative confirmation of our flow cytometry-based results. The NP-488/bacteria suspension was placed in an incubated shaker at 37°C for 30 min to allow NP-488 binding to bacteria. After washing unbound NP-488s by centrifugation with repeated PBS pH 7.4 buffer washes, bacteria were stained using *Bac*Light™ Red, a commercially available small molecule that binds to bacteria, according to manufacturer instructions. Confocal microscopy visually confirmed the pH-sensitive nature of PLGA-PLH-PEG NP-488 binding to bacteria (Figure 3.4). Close inspection (Figure 3.4E, 3.4F) demonstrates that strong fluorescence can be seen at the bacterial cell wall in the pH 6.0 NP-488 treated but not pH 7.4 NP-488 treated group. No NP-488 fluorescence can be observed in the interior of the bacteria, suggesting that PLGA-PLH-PEG NPs are unable to penetrate the cell wall, which was expected given the formidable diffusion barriers presented. In addition, after pH 6.0 NP-488 treatment, one can observe that the NP-488s have triggered agglutination of bacteria into larger aggregates as compared to what is observed with pH 7.4 NP-488 bacteria. This may be due to the positively charged NP-488s bridging two negatively charged bacteria together in the pH 6.0 NP-488 but not pH 7.4 NP-488 group.

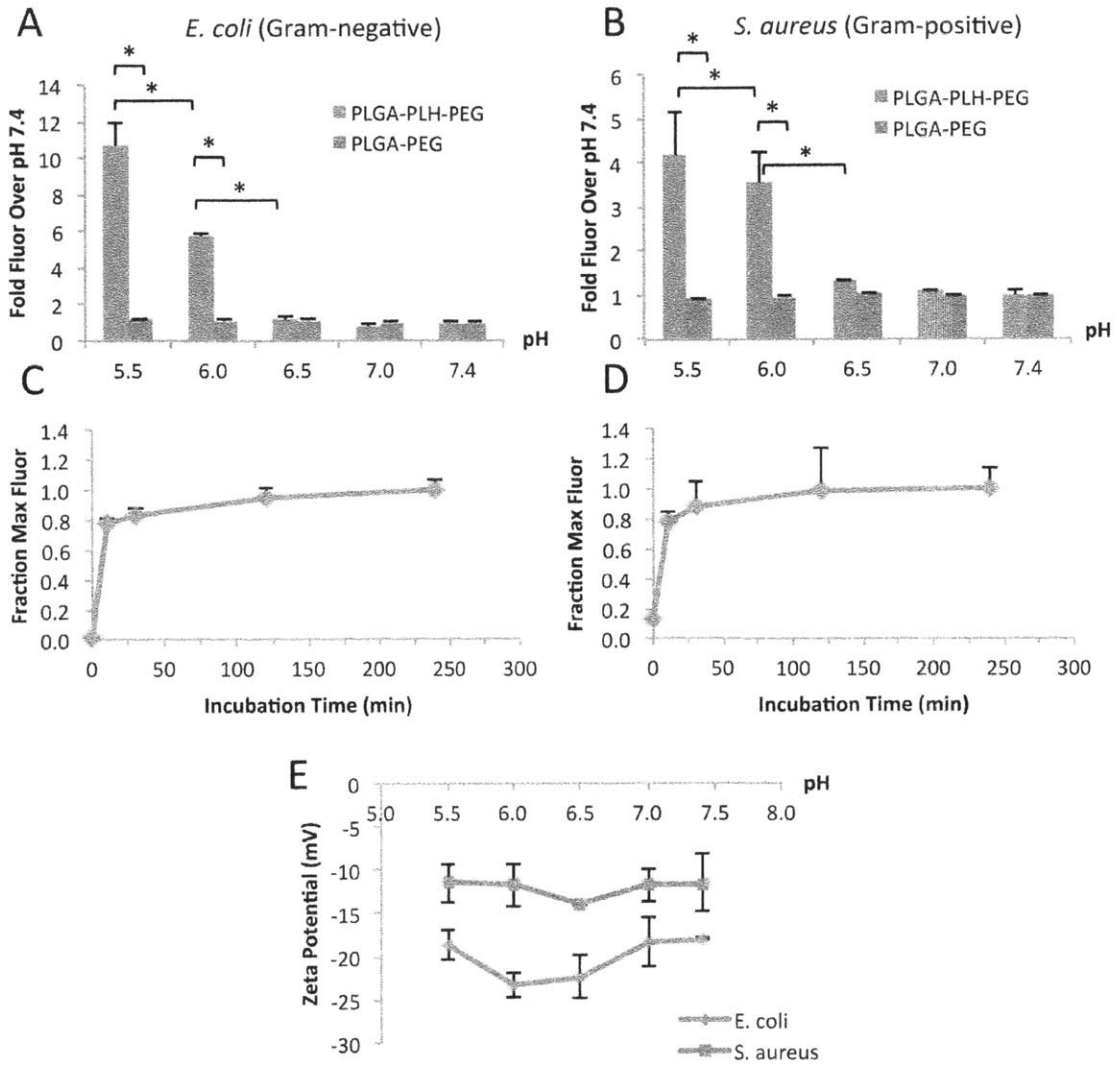

Figure 3. 3. NPs binding to representative bacteria. Alexa-488 labeled PLGA-PLH-PEG or PLGA-PEG NPs were incubated with (A) *E. coli* or (B) *S. aureus* in PBS at different pH levels ranging from 5.5 to 7.4; binding was assessed by flow cytometry and expressed as fold mean fluorescence over pH 7.4. (C) *E. coli* and (D) *S. aureus* binding kinetics studies at pH 6.0 show that bacterial binding occurs rapidly. (E) Zeta potential of bacteria with changes in pH. (* indicates $p < 0.05$). N=3 for all observations except in E, where N=2.

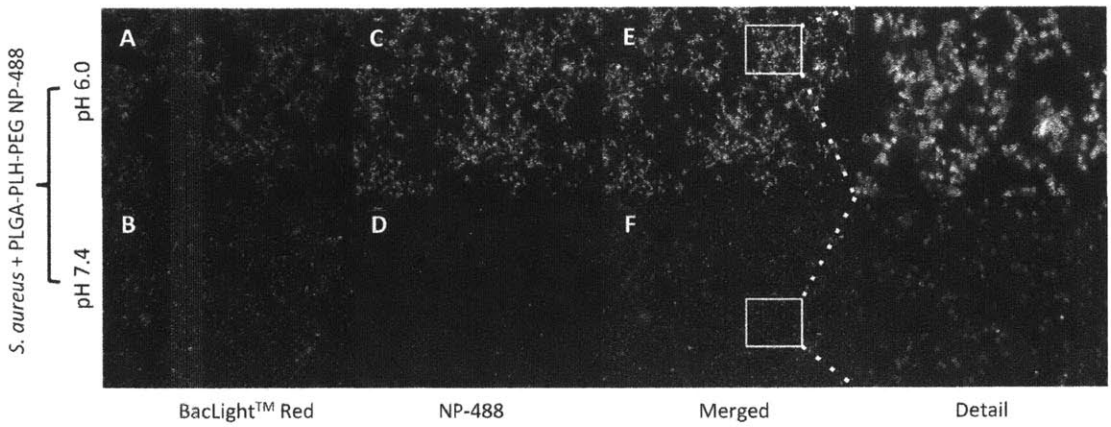

Figure 3. 4. Fluorescent confocal microscopy of pH-dependent binding. *S. aureus* bacteria labeled with *Bac*Light™ Red were treated with Alexa-488 labeled PLGA-PLH-PEG NP-488 at pH 6.0 (panels A, C, E) or pH 7.4 (panels B, D, F). (A, B) *Bac*Light™ Red (C, D) NP-488 (E, F) Merge of *Bac*Light™ Red and NP-488, with yellow indicating co-localization. The white box in E, F demonstrates a detail of the merged image, showing the bacterial cell wall-associated NP-488 at pH 6.0 but not pH 7.4.

3. 2. 4. Antimicrobial Studies. Finally, we were interested in seeing whether PLGA-PLH-PEG NP binding to the bacterial surface had an impact on antibiotic efficacy, and how this compared to PLGA-PEG NP and free drug formulations. As a proof-of-concept, we chose to examine *S. aureus* susceptibility to formulations of vancomycin, a glycopeptide antibiotic used clinically to treat infections involving *S. aureus*, particularly drug resistant strains. Vancomycin was encapsulated in NPs, washed, and resuspended in pH 6.0 or pH 7.4 PBS. Encapsulation efficiency PLGA-PLH-PEG (42.2±8.1%, N=3), PLGA-PEG (39.2±1.4%, N=3) and drug loading PLGA-PLH-PEG (7.8±1.6%, N=3), PLGA-PEG (7.3±0.3%, N=3) were evaluated. The minimum inhibitory concentration (MIC) of PLGA-PLH-PEG NP formulated vancomycin (PLGA-PLH-PEG[Vanco]), PLGA-PEG NP formulated vancomycin (PLGA-PEG[Vanco]), and free vancomycin were determined using the microplate dilution method at pH 6.0 or pH 7.4 (Figure 3.5). The minimum bactericidal concentrations were determined semi-quantitatively by

subculturing to antibiotic-free TSB agar plates. For the NP formulations of vancomycin, the vancomycin concentration is reported as the total concentration of vancomycin in the NP at the beginning of treatment. Vancomycin is released from the NP at a steady rate over a 50 hour period (Figure 3.5), which is consistent with many studies of drug release from NPs. We reasoned that the initial vancomycin concentration inside the NPs was both the most conservative and useful measure of NP antibiotic formulation efficacy. The results show (Figure 3.6, Table 3.1) that at pH 7.4, free vancomycin is the most potent formulation of the drug (MIC 1.2±0.6 ug/mL, MBC 3.1 ug/mL, N=3), but that this is strongly pH sensitive. At pH 6.0, free vancomycin loses potency by a factor of 2.0, consistent with other observations[27] (Figure 3.6). PLGA-PEG NP vancomycin formulations required higher initial vancomycin concentration than free drug to achieve antibacterial effects at physiologic pH 7.4 (MIC 6.0±0.7 ug/mL, MBC 20. ug/mL, N=4), and similarly demonstrated significant pH sensitive loss in activity by a factor of 2.3 (MIC 14.2±1.9 ug/mL, MBC 40. ug/mL, N=4). As expected, PLGA-PLH-PEG NP formulations of vancomycin behaved similar to PLGA-PEG NP formulations at pH 7.4 (MIC 6.8±2.1 ug/mL, MBC 20. ug/mL, N=4, p=0.54) but had significantly improved activity at pH 6.0, demonstrating less loss in activity with pH, by a factor of 1.3 (MIC 8.6±0.5 ug/mL, MBC 20. ug/mL, N=4, $p < 0.05$) (Figure 3.6). Further, this suggests that promoting NP-bacterium interactions under acidic conditions, such as was demonstrated, can partially mitigate the loss of activity with pH, further highlighting the potential of this delivery system for treating infections associated with localized acidity.

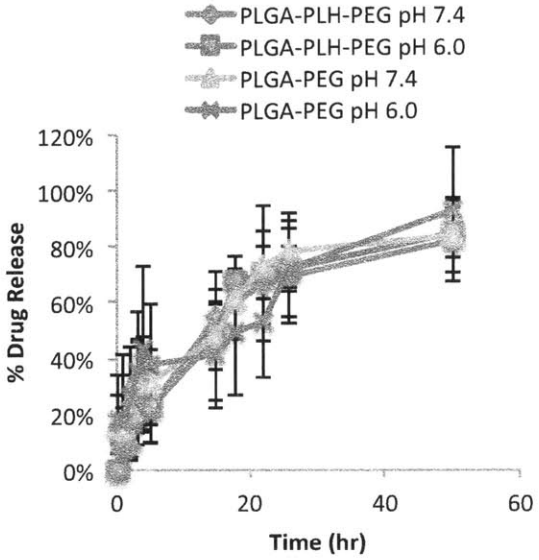

Figure 3. 5. Release of vancomycin from PLGA-PEG and PLGA-PLH-PEG NPs as a function of pH. Drug release curves demonstrate no significant difference in vancomycin release between release curves from PLGA-PEG and PLGA-PLH_{30}-PEG NPs. Drug release study performed in 4 mL pH-adjusted 1x PBS solutions at 37°C.

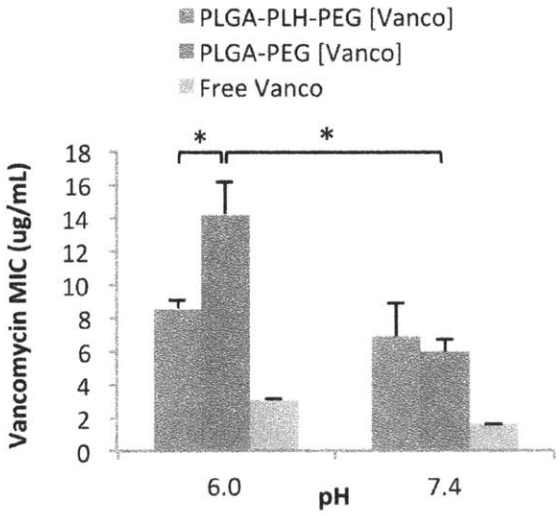

Figure 3. 6. NP-mediated vancomycin delivery to *S. aureus*. Minimum inhibitory concentrations (MIC) determined from microplate broth dilution assays at pH 6.0 or 7.4, demonstrating loss of drug activity in PLGA-PEG[Vanco] and free vancomycin but not PLGA-PLH-PEG[Vanco]. (* indicates $p < 0.05$).

Table 3. 1. Minimum bactericidal concentration (MBC) at pH 6.0 and pH 7.4 in *S. aureus*.

		Minimum Bactericidal Concentration (MBC)	
Treatment	**pH**	**[NP] (ug/mL)**	**[Vanco] (ug/mL)**
PLGA-PLH-PEG [Vanco]	6.0	250	20
PLGA-PLH-PEG [Vanco]	7.4	250	20
PLGA-PEG [Vanco]	6.0	500	40
PLGA-PEG [Vanco]	7.4	250	20
Free Vanco	6.0	N/A	6
Free Vanco	7.4	N/A	3
PLGA-PLH-PEG	6.0	> 500	N/A
PLGA-PLH-PEG	7.4	> 500	N/A
PLGA-PEG	6.0	> 500	N/A
PLGA-PEG	7.4	> 500	N/A

3. 2. 5. Binding inhibition study. To further explore the potential mechanism of binding to bacteria, we performed an inhibition study where we prepared the PLGA-PLH-PEG NPs as before, but incubated them in an excess of sodium polystyrene sulfonate solution (PSS) for ~30 min. This negatively charged polymer rendered the NPs anionic. We then incubated the PLGA-PLH-PEG NPs or the PLGA-PLH-PEG NPs + PSS with *S. aureus* bacteria for 30 min, washed, then ran on a flow cytometer. The data show that the PSS inhibited the binding of the PLGA-PLH-PEG NPs, suggesting that elimination of the charge using this anionic polymer blocks binding to bacteria (Figure 3.7).

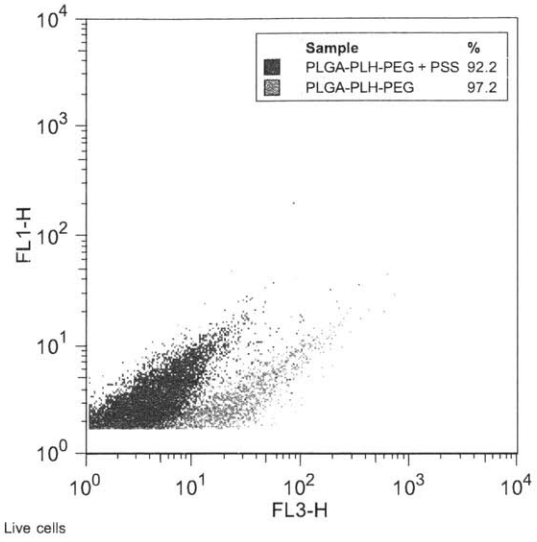

Figure 3. 7. Competition Study using Sodium Polystyrene Sulfonate (PSS). PLGA-PLH-PEG NPs were assayed for their binding to *S. aureus* bacteria either as is (red) or following a brief incubation with PSS polymer. The data suggest inhibition of binding to bacteria by preincubation with the PSS polymer. NPs were labeled with Alexa-647 and measured in the FL3-H channel (x-axis), with data in the FL1-H channel (y-axis) as a control for autofluorescence.

3. 2. 6. Summary. We have developed a pH-responsive, surface charge-switching polymeric nanoparticle drug delivery system for targeting bacterial cell walls at sites of acidic infections. We demonstrate that pH-sensitive PLGA-PLH-PEG NPs rapidly (~80% of maximum within 10 min) bind to both Gram-positive (*S. aureus*) and Gram-negative (*E. coli*) organisms under acidic conditions and that increased binding can be correlated to sharp increases in NP zeta potential with reductions in pH. Further, we demonstrate that vancomycin encapsulated in PLGA-PLH-PEG NPs demonstrates a 1.3-fold pH-dependent increase in MIC against *S. aureus*, an improvement over free vancomycin and PLGA-PEG vancomycin, which demonstrate 2.0 and 2.3 fold increase at pH 6.0, respectively. The proof-of-concept *in vitro* studies described in this work may – pending the results of further extensive *in vitro* and *in vivo* evaluation – be applied to an array of

clinical conditions in which systemic delivery approaches are desirable, where localized acidity occurs, and where antibiotic efficacy is affected by acidity, potentially suggesting methods of improving drug targeting and efficacy in these infections. Future work in this area should first explore to what extent bacterial cell wall targeting using a surface charge-switching mechanism can lead to both prolonged circulation and effective targeting as compared to untargeted NPs and free drugs *in vivo*. The pH-sensitive, surface-charge switching PLGA-PLH-PEG NPs, while potentially improving the binding specificity for bacterial cell walls as compared to pH-insensitive cationic NPs delivered systemically, still use non-specific charge-charge interactions to mediate binding locally at the site of infection. Therefore, exploring to what extent competition between bacteria, negatively charged proteins, phagocytic and non-phagocytic tissue cells at a site of infection for the charged NPs affects bacterial targeting will be important. Future studies should also: 1) compare the efficacy of antibiotics delivered using these groups *in vivo,* 2) investigate methods of improving the potency of NP-vancomycin formulations, and 3) explore the growth inhibition potential in Gram-negative infections.

3. 2. 7. Henderson-Hasselbalch Equation

We can continue understanding the underpinnings of charge-mediated targeting based on a simplified pH-sensitivity analysis using the Henderson-Hasselbalch equation (Equation 3.1).

(Equation 3.1) $$pH = pKa + log\frac{A}{HA}$$

This equation is derived from acid-base chemical equilibria; its principles are covered in most basic chemistry textbooks. As a brief reminder, its main assumptions include constant ratio of activity coefficients of the different species, attainment of chemical

equilibrium, and constant concentration of water, all of which are reasonable approximations in this case. The fraction of poly-L-histidine (PLH) that is charged is given by rearranging Equation 3.1:

(Equation 3.2) $$\frac{HA}{HA+A} = \frac{10^{pKa-pH}}{10^{pKa-pH}+1}$$

In this case, "HA" is the protonated species and "A" is the unprotonated imidazole. estimating the pKa with high precision is quite complex, as the protonable imidazole group is surrounded by a highly complex environment with PLGA, PLH, and PEG chains in a supramolecular NP structure. The pKa of the imidazole side chain of L-histidine is widely cited in textbooks to be ~6.0. Using this as a starting point in Equation 3.2, one can plot Equation 2 and perform a sensitivity analysis with different assumed pKa values in the range of 5.8-6.2 (Figure 3.8).

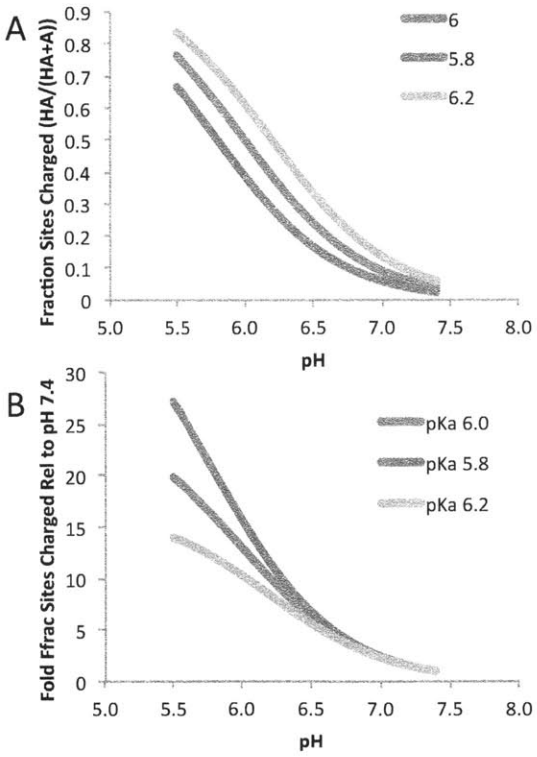

Figure 3.8. Henderson-Hasselbalch Analysis. (A) The fraction of sites on a model species of pKa 5.8, 6.0, 6.2 that are charged as a function of the pH, plotted using Equation 3.2 in the specified range. (B) Plotting the fold increase in charged sites relative to pH 7.4 on the basis of Equation 3.2.

The plot yields a notable increase in the amount of charged species as the pH is declined from 7.4. For example, at a pKa of 6.0, as the pH declines from pH 7.4 to 6.0, the fraction of the charged species increases from 3.8% to 50% (or equivalently, an increase in the ratio of charged:uncharged from 1:25 to 1:1). These exponential changes in the fraction of charged sites correlate well with the observed changes in the NP zeta potential (Figure 3.2A), which show a change in the zeta potential from -3.9±0.4 at pH 7.4 to 8.2±0.4 at pH 6.0, and also with the increase in binding to bacteria (Figure 3.3, 3.4). A pH titration of the NP binding (Figure 3.3) shows that there is little bacteria-associated fluorescence until pH 6.0, which suggests that there is a charge threshold that is reached between pH 6.0 and pH 6.5. Assuming a pKa of 6.0, there is roughly a doubling of the amount of charge as the pH is declined from pH 6.5 to 6.0 (0.24 to 0.50). While this may appear modest given the increase in binding that is observed in this region, the data suggest that this doubling had the measurable effect of increasing the NP zeta potential to past a threshold value (greater than 2.8 mV, based on the relatively low binding at pH 6.5), enabling more efficient binding to bacteria. The pH-sensitivity observed by the PLH-containing NPs in this thesis is bounded by previous reports involving PLH-containing materials. For example, a pH-sensitive micelle for tumor extracellular pH targeting using a blend of poly(L-lactic acid)-*block*-poly(ethylene glycol)-*block*-poly(L-histidine)-TAT and poly(L-histidine)-*block*-poly(ethylene glycol) demonstrated remarkable pH sensitivity, with a 30-fold increase in uptake at pH 7.0 relative to pH 7.4, likely mediated by an increase in presentation of the cell-penetrating TAT peptide.[51] Further, by dropping

the pH to 6.8, the authors found an increase of 70-fold was achieved. This dramatic pH sensitivity occurred even with the majority of the protonable groups on the poly(L-histidine) uncharged. Other pH-sensitive systems employing PLH have shown notable changes in properties with declining pH. pH-sensitive polymeric mixed micelles of poly(L-histidine) and poly(L-lactic acid) block copolymers with poly(ethylene glycol) with or without folate are another example.[48] These systems demonstrated accelerated release of adriamycin as the pH declined from 8.0 to 6.8, and lost their structural stability in the region 7.2 to 6.6. Similarly, a system using poly(L-lactic acid)-*block*-poly(ethylene glycol)-*block*-poly(L-histidine) was reported to be useful as a triggered drug release system in the range pH 7.2-6.5.[52] It appears that the changes in the properties of the poly(L-histidine) material as a function of pH can lead to a wide variety of different behaviors with changes occurring in the range of 6.0-7.2.

3. 3. Materials and Methods

3. 3. 1. Polymer Synthesis and Characterization. We synthesized the triblock copolymer poly(D, L-lactic-co-glycolic acid)-*b*-poly(L-histidine)-*b*-poly(ethylene glycol) (PLGA-PLH-PEG) using a polymer end grafting strategy. In brief, PLH was custom synthesized to contain 20 or 30 repeats of L-histidine with an N-terminal lysine and a C-terminal cysteine to facilitate conjugation reactions. First, PLH-SH and orthopyridyl disulfide (OPSS) modified PEG blocks were reacted to form a diblock copolymer using thiol-to-orthopyridyldisulfide chemistry and purified by dialysis and lyophilization. The PLGA was conjugated to the NH_2-PLH-PEG diblock copolymer using EDC/NHS

carbodiimide chemistry and purified by precipitation. The reaction products and intermediates were characterized by MALDI-TOF, GPC, and ^{1}H-NMR.

More specifically, Poly(D, L-lactide-co-glycolide)-*b*-poly(L-histidine)-*b*-poly(ethylene glycol) (PLGA-PLH-PEG) was synthesized using a sequential end-grafting process. First, the poly(L-histidine)-*b*-poly(ethylene glycol) (PLH-PEG) diblock copolymer was formed as demonstrated in "Rxn A" of Scheme S1. PLH is a 22 or 32-mer peptide synthesized and purified by HPLC by GenScript (Piscataway, NJ) with the following sequence, from N- to C-terminus: Lys-$(His)_{20}$-Cys or Lys-$(His)_{30}$-Cys. 0.0128 mmol of this reactant was dissolved in 1 mL water and pH adjusted to pH 6.5 using 0.5 M NaOH dropwise. 0.0282 mmol of mPEG-OPSS polymer obtained from Laysan Bio (MW 5000, Arab, AL) was dissolved in 3 mL DMSO. The two reactants were mixed together at room temperature for 24 hours to yield a yellowish white solution of the PLH-PEG diblock copolymer (product **1**, Scheme S1). The product was purified by dialyzing against pure water using 2,000 MWCO Slide-A-Lyzer G2 dialysis membranes (Thermo Scientific, Billerica, MA) followed by lyophilization for 48 hours. 0.0222 mmol of PLGA-COOH (inherent viscosity 0.67, LACTEL, Cupertino, CA) was dissolved in 2 mL dichloromethane and reacted with 0.9160 mmol 1-ethyl-3-(3-dimethylaminopropyl)carbodiimide (EDC) and 1.1025 mmol of N-hydroxysuccinimide (NHS) for 4 hours at room temperature while stirring (Rxn B, Scheme S1). The resulting activated PLGA-NHS ester was precipitated twice in ~ -20°C anhydrous methanol. The PLGA-NHS ester was dried *in vacuo* for 2 hours then dissolved in 3 mL of DMSO. 10 umol of PLGA-NHS in DMSO were reacted with 14.6 umol of PLH-PEG dissolved in 1 mL of DMSO. To this reaction mixture, 115 umol of N,N-diisopropylethylamine (DIEA) were added and the reaction was allowed to

proceed overnight at room temperature. The resulting crude triblock copolymer product was precipitated in a ~ -20°C 50/50 v/v mixture of methanol/diethyl ether, redissolved in DMSO, then precipitated again to produce a white polymer product. This product was dried *in vacuo* for at least 4 hours. The final purified product **2** was collected as a yellowish white brittle solid at a mass yield varying between 50-99%. The reaction products and intermediates were characterized using MALDI-TOF, ^{1}H-NMR, and gel permeation chromatography (GPC). PLGA-PEG was synthesized similarly using the same starting materials and excess reactants, with the key difference being that the PLGA-NHS was reacted with mPEG-NH_2 (MW 5,000, Laysan Bio, Arab, AL) in dichloromethane.

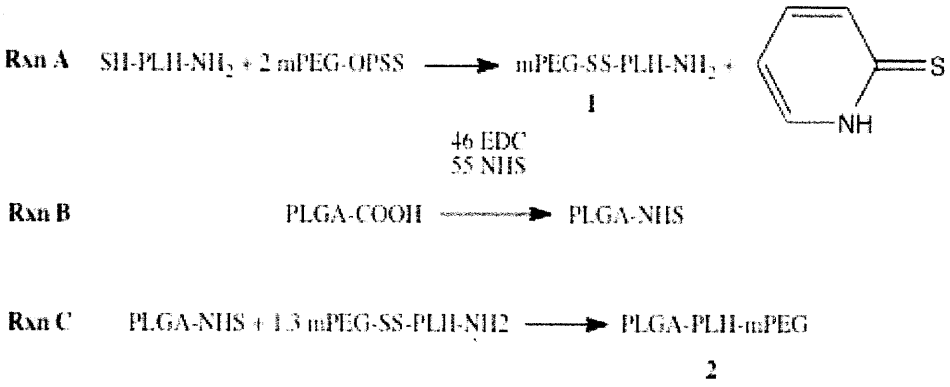

Figure 3. 9. Synthesis procedure for forming the PLGA-PLH-PEG copolymer. A three step, end-grafting strategy was employed to form the desired PLGA-PLH-PEG **2** copolymer. (Rxn A) Reacting the C-terminal Cys of the PLH block with the orthopyridyldisulfide-modified end group of PEG to form the PLH-PEG **1** diblock copolymer. (Rxn B) Activating the PLGA-COOH using 1-ethyl-3-(3-dimethylaminopropyl)carbodiimide (EDC) and N-hydroxysuccinimide (NHS). (Rxn C) Conjugating the PLGA-NHS and PEG-PLH polymers using the N-terminal Lys to form the final product **2**.

MALDI-TOF (Voyager-DE STR, JBI Scientific, Huntsville, TX) was used to confirm the conjugation of the PLH and PEG blocks using sinapinic acid to form the matrix and using

a 1-15 kDa acquisition mass range. A typical MALDI-TOF spectrum included PEG Mz = 5,315; PLH Mz 2,867; PEG-PLH Mz = 8,169. ^{1}H-NMR (400 MHz, Bruker, Billerica, MA) was used to detect the presence of the different polymer blocks at the various reaction steps. The ^{1}H-NMR spectrum of the final triblock copolymer product PLGA-PLH-PEG demonstrates peaks corresponding to the three different copolymer blocks. Proton shifts in DMSO-d_6 (ppm): 7.6 b (imidazole ring *H*, PLH), 6.8 b (imidazole ring *H*, PLH), 5.2 b (-C*H*- LA unit, PLGA), 4.9 b (-CH_2-, GA unit, PLGA), 4.4 b (α-carbon -C*H*-, PLH), 3.5 s (OCH_2CH_2, PEG), 3.0 b (-CH_2- PLH), 1.5 b (-CH_3 of LA unit, PLGA). GPC was used to measure the molecular weight of the triblock PLGA-PLH-PEG (DMF mobile phase), Mz ~ 88,000 relative to PMMA standards for all PLGA-PLH-PEG polymers.

3. 3. 2. NP Formulation. NPs were formulated (PLGA-PLH-PEG or PLGA-PEG in the same manner) using modified emulsion/solvent evaporation techniques (see SI for details). In brief, a typical vancomycin-containing NP formulation was prepared by sonicating 50 uL of a 4 g/L solution of vancomycin hydrochloride (Sigma Aldrich, St. Louis, MO) into 500 uL ethyl acetate containing 2 g/L polymer. This primary emulsion was sonicated into 2 mL 10% w/v NaCl solution to form the W/O/W double emulsion, diluted into 8 mL 5% w/v NaCl, and solvent allowed to evaporate for 4 hours prior to purification using ultrafiltration. To form green fluorescent NPs, Alexa-488-modified PLGA was blended into the organic phase at 15% w/w total polymer and no salt or vancomycin were used in the emulsion process.

More specifically, to form vancomycin-encapsulated NPs, 1 mg of polymer (PLGA-PLH-PEG or PLGA-PEG) dissolved in 15/85 v/v DMSO/ethyl acetate solution was diluted into a final volume of 500 uL of ethyl acetate (with trace DMSO) to form the organic

phase. The drug-containing aqueous phase would typically consist of 50 uL of a 4 g/L solution of vancomycin hydrochloride (Sigma Aldrich, St. Louis, MO) dissolved in pure water. The aqueous phase was sonicated into the polymer-containing organic phase for 15 sec at 40% amplitude using a probe tip sonicator (Misonix Sonicator S-4000, Farmingdale, NY). This primary emulsion was then emulsified into 2 mL of a 10% w/v NaCl solution at 40% amplitude for 30 sec. This concentrated double emulsion was diluted into 8 mL of a 5% w/v NaCl solution under magnetic stirring. The NPs were allowed to harden by allowing slow organic solvent evaporation for 4 hours in the hood. NPs were purified by triple filtration using Amicon Ultra-4 100,000 NMWL centrifugal filter units (Millipore, Billerica, MA) using sterile water. To form green fluorescent NP-488s, PLGA-COOH (inherent viscosity 0.67, LACTEL, Cupertino, CA) was coupled to amine-modified Alexa-488 (Life Technologies, Carlsbad, CA) using EDC/NHS chemistry and purified by precipitation and drying *in vacuo*. The resulting Alexa-488-PLGA product was (15% w/w of the total polymer mass) was co-dissolved in the organic phase with the PLGA-PLH-PEG or PLGA-PEG polymer in a final volume of 500 uL. The 500 uL were then sonicated into 2 mL of sterile water at a 40% amplitude setting for 30 seconds. This emulsion was diluted into an additional 8 mL of water, solvent evaporation, then NP-488 purification as described for vancomycin-containing NPs. Fluorescence per mg of NP-488 was not significantly different between triblock and diblock NPs or at different pH, as measured using a plate reader.

3. 3. 3. Drug Encapsulation and Release Studies. 2.0 mg of PLGA-PEG or PLGA-PLH_{30}-PEG NPs were formulated with 0.4 mg initial vancomycin. Drug encapsulation

was determined by quantifying the amount of unencapsulated drug relative to the initial amount of drug by UV absorbance at 220 nm relative to a standard curve. Drug release was conducted by suspending NPs in 4 mL of pH-adjusted PBS (6.0 or 7.4), separating NPs and free drug by ultrafiltration, and quantifying free drug at each time point in triplicate.

3. 3. 4. pH-Dependent Physicochemical Property Characterization. ***ZetaPALS analysis.*** NPs made with different PLH lengths were prepared without vancomycin, purified, and resuspended in pH-adjusted solution in triplicate. Similarly, bacteria were centrifuged, washed, and resuspended in pH-adjusted solutions. Size and zeta potential were measured for each solution by quasi-elastic laser light scattering using a ZetaPALS dynamic light scattering detector (15 mW laser, incident beam 676 nm, Brookhaven Instrument Corporation).

Transmission Electron Microscopy. PLGA-PLH_{20}-PEG NPs were prepared, washed to remove residual organic solvent, resuspended at 5 mg/mL in a 1% w/v uranyl acetate solution (pH ~5.5), deposited onto carbon supported copper TEM grids for 5 min, dried, then imaged on a JEOL 200 CX TEM (MIT CMSE) at an accelerating voltage of 200 kV.

3. 3. 5. Nanoparticle-Bacterium Binding Studies. ***Bacterial Culture.*** *Escherichia coli* (ATCC# 11229) were cultured in LB broth (BD# 244620). Colonies were streaked on an LB-agar plate, selected, inoculated into 5 mL of growth medium and allowed to grow overnight in an incubated shaker at 37°C. *Staphylococcus aureus* (ATCC# 25923) were cultured in similar fashion using Tryptic Soy Broth (TSB, BD#211825).

Flow Cytometry NP-488 Binding Assays. PLGA-PLH_{20}-PEG and PLGA-PEG NP-488s were prepared, purified, and concentrated into 100 uL of pure water. Bacteria were

overgrown overnight in 5 mL of growth medium, spun down, washed in saline solution, then resuspended in salt solution previously pH-adjusted to 5.5, 6.0, 6.5, 7.0, or 7.4 using a dilute aqueous HCl solution. NP-488 were added to the bacteria and incubated for 30 minutes. For binding kinetic studies, time points ranged from 10 minutes to 4 hours. For the inhibition study, NPs were preincubated in an excess sodium polystyrene sulfonate (PSS) solution for ~30 minutes prior to incubation with bacteria. After incubation was complete, bacteria were spun down, unbound NP-488 in the supernatant were removed, bacteria were resuspended in PBS pH 7.4, and run on a flow cytometer (FACSCalibur, BD Biosciences, Koch Institute Flow Cytometry Core). Forward scatter (FSC), side scatter (SSC), green fluorescence (ex: 488, filter: 530/30), and red fluorescence (ex: 488, filter: 650 LP) data were collected on a minimum of 10,000 events per sample. Bacteria were gated for live using FSC vs. SSC plots using an untreated negative control for reference.

Fluorescence Confocal Imaging. Overnight overgrown cultures of *S. aureus* were spun down at 3,000 RCF for 5 min. A 1:10 dilution of the bacteria in solution was washed in saline solution then resuspended in 500 uL solution pH-adjusted to pH 6.0 or pH 7.4 using dilute HCl solution. Freshly prepared PLGA-PLH_{20}-PEG NP-488 were prepared, purified, resuspended in a small volume of sterile water, then diluted into the bacterial pH-buffered suspension. The bacteria and NP-488 were placed in an incubated shaker for 30 min at 37°C to allow NP-488 binding to occur. At the 30 minute time point, the suspension was centrifuged at 3,000 RCF for 5 min to pellet bacteria and bacteria-NP-488 aggregates. The pellet was washed 3x in PBS pH 7.4 and resuspended in 100 uL of PBS pH 7.4. Bacteria were stained using *Bac*Light™ Red (Life Technologies #B-35001,

Carlsbad, CA) for 30 min following the manufacturer's protocol, placed on a glass slide, coverslipped, then taken immediately for fluorescent laser scanning confocal imaging (Zeiss LSM 510 meta, W. M. Keck Microscopy Facility, Whitehead Institute at MIT). Excitation lasers used: 488 nm for green channel, 543 nm for red channel.

3. 3. 6. Antibacterial Studies. ***Minimum Inhibitory Concentration (MIC).*** The MIC of the different vancomycin formulations against *S. aureus* were determined using the microplate broth dilution method. Briefly, *S. aureus* from overnight cultures were inoculated into 5 mL TSB and allowed to enter log phase (OD_{600} ~0.3) after approximately 2 hours of incubation. NPs (PLGA-PLH_{30}-PEG or PLGA-PEG) encapsulating vancomycin were freshly prepared, purified, and serially diluted into a final volume of 100 uL of sterile water in triplicate at a 2x concentration in clear, flat bottom 96 well plates. Bacteria in log phase were diluted to a theoretical OD_{600} of 0.001 in either TSB pH adjusted to pH 7.4 or pH 6.0 using a dilute sterile HCl solution and seeded onto the microplates to produce a final volume per well of 200 uL. The OD_{600} was measured immediately before placing into an incubated shaker at 37°C, 18 hours later. The drug concentration is the total drug concentration present inside the nanoparticles, as determined by encapsulation efficiency and drug release studies. The MIC was determined as suggested by Lambert and Pearson[53] by fitting Gompertz functions to bacterial growth data using least squares regression techniques. No change in pH with time was detected.

Minimum Bactericidal Concentration (MBC). The MBC was determined by plating bacterial inoculum from the MIC studies onto antibiotic-free TSB agar plates. The MBC

was reported as the smallest concentration that results in no visible bacterial growth within 24 hours.

3. 3. 7. Statistics All data are expressed as mean ± SD. Differences between groups were assessed using one-way ANOVA (comparisons of vancomycin formulation efficacy were performed on MIC data only). Post hoc group comparisons were done using Fisher's LSD method. Least squares regressions were used to fit Gompertz functions to bacterial growth inhibition data. A significance level of $p < 0.05$ was used for all comparisons.

3. 4. References

1. Lobatto, M. E.; Fuster, V.; Fayad, Z. A.; Mulder, W. J., Perspectives and Opportunities for Nanomedicine in the Management of Atherosclerosis. *Nat Rev Drug Discov* 2011, 10, 835-852.

2. Peer, D.; Karp, J. M.; Hong, S.; Farokhzad, O. C.; Margalit, R.; Langer, R., Nanocarriers as an Emerging Platform for Cancer Therapy. *Nat Nanotechnol* 2007, 2, 751-760.

3. Zhang, L.; Pornpattananangku, D.; Hu, C. M.; Huang, C. M., Development of Nanoparticles for Antimicrobial Drug Delivery. *Curr Med Chem* 2010, 17, 585-594.

4. Gu, F.; Zhang, L.; Teply, B. A.; Mann, N.; Wang, A.; Radovic-Moreno, A. F.; Langer, R.; Farokhzad, O. C., Precise Engineering of Targeted Nanoparticles by Using Self-Assembled Biointegrated Block Copolymers. *Proc Natl Acad Sci U S A* 2008, 105, 2586-2591.

5. Hu-Lieskovan, S.; Heidel, J. D.; Bartlett, D. W.; Davis, M. E.; Triche, T. J., Sequence-Specific Knockdown of EWS-FLI1 by Targeted, Nonviral Delivery of Small Interfering RNA Inhibits Tumor Growth in a Murine Model of Metastatic Ewing's Sarcoma. *Cancer Research* 2005, 65, 8984-8992.

6. von Maltzahn, G.; Park, J. H.; Lin, K. Y.; Singh, N.; Schwoppe, C.; Mesters, R.; Berdel, W. E.; Ruoslahti, E.; Sailor, M. J.; Bhatia, S. N., Nanoparticles that Communicate *In Vivo* to Amplify Tumour Targeting. *Nat Mater* 2011, 10, 545-552.

7. Poon, Z.; Chang, D.; Zhao, X.; Hammond, P. T., Layer-by-Layer Nanoparticles with a pH-Sheddable Layer for *In Vivo* Targeting of Tumor Hypoxia. *ACS Nano* 2011, 5, 4284-4292.

8. Pornpattananangkul, D.; Zhang, L.; Olson, S.; Aryal, S.; Obonyo, M.; Vecchio, K.; Huang, C. M., Bacterial Toxin-Triggered Drug Release from Gold Nanoparticle-Stabilized Liposomes for the Treatment of Bacterial Infection. *J Am Chem Soc* 2011, 133, 4132-4139.

9. Petros, R. A.; DeSimone, J. M., Strategies in the Design of Nanoparticles for Therapeutic Applications. *Nat Rev Drug Discov* 2010, 9, 615-627.

10. Euliss, L. E.; DuPont, J. A.; Gratton, S.; DeSimone, J., Imparting Size, Shape, and Composition Control of Materials for Nanomedicine. *Chem Soc Rev* 2006, 35, 1095-1104.

11. Cheow, W. S.; Chang, M. W.; Hadinoto, K., Antibacterial Efficacy of Inhalable Levofloxacin-Loaded Polymeric Nanoparticles against *E. coli* Biofilm Cells: the Effect of Antibiotic Release Profile. *Pharm Res* 2010, 27, 1597-1609.

12. Wang, A. Z.; Langer, R.; Farokhzad, O. C., Nanoparticle Delivery of Cancer Drugs. *Annual Review of Medicine* 2012, 63, 185-198.

13. Nederberg, F.; Zhang, Y.; Tan, J. P.; Xu, K.; Wang, H.; Yang, C.; Gao, S.; Guo, X. D.; Fukushima, K.; Li, L.; Hedrick, J. L.; Yang, Y. Y., Biodegradable Nanostructures with Selective Lysis of Microbial Membranes. *Nat Chem* 2011, 3, 409-414.

14. Moogooee, M.; Ramezanzadeh, H.; Jasoori, S.; Omidi, Y.; Davaran, S., Synthesis and *In Vitro* Studies of Cross-Linked Hydrogel Nanoparticles Containing Amoxicillin. *J Pharm Sci* 2010, 100, 1057-1066.

15. Pinto-Alphandary, H.; Andremont, A.; Couvreur, P., Targeted Delivery of Antibiotics Using Liposomes and Nanoparticles: Research and Applications. *Int J Antimicrob Agents* 2000, 13, 155-168.

16. Italia, J. L.; Sharp, A.; Carter, K. C.; Warn, P.; Kumar, M. N., Peroral Amphotericin B Polymer Nanoparticles Lead to Comparable Or Superior *In Vivo* Antifungal Activity to that of Intravenous Ambisome or Fungizone. *PLoS One* 2011, 6, e25744.

17. Griffiths, G.; Nystrom, B.; Sable, S. B.; Khuller, G. K., Nanobead-Based Interventions for the Treatment and Prevention of Tuberculosis. *Nat Rev Microbiol* 2010, 8, 827-834.

18. Mohammadi, G.; Valizadeh, H.; Barzegar-Jalali, M.; Lotfipour, F.; Adibkia, K.; Milani, M.; Azhdarzadeh, M.; Kiafar, F.; Nokhodchi, A., Development of Azithromycin-PLGA Nanoparticles: Physicochemical Characterization and Antibacterial Effect Against *Salmonella typhi*. *Colloids Surf B Biointerfaces* 2010, 80, 34-39.

19. Maeda, H., Tumor-Selective Delivery of Macromolecular Drugs Via the EPR Effect: Background and Future Prospects. *Bioconjug Chem* 2010, 21, 797-802.

20. Kohanski, M. A.; DePristo, M. A.; Collins, J. J., Sublethal Antibiotic Treatment Leads to Multidrug Resistance Via Radical-Induced Mutagenesis. *Mol Cell* 2010, 37, 311-320.

21. Levy, S. B.; Marshall, B., Antibacterial Resistance Worldwide: Causes, Challenges and Responses. *Nat Med* 2004, 10, S122-S129.

22. Huh, A. J.; Kwon, Y. J., "Nanoantibiotics": A New Paradigm for Treating Infectious Diseases Using Nanomaterials in the Antibiotics Resistant Era. *J Control Release* 2011, 156, 128-145.

23. Chung, Y. C.; Wang, H. L.; Chen, Y. M.; Li, S. L., Effect of Abiotic Factors on the Antibacterial Activity of Chitosan Against Waterborne Pathogens. *Bioresour Technol* 2003, 88, 179-184.

24. Lopez, A. I.; Reins, R. Y.; McDermott, A. M.; Trautner, B. W.; Cai, C., Antibacterial Activity and Cytotoxicity of PEGylated Poly(amidoamine) Dendrimers. *Molecular BioSystems* 2009, 5, 1148-1156.

25. Wang, J.; Byrne, J. D.; Napier, M. E.; DeSimone, J. M., More Effective Nanomedicines Through Particle Design. *Small* 2011, 7, 1919-1931.

26. He, C.; Hu, Y.; Yin, L.; Tang, C.; Yin, C., Effects of Particle Size and Surface Charge on Cellular Uptake and Biodistribution of Polymeric Nanoparticles. *Biomaterials* 2010, 31, 3657-3666.

27. Mercier, R. C.; Stumpo, C.; Rybak, M. J., Effect of Growth Phase and pH on the *In Vitro* Activity of a New Glycopeptide, Oritavancin (LY333328), Against *Staphylococcus aureus* and *Enterococcus faecium*. *J Antimicrob Chemother* 2002, 50, 19-24.

28. Simmen, H. P.; Battaglia, H.; Giovanoli, P.; Blaser, J., Analysis of pH, pO2 and pCO2 in Drainage Fluid Allows for Rapid Detection of Infectious Complications During the Follow-Up Period After Abdominal Surgery. *Infection* 1994, 22, 386-389.

29. Barrett, K. E., *Gastrointestinal Physiology*. The McGraw-Hill Companies, Inc.: 2006.

30. Barrett, K. E.; Barman, S. M.; Boitano, S.; Heddwen, B., *Ganong's Review of Medical Physiology*. 23 ed.; 2010.

31. Fuchs, S.; Pane-Farre, J.; Kohler, C.; Hecker, M.; Engelmann, S., Anaerobic Gene Expression in *Staphylococcus aureus*. *J Bacteriol* 2007, 189, 4275-4289.

32. Trevani, A. S.; Andonegui, G.; Giordano, M.; Lopez, D. H.; Gamberale, R.; Minucci, F.; Geffner, J. R., Extracellular Acidification Induces Human Neutrophil Activation. *J Immunol* 1999, 162, 4849-4857.

33. Dubos, R. J., The Micro-Environment of Inflammation of Metchnikoff Revisited. *Lancet* 1955, 266, xxiv-5.

34. Simmen, H. P.; Blaser, J., Analysis of pH and pO2 in Abscesses, Peritoneal Fluid, and Drainage Fluid in the Presence or Absence of Bacterial Infection During and After Abdominal Surgery. *Am J Surg* 1993, 166, 24-27.

35. Vermeulen, M.; Giordano, M.; Trevani, A. S.; Sedlik, C.; Gamberale, R.; Fernandez-Calotti, P.; Salamone, G.; Raiden, S.; Sanjurjo, J.; Geffner, J. R., Acidosis Improves Uptake of Antigens and MHC Class I-Restricted Presentation by Dendritic Cells. *J Immunol* 2004, 172, 3196-3204.

36. Tate, S.; MacGregor, G.; Davis, M.; Innes, J. A.; Greening, A. P., Airways in Cystic Fibrosis are Acidified: Detection by Exhaled Breath Condensate. *Thorax* 2002, 57, 926-929.

37. Poschet, J.; Perkett, E.; Deretic, V., Hyperacidification in Cystic Fibrosis: Links with Lung Disease and New Prospects for Treatment. *Trends Mol Med* 2002, 8, 512-519.

38. Tomb, J. F.; White, O.; Kerlavage, A. R.; Clayton, R. A.; Sutton, G. G.; Fleischmann, R. D.; Ketchum, K. A.; Klenk, H. P.; Gill, S.; Dougherty, B. A.; Nelson, K.; Quackenbush, J.; Zhou, L.; Kirkness, E. F.; Peterson, S.; Loftus, B.; Richardson, D.; Dodson, R.; Khalak, H. G.; Glodek, A.; McKenney, K.; Fitzegerald, L. M.; Lee, N.; Adams, M. D.; Hickey, E. K.; Berg, D. E.; Gocayne, J. D.; Utterback, T. R.; Peterson, J. D.; Kelley, J. M.; Cotton, M. D.; Weidman, J. M.; Fujii, C.; Bowman, C.; Watthey, L.; Wallin, E.; Hayes, W. S.; Borodovsky, M.; Karp, P. D.; Smith, H. O.; Fraser, C. M.; Venter, J. C., The Complete Genome Sequence of the Gastric Pathogen *Helicobacter pylori*. *Nature* 1997, 388, 539-547.

39. Simon, R. H., Cystic Fibrosis: Antibiotic Therapy for Lung Disease. In *UpToDate*, Basow, D. S., Ed. UpToDate: Waltham, MA, 2012.

40. Brooks, G. F.; Carroll, K. C.; Butel, J. S.; Morse, S. A.; Mietzner, T. A., *Jawetz, Melnick, & Adelberg's Medical Microbiology, 25th Edition*. 25 ed.; The McGraw-Hill Companies, Inc.: USA, 2010.

41. Fang, B.; Gon, S.; Park, M.; Kumar, K. N.; Rotello, V. M.; Nusslein, K.; Santore, M. M., Bacterial Adhesion on Hybrid Cationic Nanoparticle-Polymer Brush Surfaces: Ionic Strength Tunes Capture from Monovalent to Multivalent Binding. *Colloids Surf B Biointerfaces* 2011, 87, 109-115.

42. Dillen, K.; Bridts, C.; Van der Veken, P.; Cos, P.; Vandervoort, J.; Augustyns, K.; Stevens, W.; Ludwig, A., Adhesion of PLGA or Eudragit/PLGA Nanoparticles to *Staphylococcus* and *Pseudomonas*. *Int J Pharm* 2008, 349, 234-240.

43. Hancock, R. E., Peptide Antibiotics. *Lancet* 1997, 349, 418-422.

44. Liu, L.; Xu, K.; Wang, H.; Tan, P. K.; Fan, W.; Venkatraman, S. S.; Li, L.; Yang, Y. Y., Self-Assembled Cationic Peptide Nanoparticles as an Efficient Antimicrobial Agent. *Nat Nanotechnol* 2009, 4, 457-463.

45. Vukomanovic, M.; Skapin, S. D.; Jancar, B.; Maksin, T.; Ignjatovic, N.; Uskokovic, V.; Uskokovic, D., Poly(D,L-lactide-co-glycolide)/Hydroxyapatite Core-Shell Nanospheres. Part 1: A Multifunctional System for Controlled Drug Delivery. *Colloids Surf B Biointerfaces* 2011, 82, 404-413.

46. Misra, R.; Acharya, S.; Dilnawaz, F.; Sahoo, S. K., Sustained Antibacterial Activity of Doxycycline-Loaded Poly(D,L-lactide-co-glycolide) and Poly(epsilon-caprolactone) Nanoparticles. *Nanomedicine (Lond)* 2009, 4, 519-530.

47. Gref, R.; Minamitake, Y.; Peracchia, M. T.; Trubetskoy, V.; Torchilin, V.; Langer, R., Biodegradable Long-Circulating Polymeric Nanospheres. *Science* 1994, 263, 1600-1603.

48. Lee, E. S.; Na, K.; Bae, Y. H., Polymeric Micelle for Tumor pH and Folate-Mediated Targeting. *J Control Release* 2003, 91, 103-113.

49. Yin, H.; Lee, E. S.; Kim, D.; Lee, K. H.; Oh, K. T.; Bae, Y. H., Physicochemical Characteristics of pH-Sensitive Poly(L-histidine)-b-poly(ethylene glycol)/poly(L-lactide)-b-poly(ethylene glycol) Mixed Micelles. *J Control Release* 2008, 126, 130-138.

50. Perez, C.; Sanchez, A.; Putnam, D.; Ting, D.; Langer, R.; Alonso, M. J., Poly(lactic acid)-poly(ethylene glycol) Nanoparticles as New Carriers for the Delivery of Plasmid DNA. *J Control Release* 2001, 75, 211-224.

51. Lee, E. S.; Gao, Z. G.; Kim, D.; Park, K.; Kwon, I. C.; Bae, Y. H., Super pH-sensitive multifunctional polymeric micelle for tumor pH(e) specific TAT exposure and multidrug resistance. *Journal of Controlled Release* 2008, 129, 228-236.

52. Lee, E. S.; Oh, K. T.; Kim, D.; Youn, Y. S.; Bae, Y. H., Tumor pH-responsive flower-like micelles of poly(L-lactic acid)-b-poly (ethylene glycol)-b-poly(L-histidine). *Journal of Controlled Release* 2007, 123, 19-26.

53. Lambert, R. J.; Pearson, J., Susceptibility Testing: Accurate and Reproducible Minimum Inhibitory Concentration (MIC) and Non-Inhibitory Concentration (NIC) Values. *J Appl Microbiol* 2000, 88, 784-790.

Chapter 4

Mammalian Cell and Protein Interactions *In Vitro* and Preliminary Evaluation *In Vivo*

This chapter has been reproduced in part from: Radovic-Moreno A. F., Lu T. K., Puscasu V. A., Yoon C. J., Langer R., Farokhzad O. C. *ACS Nano* **2012**, *6*, 4279-4287.

4. 1. Introduction

Resistance to antibiotics remains one of the major challenges in modern medicine despite almost 80 years of widespread clinical experience with this phenomenon. For decades following the introduction of the first antibiotics to the clinic, such as the penicillins (penicillin, 1928) and aminoglycosides (streptomycin, 1943) resistance was controlled through a combination of containment and new antibiotic discovery. These approaches were largely successful due to the remarkable productivity of the "golden era" of antibiotic discovery (~1940-1970). This period introduced many new antibiotic classes including the macrolides (erythromycin, 1949), tetracyclines (tetracycline, 1952), glycopeptides (vancomycin, 1958), and quinolones (naldixic acid, 1962), among several others. This was followed by decades of successes in modifying antibiotics to compensate for bacterial resistance. Over this period, resistance to one type of antibiotic could be handled by turning to another drug class or by using a newer drug within the same class, such as using methicillin when β-lactamase became widespread.[1-5]

However, new antibiotic development has stalled in the last several decades. The lipopeptide daptomycin (1980s) and the oxazolidinone linezolid (1990s) are among the newest antibiotic drug classes to be developed, but relatively little new development has occurred since then and resistance has been documented against both of these drugs.

Given the rising threat of multi-drug resistant organisms, it is imperative to explore new paradigms in antibacterial drug development.[6, 7]

Various alternatives to small molecule antibiotics are in development, including bacteriophages, drug potentiators, antivirulence factors, antimicrobial peptide or peptidomimetics and nanoparticles (NPs).[8-10] Of these alternatives, NPs are potentially well-suited to contribute to new antibacterial drug design due to their small size, unique properties, and high surface area-to-volume ratio.[1, 11, 12] NPs have been shown to improve drug function, drug delivery, overcome resistance, and introduce novel mechanisms of action. Particularly significant is the ability to use NPs to target drugs to a site of infection.[13, 14] Improved drug targeting can increase drug effectiveness, reduce toxicity, optimize exposure, and potentially reduce the likelihood of drug resistance emerging (Chapter 2). This strategy might be able to extend the useful lifetime of a drug, widen the types of clinical indications, and potentially improve patient outcomes.

Previously, our group had reported a biodegradable and nontoxic polymeric NP for targeting vancomycin to bacterial cell walls.[15] These NPs were designed to switch their surface charge from near neutral to cationic under conditions of slight acidity (pH < 6.5), a state reported to occur locally at the site of certain infections. This surface charge-switching capability was important since positively charged NPs, when in the bloodstream, tend to interact non-specifically with a wide variety of cells and proteins, greatly reducing the potential circulating half-life and thereby the NP's systemic applicability. Our results showed that the cationic surface charge produced under low pH conditions enabled binding to the cell walls of both Gram-positive and Gram-negative

bacteria using both flow cytometry and confocal fluorescent microscopy techniques, highlighting the potential of this targeting system.

Nevertheless, a common challenge to using electrostatic interactions as the basis for targeting *in vivo* is lack of specificity. An infection site is a rich tapestry of eukaryotic cells, bacteria, small molecules, and proteins, many of which are negatively charged and may interfere with NP-bacterial specificity (Chapter 2, Figure 2.2). The goal of our present work was to further explore the interactions between NPs based on poly(D,L-lactic-co-glycolic acid)-*block*-poly(L-histidine)-*block*-poly(ethylene glycol) (PLGA-PLH-PEG) and model eukaryotic cells, as well as NPs and bacteria in the presence of a model negatively charged protein. These studies can inform the design of cationically-charged NP-bacteria targeting mechanisms *in vivo*, one of the most widely used strategies to target bacteria.

Our results show that mixing poly(D,L-lactic-co-glycolic acid)-*block*-poly(L-histidine)-*block*-poly(ethylene glycol) (PLGA-PLH-PEG) and PLGA-PEG to form mixed NPs yields improved bacterial binding sensitivity and specificity in high protein concentration as well as the circulation half-life compared to controls. NPs with a PLGA-PLH-PEG content between 40-60% (w/w) showed greater binding to *Staphylococcus aureus* as measured by flow cytometry in the presence of serum levels of bovine serum albumin (BSA, 4 g/dL) than NPs of other composition and controls, though this was significantly less than what was observed in the absence of BSA. Mixed NPs also demonstrated less binding/uptake to model eukaryotic cells in a composition-dependent manner *in vitro*. Of the preferred 40-60% NP composition range, a longer circulation half-life was obtained with ~40% (w/w) PLGA-PLH-PEG than ~60% PLGA-PLH-PEG. The circulation half-

life of ~40% PLGA-PLH-PEG was comparable to PLGA-PEG NP controls. These studies may inform future studies aimed at optimizing cationic charge-mediated targeting of bacteria in complex environments.

4. 2. Results and Discussion

4. 2. 1. NP design, formulation, and characterization. Previously, we designed a triblock copolymer with a PLGA-PLH-PEG structure, which we formulated into NPs using a modified double emulsion/solvent evaporation technique. We were interested in further exploring the bacterial targeting potential of NPs containing PLGA-PLH-PEG. To do so, we formed mixed NPs with PLGA-PEG by blending PLGA-PLH-PEG and PLGA-PEG together in the organic phase prior to NP formulation. We hypothesized that blending these two polymers together might yield NPs with improved bacterial targeting specificity by increasing the density of PEG on the NP surface, which might reduce nonspecific protein binding while potentially still retaining bacterial binding ability. This was based on previous studies showing that relatively small changes in PEG density can result in large changes in protein adsorption.[16, 17] Forming mixed NPs was also motivated by initial studies, which showed significant attenuation of PLGA-PLH-PEG NP binding to bacteria at 4 g/dL BSA (17.3±3.5% of binding at 0 g/dL), as well as quantification of the surface composition of PLGA-PLH-PEG NPs using XPS (Table 4.1). The XPS data showed elevated levels of nitrogen and reduced levels of oxygen in the top ~10 nm of the NPs, consistent with reduced PEG density on the NP surface.

Table 4. 1. XPS Analysis of PLGA-PLH-PEG and PLGA-PEG NPs

XPS Analysis	Mol %, Top ~10 nm of NP surface (electron)

Nanoparticle	C (C 1s)	O (O 1s)	N (N 1s)
PLGA-PLH-PEG	61.4	36.3	2.2
PLGA-PEG	59.1	40.9	0.0

Reduced PEG density in the PLGA-PLH-PEG NPs compared to PLGA-PEG is likely due to a combination of incomplete PEGylation of the PLGA-PLH-PEG polymer and PEG "burying" inside the NP during the NP self-assembly. The latter can be understood by considering that the polymers self-assemble into NPs based on hydrophilic/hydrophobic forces, which tend to orient the more hydrophobic PLGA portion towards the NP core. Under typical NP formulation conditions (pH ~5-6) the PLH segment is cationically charged (pKa of histidine imidazole ~6.0-6.5), making this polymer more hydrophilic and capable of competing with PEG for the limited NP surface, which is in contact with water. In contrast, PLGA-PEG polymers are more likely to orient themselves with PEG on the NP surface due to the greater difference in hydrophobicity between the PLGA and PEG blocks.

To form mixed PLGA-PLH-PEG / PLGA-PEG NPs, we blended the different polymers in varying weight ratios together in the organic phase of the emulsion. The resulting NPs demonstrated zeta potential in acidic conditions (pH ~6.0) that was between the two pure species, suggesting formation of mixed NPs (Figure 4.1). Of note, a minimal level of ~30% PLGA-PLH-PEG is needed to yield positively charged NPs at acidic pH and a plateau is reached at ~80% PLGA-PLH-PEG, where greater PLGA-PLH-PEG levels do not appear to increase the amount of cationic charge. Otherwise, the relationship between

zeta potential and PLGA-PLH-PEG content is relatively linear in the range ~20-80% PLGA-PLH-PEG (Figure 4.1).

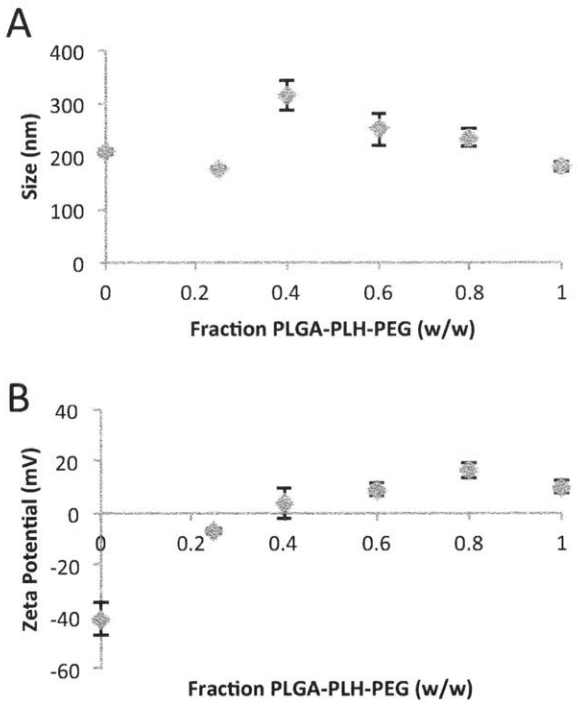

Figure 4. 1. Mixed PLGA-PLH-PEG / PLGA-PEG NP Size and Zeta Potential Characterization. (A) NP size. (B) NPs formed containing mixtures of PLGA-PLH-PEG and PLGA-PEG demonstrate mixed zeta potential, consistent with formation of mixed PLGA-PLH-PEG / PLGA-PEG NPs.

4. 2. 2. NP binding to bacteria in the presence of bovine serum albumin. Next, we wanted to examine the effect of mixed NP binding to bacteria in the presence of a model negatively charged protein. We selected BSA because it is one of the major proteins in the body, with a concentration of ~4 g/dL in serum and on the order of g/dL at typical infection sites.[18] As a model bacterium, we selected *Staphylococcus* aureus, a major clinically relevant pathogen that has high incidence of drug resistance.[4, 19, 20] We examined NP binding to *S. aureus* by incubating ~150 ug/mL of Alexa-488-PLGA-labeled PLGA-PLH-PEG NPs with bacteria (OD_{600} ~0.3) at 37°C with different

concentrations of BSA (Figure 4.3), collecting the bacteria, then running on a flow cytometer to assess bacteria-associated fluorescence. The results show a logarithmic dependence of bacteria-associated fluorescence with BSA concentration, with a significant attenuation of NP binding to bacteria at 4 g/dL (17.3±3.5% of binding at 0 g/dL).

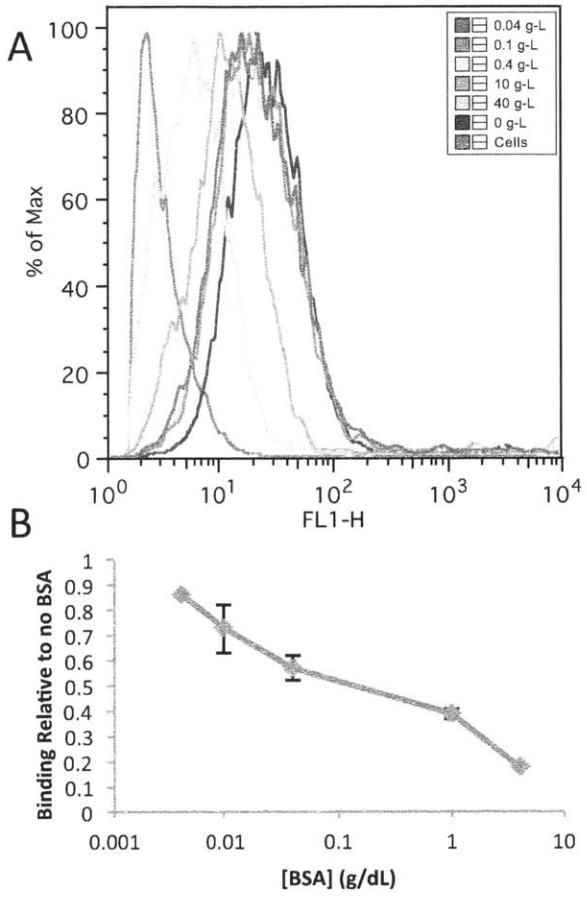

Figure 4. 2. PLGA-PLH-PEG NP Uptake in the Presence of Bovine Serum Albumin (BSA). Alexa-488 labeled NPs were incubated with *S. aureus* and BSA at the indicated concentration for 30 min, washed, and then evaluated in terms of their cell-associated fluorescence using flow cytometry. (A) Representative histogram of cell-associated fluorescence (FL1-H indicates fluorescence obtained in the green fluorescent channel). (B) The data expressed as binding relative to no BSA, with additional repeated experiments included (N=3). The data suggests binding to *S. aureus* is inhibited in the presence of BSA in a logarithmic manner.

Next, we formed mixed NPs of PLGA-PLH-PEG / PLGA-PEG with 0-80% (w/w) PLGA-PLH-PEG content and similarly evaluated bacteria-associated fluorescence following incubation in the presence of varying BSA levels (reserving 20% of each for fluorescently modified PLGA polymer). We found that the amount of bacteria-associated fluorescence, similar to pure PLGA-PLH-PEG NPs, had a logarithmic dependence with BSA concentration (Figure 4.3A), but that this strongly depended on the composition of the NPs. At 20-40% PLGA-PLH-PEG, there was an overall reduction in the amount of bacteria-binding but that the quantity of binding at 0 g/dL was retained better than the other formulations, suggesting relatively lower dependence of binding on BSA level at this composition. This is consistent with a higher PEG density in this composition range, which would prevent adsorption of BSA. The 60-80% PLGA-PLH-PEG NPs demonstrate higher binding to bacteria at low BSA levels, but bacterial binding is affected more prominently at high BSA levels. Interestingly, 80% PLGA-PLH-PEG NPs demonstrated less binding at 4 g/dL BSA than 60% (Figure 4.3B), suggesting BSA adsorption that was so high as to inhibit most NP bacterial binding.

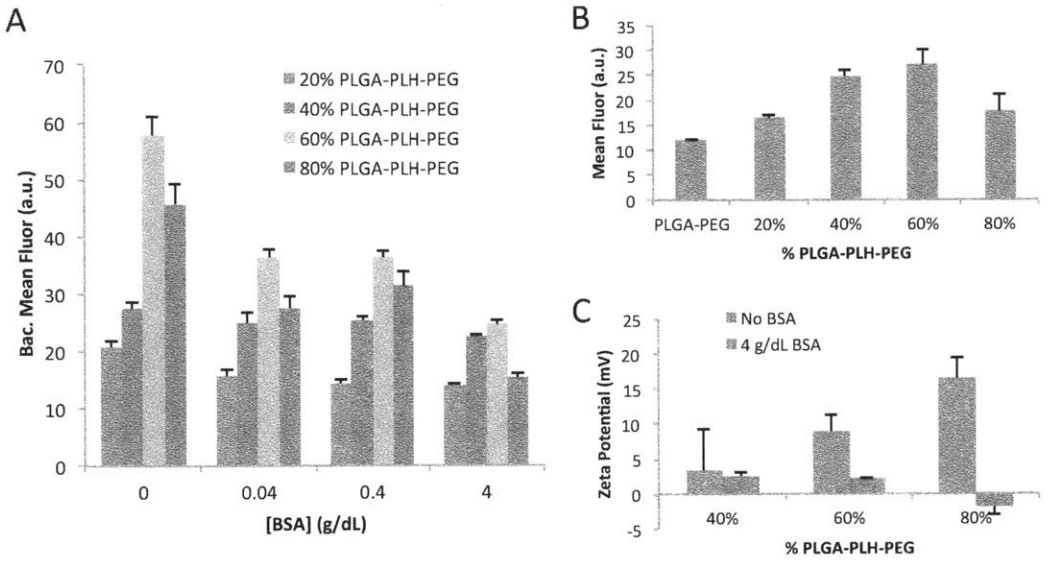

Figure 4. 3. Mixed PLGA-PLH-PEG / PLGA-PEG NP Binding to *S. aureus*. (A) Mean bacteria-associated fluorescence obtained via flow cytometry for different mixtures at the indicated BSA concentration, showing a general decline in bacterial binding at higher protein concentrations. (B) Bacteria-associated uptake at 4 g/dL BSA, demonstrating a reduction in uptake at 80% PLGA-PLH-PEG NPs. (C) Zeta potential of NPs with or without 4 g/dL BSA, demonstrating high BSA adsorption in 80% PLGA-PLH-PEG NPs leading to surface charge reversal, which correlates with reduced binding to bacteria.

To gain greater understanding of NP bacterial binding, particularly the reversal that occurs in binding at higher PLGA-PLH-PEG content, we evaluated the zeta potential of the NPs as a function of the BSA concentration. At 40% PLGA-PLH-PEG, there is a mild cationic charge on the NP surface (3.4±5.9 mV at 0 g/dL; 2.6±0.5 mV at 4 g/dL) that is independent of BSA concentration (Figure 4.3C). This correlates well with bacterial binding at this composition, which similarly appeared largely independent of BSA concentration (27.3±1.1 at 0 g/dL; 22.4±0.5 at 4 g/dL, arbitrary fluorescence units). At 60% PLGA-PLH-PEG, the increased PLGA-PLH-PEG content leads to an increase in the zeta potential of the NPs in the absence of BSA, but this demonstrates a more noticeable decline at 4 g/dL (8.9±2.3 mV at 0 g/dL; 2.3±0.1 mV at 4 g/dL) but the NPs

remain cationic. In contrast, 80% PLGA-PLH-PEG NPs demonstrate the highest zeta potential at 0 g/dL (16.5±2.8 mV) but demonstrate a large reduction in zeta at 4 g/dL, so much so that the NPs become anionic (-1.8±1.2 mV). These data correlate well with the amount of bacteria binding as a function of BSA concentration, where the 80% PLGA-PLH-PEG NPs demonstrate binding that is equivalent to 20% PLGA-PLH-PEG at 4 g/dL despite much higher binding at 0 g/dL.

Taken together, these results suggest that the optimal range for continued evaluation of these NPs is 40-60% PLGA-PLH-PEG, which show a balance being achieved between inhibiting BSA binding but retaining enough cationic charge to yield NP binding to bacteria, even in the presence of serum BSA levels.

4. 2. 3. NP interactions with model mammalian cells – *in vitro* studies. In addition to bacteria and protein, a site of infection will be populated by various different eukaryotic (host) cells. Greater insight into the potential of a charge-based bacterial targeting strategy could be obtained by evaluating the extent and kinetics of binding of PLGA-PLH-PEG NPs to infection-resident host cells. As model cells, we selected two cell lines: a model phagocytic cell line, RAW 264.7 murine macrophages, and a model tissue epithelial cell line, LNCaP prostate adenocarcinoma cells. Positively charged NPs have been shown to bind to and be internalized by various eukaryotic cells previously.[21-23] In general, this is believed to occur due to the negative surface charge imparted by the phosphate-rich glycocalyx and negatively charged cell membrane proteins, among others. To evaluate the binding/uptake properties of PLGA-PLH-PEG NPs to these cell lines, we incubated Alexa-488-PLGA-labeled PLGA-PLH-PEG NPs with cells grown to ~70%

confluence at either pH 5.5 or pH 7.4. The NPs were removed, washed, then run on a flow cytometer to evaluate cell-associated fluorescence. The results demonstrate a pH-dependent increase in the amount of binding/uptake to both cell lines, though the effect is significantly more prominent in the LNCaP cell line (Figure 4.4A, C). To determine the kinetics of uptake, the NPs were incubated with the cells in similar fashion but collected at different time points (Figure 4.4B, D). The RAW 264.7 macrophages demonstrated a significant initial lag in uptake, with less than 20% of maximum observed within the first hour of incubation. The NPs showed near half saturation after 2 hours of incubation. LNCaP cells showed a gradual saturation of uptake that began immediately, with full saturation being observed after 2 hours of incubation. Both cell lines showed approximately the same zeta potential (Figure 4.4E), suggesting that the observed differences may be due to differences in NP internalization rates. To gain further degree of discrimination of the pH-dependent uptake properties in LNCaP cells, we incubated the NPs with ~70% confluent LNCaP cells and measured the NP uptake at different pH levels (Figure 4.5). The greatest increase in NP uptake occurred as the pH declined from 6.5 to 6.0 (1.3±0.1 fold increase relative to pH 7.4 at pH 6.5, 2.3±0.1 fold increase at pH 6.0), which correlates well with the NP changes in zeta potential (Chapter 3). Maximal increases in binding/uptake are observed at pH 5.5 (3.3±0.2 fold increase). In contrast, PLGA-PEG NPs demonstrated relatively little changes in uptake, particularly for the RAW 264.7 cell line (Figure 4.6). This suggests that PLGA-PLH-PEG NPs are associated with cells in a pH-dependent manner.

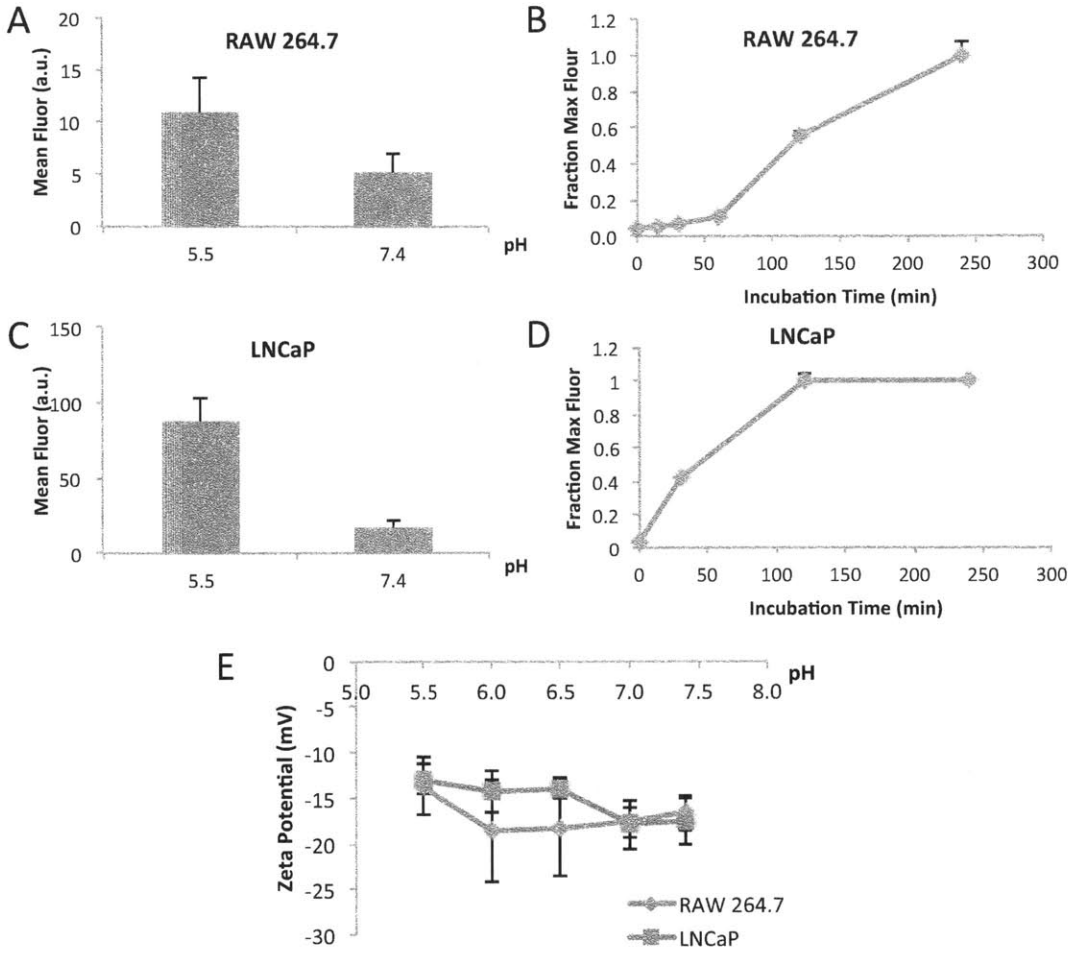

Figure 4. 4. Nanoparticle-Mammalian Cell Uptake. Alexa-488 labeled PLGA-PLH-PEG or PLGA-PEG NPs were incubated with a model phagocytic cell line, RAW 264.7 (A, B) or a model tissue resident cell line, LNCaP (C, D) to study NP uptake characteristics. Mean cell-associated fluorescence after NP incubation at pH 5.5 or 7.4 as determined using flow cytometry in RAW 264.7 (A) or LNCaP (C) cell lines. Binding kinetics of (B) RAW 264.7 and (D) LNCaP cells at low pH. (E) Zeta potential of cell lines with changes in pH.

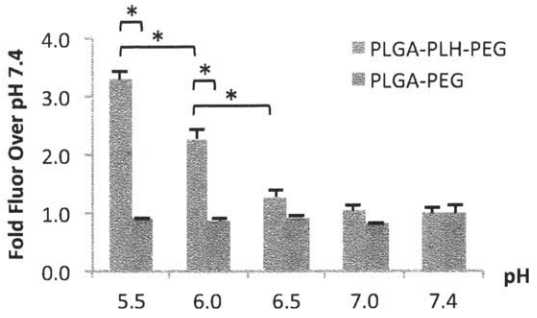

Figure 4. 5. pH-Titration of NP Uptake in LNCaP Cells. To obtain greater understanding of the pH-dependent uptake properties, the indicated NPs were incubated with LNCaP cells, uptake was assessed by flow cytometry, and expressed as fold fluorescence over that observed at pH 7.4. The data suggests that pH-sensitive PLGA-PLH-PEG NPs demonstrate increased uptake as pH < 6.5 whereas PLGA-PEG NPs do not. (* indicates $p < 0.05$ by ANOVA).

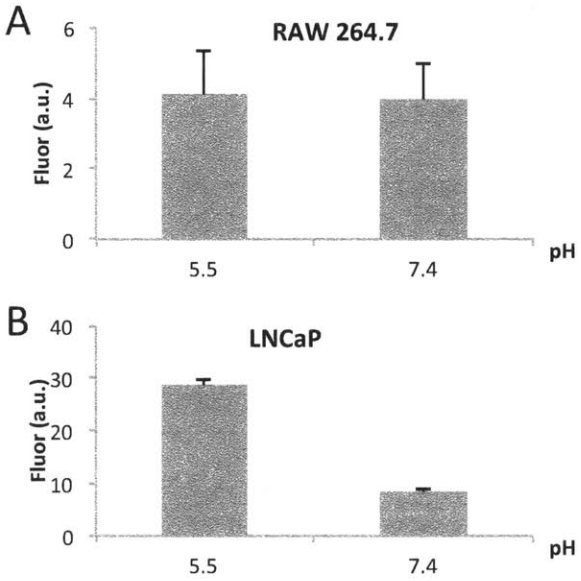

Figure 4. 6. pH-dependent Uptake of PLGA-PEG NPs. (A) Uptake in a model phagocytic cell line, RAW 264.7 appears to be pH-independent. (B) Uptake in a model tissue cell, LNCaP, demonstrates some pH-sensitivity, but this is considerably smaller than what is observed in PLGA-PLH-PEG NPs (Figure 4. 4C).

To confirm the pH-dependent uptake properties in the LNCaP cells and grossly evaluate their subcellular localization, we turned to fluorescent confocal microscopy. Alexa-488-PLGA-labeled PLGA-PLH-PEG or PLGA-PEG NPs were incubated with LNCaP cells at

time points of 30 min or 2 hr at pH 5.5, washed, fixed, then imaged (Figure 4.7). The PLGA-PLH-PEG NPs demonstrated an increase in uptake that was not observed with PLGA-PEG NPs. Further, the amount of uptake appeared to be time-dependent, with much more noticeable uptake at the 2 hr time point. Interestingly, at 2 hr, the NPs appeared to be distributed both on the cell membrane as well as the inside of cells, with a punctate pattern of fluorescence consistent with localization inside of endolysosomes. To further explore the mechanism of internalization, PLGA-PLH-PEG NPs were incubated with LNCaP cells at pH 5.5 in the presence (or absence) of inhibitors of clathrin-dependent endocytosis (CME) (monodansylcadaverine, MDC) or macropinocytosis (rottlerin) (Figure 4.8). Both of the inhibitor-treated cells demonstrated a reduction in the amount of NP uptake (MDC 66±13% of no inhibitor, rottlerin 69±3%), suggesting that both CME and macropinocytosis play a role in PLGA-PLH-PEG NP internalization. Notably, the majority of fluorescence was retained despite the presence of these inhibitors, suggesting that a substantial fraction of NPs are present on the surface. This is consistent with what is observed in the fluorescent confocal images (Figure 4.7).

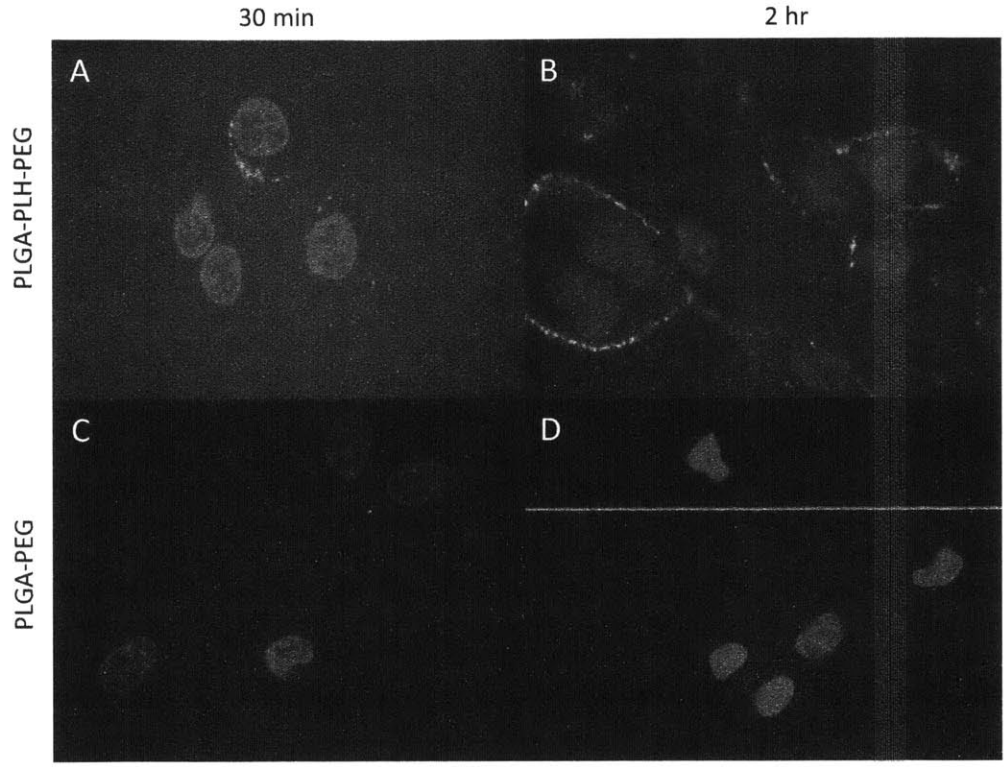

Figure 4. 7. Fluorescence Image of NP Uptake in LNCaP Cells. Alexa-488 modified NPs were incubated with a model tissue cell, LNCaP, at low pH for the indicated period of time and imaged using fluorescence microscopy. Greater uptake is observed in pH-sensitive PLGA-PLH-PEG NPs. In addition, considerable NP fluorescence appears to be associated with the cell surface, especially after 2 hours of incubation.

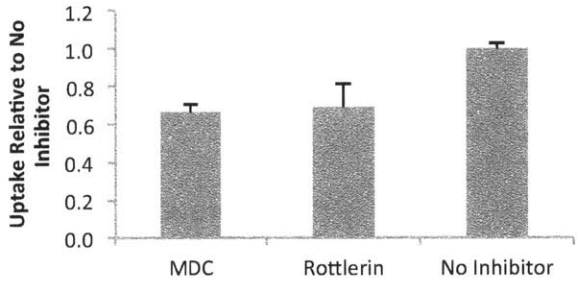

Figure 4. 8. Inhibitor Study of Uptake of PLGA-PLH-PEG NPs in LNCaP cells at low pH. NPs were incubated with LNCaP cells in the presence of inhibitors of clathrin-mediated endocytosis (monodansylcadaverine, MDC), macropinocytosis (rottlerin), or no inhibitor, collected, and their cell-associated fluorescence evaluated using flow cytometry. The data suggests that both pathways are involved in NP uptake, but that significant fluorescence remains, consistent with NP surface association.

Next, we sought to evaluate the impact that mixed PLGA-PLH-PEG / PLGA-PEG NPs have on eukaryotic cell binding/uptake properties. We incubated mixed NPs with either

RAW 264.7 or LNCaP cells at pH 5.5 or 7.4, washed, collected the cells, then ran on a flow cytometer to evaluate cell-associated fluorescence (Figure 4.9). Both cell lines demonstrated an increase in binding/uptake at pH 5.5 relative to pH 7.4, but this was dependent on the PLGA-PLH-PEG content. In general, a linear reduction in the PLGA-PLH-PEG content resulted in a corresponding reduction in NP binding/uptake at pH 5.5, but not pH 7.4. This suggests that the mixed NPs demonstrate a reduction in binding/uptake to eukaryotic cells as the PLGA-PLH-PEG content is reduced.

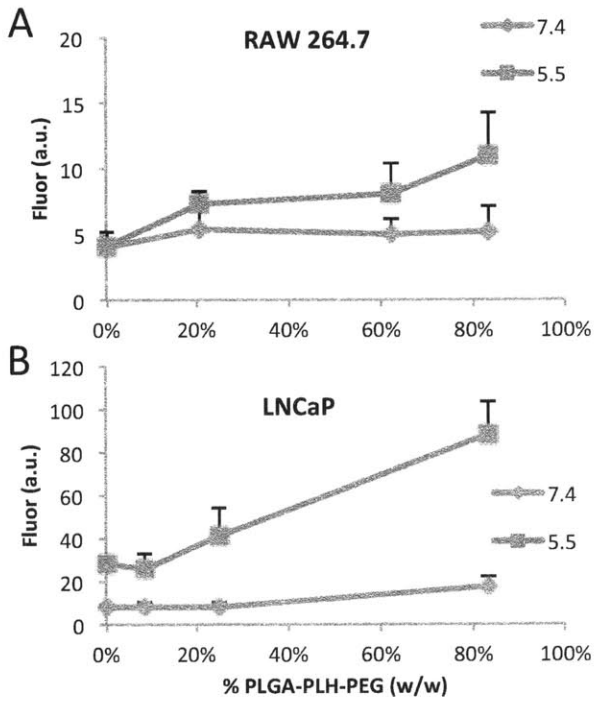

Figure 4. 9. Mixed PLGA-PLH-PEG / PLGA-PEG NP Uptake in Mammalian Cells. Mean cell-associated fluorescence obtained via flow cytometry for different PLGA-PLH-PEG / PLGA-PEG mixtures, showing an increase in pH-dependent binding at higher % PLGA-PLH-PEG for both (A) RAW 264.7 and (B) LNCaP cell lines. N=3 or more for observations.

We then sought to determine whether NP binding to *S. aureus* could occur in the presence of protein and eukaryotic cells. Given the more prominent uptake in the LNCaP cell line, NPs were incubated with bacteria and LNCaP cells to explore the degree of

uptake competition (Figure 4.10A, B). The results show that at the given conditions, the PLGA-PLH-PEG NPs were able to bind to bacteria, but that some competition was observed (62.8±7.3% of fluor in the LNCaP group). This is consistent with the observation that LNCaP cells are able to capture NPs. The bacterial binding, even in the presence of LNCaP cells, may be mediated by more rapid binding kinetics to bacteria than LNCaP cells (Figure 4.10C).

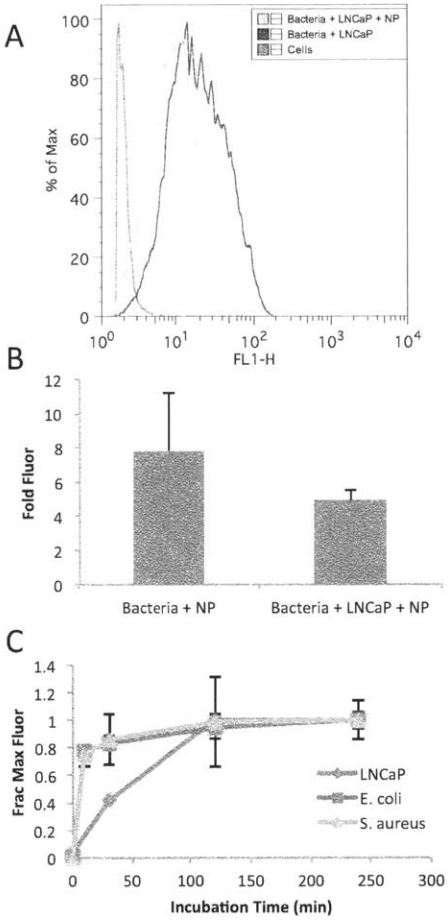

Figure 4. 10. Impact of LNCaP Cell Monolayer on Bacteria Targeting Ability. Alexa-488 modified NPs were incubated with *S. aureus* in the presence of a monolayer of LNCaP cells to evaluate the ability to target bacteria in the presence of mammalian cell competition. (A) Representative histogram of bacteria-associated fluorescence (FL1-H indicates fluorescence obtained in the green channel). (B) Bacteria-associated fluorescence in the presence and absence of LNCaP cells indicating reduced bacterial targeting ability. (C) Uptake or binding kinetic study, showing rapid binding to bacteria and relatively slower uptake saturation in LNCaP cells. N=3 or more for observations.

4. 2. 4. *In vivo* evaluation of NPs – pharmacokinetics. To further explore the *in vivo* applicability of PLGA-PLH-PEG NP-based targeting, we wanted to explore the impact of NP composition on the circulation pharmacokinetics (PK). Two NP formulations in the range of 40-60% PLGA-PLH-PEG (43% and 57%) and control PLGA-PEG NPs were fluorescently labeled by incorporation of Alexa-674-PLGA into the NPs. The NPs were delivered i.v. at 2 mg/mouse (~80 mg/kg NP) in 200 uL of PBS. At the given time point, a sample of blood was collected and measured for its NP fluorescence using an IVIS imaging system. The PLGA-PEG NPs demonstrated the longest circulation time, followed by the 43% then 57% PLGA-PLH-PEG (Figure 4.11). To model the NP PK, a two-compartment model was assumed and the data fit using a non-linear least squares regression technique (Table 4.2).

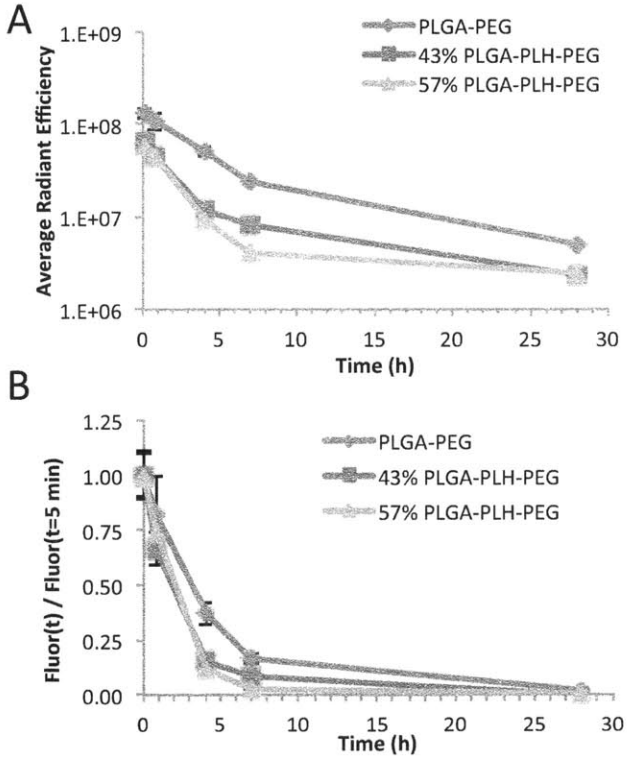

Figure 4. 11. Mixed PLGA-PLH-PEG / PLGA-PEG NP Pharmacokinetics. Alexa-647 modified NPs were injected intravenously into the tail vein of male Balb/c mice, blood was collected at the indicated time point, and the amount of fluorescence quantified. (A) Average radiant efficiency of a drop of blood over time. (B) Data in (A) expressed as a fraction of the amount of fluorescence observed at t=5 min. N=4 for all observations.

Table 4. 2. Pharmacokinetic parameters – Two Compartmental Fit

	Distribution $t_{1/2}$ (h)	Elimination $t_{1/2}$ (h)
PLGA-PEG	2.8 ± 0.7	8.0 ± 1.1
43% PLGA-PLH-PEG	2.0 ± 0.4	11.1 ± 1.9
57% PLGA-PLH-PEG	1.8 ± 0.1	16.4 ± 3.4

The PK properties of the NPs suggest that a higher PLGA-PEG content leads to more extended NP circulation time in the blood. This may be due to a number of factors. Increased PEG density in NPs with greater PLGA-PEG content is a likely mechanism, which is corroborated by the XPS data (Table 4.1) and the observation of reduced changes in zeta potential in the presence of BSA (Figure 4.4C). In addition, greater PEG chain flexibility when attached to PLGA, which would improve the steric barrier function of the PEG, may be contributing. We also cannot rule out the possibility of more specific interactions between the PLH and BSA (and not electrostatic only), though to the best of our knowledge this has not been reported previously. It should be noted that all NP formulations demonstrated extended circulation times, with a distribution half-life of at least 1.8 hr or more. In addition, there did not appear to be a significant difference in the distribution half-life of the 43% PLGA-PLH-PEG and PLGA-PEG NPs. These extended

circulation times are significantly longer than the reported circulation time of PLGA or of typical cationic NPs, both of which are significantly shorter.[17, 21]

4. 2. 5. *In vivo* evaluation of NPs – biodistribution. Next, we sought to evaluate the biodistribution properties of the NPs following an i.v. injection. We selected an intermediate PLGA-PLH-PEG composition, 53%, formed Alexa-647-labeled NPs as previously, and delivered 2 mg/mouse via the tail vein as a bolus together with PLGA-PEG as a control. On the basis of the PK studies, the NPs were given enough time to completely leave the circulation, at which point the mice were necropsied to collect their organs. Organs were weighed then assessed for their NP-associated fluorescence using an IVIS system. The data demonstrate that no significant difference in the biodistribution of the 53% PLGA-PLH-PEG NPs as compared to PLGA-PEG could be observed, with the majority of accumulation occurring in the spleen and liver, consistent with various reports with similar NPs (Figure 4.12).[24, 25] To confirm the quantitative data and evaluate the organ-level distribution of the NPs, frozen sections of the organs were imaged using fluorescent confocal microscopy (Figure 4.13). The images demonstrate NP accumulation primarily in the spleen and liver, with a distribution pattern consistent with phagocytic cell clearance. Further, we were interested in whether PLGA-PLH-PEG-containing NPs would accumulate in organs that have a local acidic environment. Most notably, this can occur in two regions: the lumen of the stomach (pH 1-2) and the medulla of the kidney (pH ~4-8).[26] The 53% PLGA-PLH-PEG NPs did not appear to accumulate in either of these regions (Figure 4.13). In the case of the lumen of the stomach, it is likely that the NPs were never in contact with acidic regions, instead remaining in the pH ~7.4 vasculature during their transit through this organ. The situation

in the renal medulla is a bit more complex, as some have reported a lower intravascular pH in this region.[26] Our data suggest that the 53% PLGA-PLH-PEG NPs do not appear to accumulate in this region under the given experimental conditions. However, it should be noted that medullary pH is well-known to depend on the acid-base balance of the animal, which can be strongly affected by diet. Consequently, we cannot yet rule out the possibility of accumulation in this region in cases where the urine pH is more acidic.

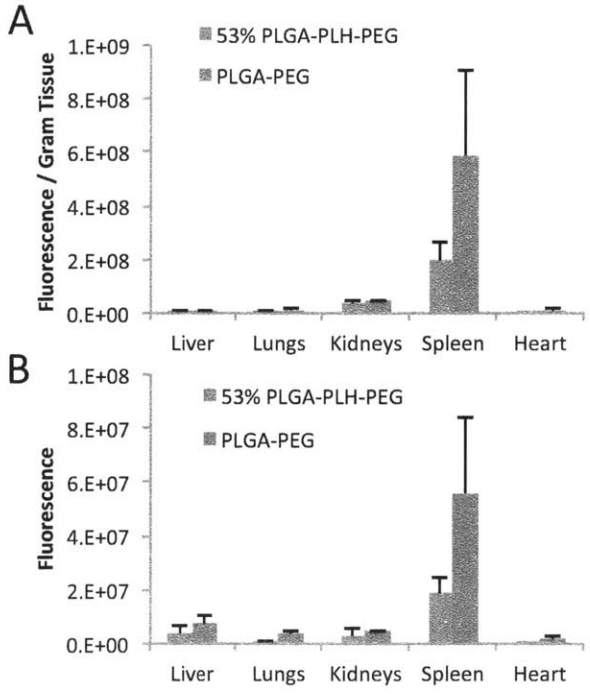

Figure 4. 12. Mixed PLGA-PLH-PEG / PLGA-PEG NP Biodistribution. Alexa-647 modified NPs were injected intravenously into the tail vein of male Balb/c mice, allowed to leave the circulation (no fluorescence was detected in the blood), then organs were harvested and assayed in terms of their fluorescence. (A) Organ-associated fluorescence per gram of tissue. (B) Data in (A) expressed as total fluorescence. N=3 for all observations. No significant differences were observed between mixed PLGA-PLH-PEG and PLGA-PEG NPs.

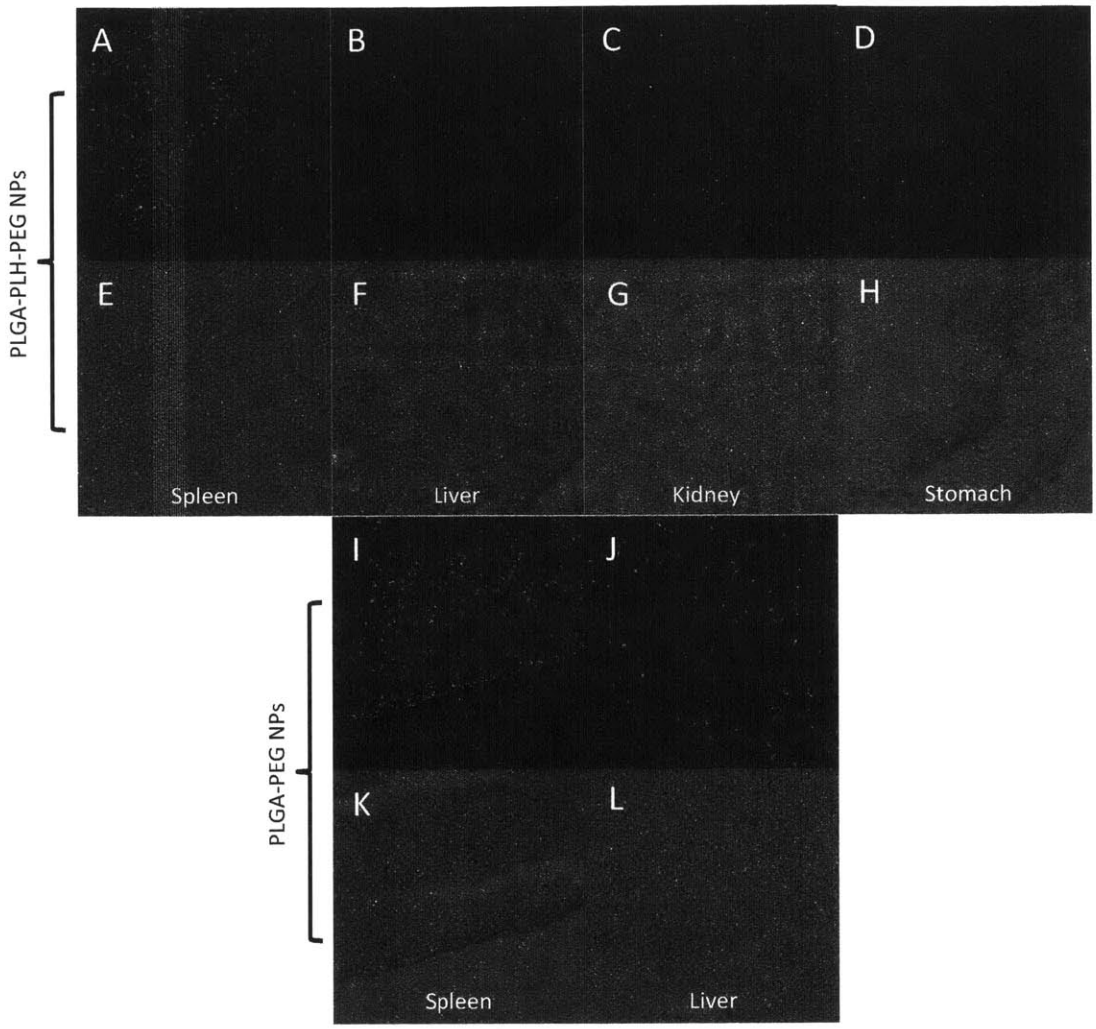

Figure 4. 13. Mixed PLGA-PLH-PEG / PLGA-PEG NP Biodistribution – Confocal Images. Alexa-647 modified 53.3% PLGA-PLH-PEG or PLGA-PEG NPs were injected intravenously into the tail vein of male Balb/c mice, allowed to leave the circulation (no fluorescence was detected in the blood), then organs were harvested and assayed in terms of their fluorescence by confocal imaging. Spleen (A, 647 Fluor; E, Bright field), Liver (B, 647 Fluor; F, Bright field), Kidney (C, 647 Fluor; G, Bright field).

4. 2. 6. Summary. In summary, we have continued to explore the potential of PLGA-PLH-PEG NPs to target *Staphylococcus aureus* infections by seeking a greater understanding of NP bacterial targeting in high protein concentration (up to 4 g/dL BSA), evaluating NP binding/uptake to model phagocytic cells and tissue cells, as well as evaluating NP pharmacokinetics and biodistribution *in vivo*. We determined that blending

PLGA-PLH-PEG with PLGA-PEG to form mixed NPs, particularly with a composition of 40-60% PLGA-PLH-PEG, has the potential to improve bacterial targeting specificity in high background levels of the negatively charged protein BSA, though this occurs at the expense of binding sensitivity. Further, the mixed NPs demonstrated pH-dependent binding/uptake to model host phagocytic cells and tissue cells, though saturation occurred more slowly than with bacteria and the majority of binding to bacteria was retained in the presence of a monolayer of eukaryotic cells. When injected i.v., mixed NPs demonstrated extended circulation time with a half-life of at least 1.8 hr, and had a biodistribution similar to that of PLGA-PEG, suggesting that these two NPs behaved similarly at physiologic pH *in vivo*. These data suggest that mixed NPs may have the potential to target acidic sites of bacterial infections, though more evaluation in animal models of infection is needed. More specifically, future work should focus on methods of increasing the sensitivity of binding to bacteria of mixed NPs in high protein, while retaining the long circulating ability in the circulation.

4. 3. Materials and Methods

4. 3. 1. Chemicals

All chemicals were obtained from Sigma-Aldrich and used as received unless otherwise specified.

4. 3. 2. Animals

All procedures were performed in accordance with principles as set forth by the MIT Committee on Animal Care as quickly as possible with the intent to minimize pain and

distress. Procedures were approved by the MIT Committee on Animal Care under Langer protocol #0710-055-13.

4. 3. 3. Polymer Synthesis and NP Formulation. The triblock copolymer poly(D, L-lactic-co-glycolic acid)-*b*-poly(L-histidine)-*b*-poly(ethylene glycol) (PLGA-PLH-PEG) was synthesized using a polymer end grafting strategy, as detailed in Chapter 3. NPs were formulated (PLGA-PLH-PEG or PLGA-PEG in the same manner) using modified emulsion/solvent evaporation techniques. In brief, a typical NP formulation was prepared by sonicating 500 uL ethyl acetate containing 2 g/L polymer into 2 mL aqueous solution to form an O/W emulsion, diluted into 8 mL water, and solvent allowed to evaporate for 4 hours prior to purification using ultrafiltration. The reported composition of the NPs includes the percent by weight of PLGA-PLH-PEG that went into the formulation, with the remaining mass being accounted for by PLGA-PEG and either fluorescently labeled PLGA (Alexa-488- or Alexa-647-PLGA) or plain PLGA at 20% by mass.

4. 3. 4. Physicochemical Characterization. ***ZetaPALS analysis.*** NPs were prepared, purified, and resuspended in pH-adjusted aqueous solution at ~1 mg/mL. Similarly, cells were centrifuged, washed, and resuspended in pH-adjusted salt solutions at ~350k/mL. To measure the zeta potential in BSA, ~1 mg/mL NPs were resuspended in pH ~6.0 solution with or without 4 g/dL BSA and allowed to equilibrate for 30 min prior to analysis. Size and zeta potential were measured by quasi-elastic laser light scattering using a ZetaPALS dynamic light scattering detector (15 mW laser, incident beam 676 nm, Brookhaven Instrument Corporation), collecting data from 3 or more runs per sample.

X-ray Photoelectron Spectroscopy (XPS). NPs were prepared, purified, then lyophilized to yield 1-3 mg of powder per sample. The NP powder was then analyzed on a PH1

VersaProbe II XPS (MIT Center for Materials Science and Engineering) with the expert technical help of Elisabeth Shaw using 3 sweeps with PE 187.85, 50W, and 200 um.

4. 3. 5. Nanoparticle-Bacterium Binding Studies. ***Bacterial Culture.*** *Staphylococcus aureus* (ATCC# 25923) were cultured in tryptic soy broth (BD# 211825). Initially, colonies were streaked on a TSB-agar plate, selected, inoculated into 5 mL of growth medium and allowed to grow overnight in an incubated shaker at 37°C. The resulting suspension was diluted into 80% sterile glycerol solution and frozen at -80°C. For experimentation, a small amount of frozen bacteria were collected using a sterile inoculating loop and transferred to 5 mL of TSB media. This suspension was then allowed to grow overnight prior to experimental manipulation.

Flow Cytometry NP-488-Bacteria Binding Assays. PLGA-PLH-PEG, PLGA-PEG, or mixed PLGA-PLH-PEG / PLGA-PEG NP-488s were prepared, purified, and concentrated into 100 uL of pure water. *S. aureus* bacteria were overgrown overnight in 5 mL of growth medium, spun down, washed in saline solution, then resuspended in pH-adjusted solutions using a dilute aqueous HCl solution to an OD_{600} ~0.3. NP-488 were added to the bacteria at 150 ug/mL with or without bovine serum albumin (BSA) at the desired concentration and incubated for ~30 minutes. After incubation was complete, bacteria were spun down, unbound NP-488 in the supernatant were removed, bacteria were resuspended in PBS pH 7.4, and run on a flow cytometer (FACSCalibur, BD Biosciences, Koch Institute Flow Cytometry Core). Forward scatter (FSC), side scatter (SSC), green fluorescence (ex: 488, filter: 530/30), and red fluorescence (ex: 488, filter: 650 LP) data were collected on a minimum of 10,000 events per sample. Bacteria were gated for live using FSC vs. SSC plots using an untreated negative control for reference.

The mean fluorescence of the distributions in the green fluorescence channel were calculated using FlowJo v9.5 or higher software and recorded in at least triplicate. Binding relative to no BSA was calculated as the percentage of bacteria-associated fluorescence divided by the mean fluorescence of NP and bacteria treated incubated without any BSA present.

4. 3. 6. Nanoparticle-Mammalian Cell Binding Studies. ***Cell Culture.*** RAW 264.7 murine macrophages (ATCC# TIB-71) were cultured in Dulbecco's Modified Eagle's Medium (DMEM) with 10% fetal bovine serum (FBS) at 37°C and 5% CO_2. Cells were subcultured by scraping and passaging in 1:3 to 1:6 ratios up to and including passage ~9. LNCaP prostate adenocarcinoma cells (ATCC# CRL-1740) were cultured in phenol red-free RPMI-1640 medium supplemented with 10% FBS and 1% penicillin/streptomycin at 37°C and 5% CO_2. LNCaPs were subcultured by using 0.05-0.25% trypsin/EDTA-based methods at a passage ratio of 1:3 with no more than ~15 passages.

Flow Cytometry NP-488 Binding Assays. The day before conducting the experiment, RAW 264.7 cells or LNCaP cells were collected and plated onto 6-well plates to yield a 70%+ confluent monolayer within 24 hours. On the day of experiments, PLGA-PLH-PEG, PLGA-PEG, or mixed PLGA-PLH-PEG / PLGA-PEG NP-488s were prepared, purified, and concentrated into 100 uL of pure water. NP-488 were added to the cells in a pH-adjusted salt solution (pH 5.5, 7.4, or the indicated pH, as appropriate) and incubated for ~2 hr, or for the indicated period of time in the case of kinetic studies. After incubation was complete, unbound NP-488 in the supernatant were removed, cells were washed at least 3x using PBS pH 7.4, then run on a flow cytometer (FACSCalibur, BD Biosciences, Koch Institute Flow Cytometry Core). Forward scatter (FSC), side scatter

(SSC), green fluorescence (ex: 488, filter: 530/30), and red fluorescence (ex: 488, filter: 650 LP) data were collected on a minimum of 10,000 events per sample. Cells were gated for live using FSC vs. SSC plots using an untreated negative control for reference. The mean fluorescence was calculated using FlowJo v9.5 or higher software.

Bacteria-LNCaP Cell Competition Assay. To evaluate bacteria-associated fluorescence in the presence of a LNCaP monolayer, *S. aureus* bacteria were cultured as before and added to a ~70% confluent layer of LNCaP cells in 6-well plates in a pre-warmed pH 6.0 PBS solution to yield an OD_{600} ~0.3. NP-488 (150 ug/mL) were added to the suspension containing bacteria and a LNCaP cell monolayer and incubated for ~30 minutes. After this period, the bacteria solution was collected, spun down, resuspended in pH 7.4 PBS, then run on a flow cytometer to assess bacteria-associated green fluorescence, as described previously. The mean fluorescence of the distribution was analyzed using FlowJo v9.5 or higher software and expressed as fold fluorescence relative to untreated control.

Mechanism of Uptake Studies. The NP mechanism of uptake was evaluated using specific inhibitors of uptake pathways. LNCaP cells were plated onto 6-well plates at ~70% confluence (approximately 40,000 cells per cm^2) in phenol red-free complete growth medium. To perform the experiments, the specific inhibitors were incubated with the cells in PBS pH-adjusted to pH 5.5 using a dilute HCl solution. Clathrin-mediated endocytosis (CME) was blocked by pre-incubation with monodansylcadaverine (MDC) at 200 uM for 10 min. Macropinocytosis was blocked by pre-incubation with 2 uM rottlerin for 30 min. Following the preincubation, the NPs were added to the mixture and

incubated for ~2 hr at 37°C and 5% CO_2 in the dark. Following incubation, the cells were washed with PBS pH 7.4, collected, and analyzed on a flow cytometer as before.

Fluorescence Imaging. On the day before experiments, cells were plated onto Lab-Tek II CC^2 chamber slides (Thermo Scientific #154917) to achieve approximately 70% confluence within 24 hours. On the day of experiments NP-488 were prepared, purified, resuspended in a small volume of sterile water, then added to the cells in pH-adjusted PBS media at pH 5.5. The chamber slides were placed in an incubated shaker for either 30 min or 2 hours at 37°C to allow NP-488 binding/uptake to occur. Following incubation, the cells were washed with PBS pH 7.4, fixed in 4% formalin solution, washed again with PBS, covered with a drop of VECTASHIELD mounting medium with DAPI (Vector Laboratories) per well, coverslipped, then taken immediately for fluorescent laser scanning confocal imaging (Zeiss LSM 510 meta, W. M. Keck Microscopy Facility, Whitehead Institute at MIT). Excitation lasers used: 405 nm for blue channel and 488 nm for green channel.

4. 3. 7. Pharmacokinetics. ***Data Collection.*** Male Balb/c mice that were at least 4 weeks old (Charles River Laboratories) were allowed food and water *ad libitum*. On the day of experiments, the mice (N=4 per group) were gently restrained and dosed with 2 mg of Alexa-647-PLGA-modified NPs per mouse (~80 mg/kg) in a total volume of 400 uL per mouse, delivered as a bolus push into the tail vein. At the desired time point, a drop of blood (~100 uL) was collected by performing a small incision across the tail vein. The NP-associated fluorescence was measuring using an IVIS Spectrum-bioluminescent and fluorescent imaging system (Xenogen Corporation), excitation 640 nm, emission 800 nm,

3 sec exposure time. The drop of blood was circled as a region of interest (ROI) and the average radiant efficiency calculated.

Pharmacokinetic Modeling. To evaluate the pharmacokinetic parameters, a two compartment model was assumed:

(Equation 4.1) $$F = Ae^{-\alpha t} + Be^{-\beta t}$$

Here, α and β are related to the distribution and elimination half-lives, respectively, according to the following:

(Equation 4.2) $$t_{\frac{1}{2},distribution} = \frac{\ln(2)}{\alpha}$$

(Equation 4.3) $$t_{\frac{1}{2},elimination} = \frac{\ln(2)}{\beta}$$

To fit the data to this model (Equation 4.1), the average radiant efficiency at the t = 5 min time point was assumed to be equal to 100% of the dose and background was subtracted to yield data ranging from 0 to 1. The parameters were determined by minimizing the sum of the residuals using the nonlinear optimization algorithm "GRG nonlinear" available through Microsoft Excel's "Solver" toolkit and confirmed independently using MatLab's NLINFIT program.

4. 3. 8. Biodistribution. ***Quantitative analysis.*** Alexa-647-PLGA-modified NPs (53% PLGA-PLH-PEG or PLGA-PEG) were prepared and purified. 4 week old or greater male Balb/c mice were injected with 2 mg NP/mouse as a single bolus suspended in 200 uL PBS solution via the tail vein. Six hours later, the mice were euthanized via CO_2 inhalation and necropsied, collecting the liver, lungs, kidneys, spleen, heart, and stomach with N=3. Each organ was weighed individually and the fluorescence per organ evaluated using an IVIS system (Xenogen Corporation), excitation = 640 nm, emission = 800 nm, exposure time = 3 sec. The average radiant efficiency from each organ was evaluated by

circling each organ as a region of interest, and the background was subtracted from an untreated mouse (N=2).

Confocal microscopy. The organ-level distribution of NPs was evaluated by collecting organs where the NPs were likely to have accumulated – the spleen, liver, kidney, and stomach. These organs were collected, embedded in O.C.T., then slowly frozen on dry ice for approximately 2 hours. The frozen tissue blocks were then transferred to a -80°C freezer until ready for sectioning. Sectioning was performed by the MIT Koch Institute Histology Core Facility with the expert technical assistance of Michael Brown, mounted onto glass slides, then stored at -80°C until microscopy. The slides were then imaged using a PerkinElmer Ultraview Spinning Disk Confocal microscope (W. M. Keck Microscopy Facility, Whitehead Institute, MIT), excitation 640 nm.

4. 3. 9. Statistics All data are expressed as mean ± SD. Differences between groups were assessed using one-way ANOVA. Post hoc group comparisons were done using Fisher's LSD method. A significance level of $p < 0.05$ was used for all comparisons.

4. 4. Acknowledgments. The *in vivo* PK and biodistribution studies were designed, executed, and analyzed with the expert assistance or advice of Eric Pridgen, Pedro Valencia, and Nicolas Bertrand. Confocal imaging was performed with expert assistance of Wendy Salmon.

4. 5. References

1. Huh, A. J.; Kwon, Y. J., "Nanoantibiotics": A New Paradigm for Treating Infectious Diseases Using Nanomaterials in the Antibiotics Resistant Era. *J Control Release* 2011, 156, 128-145.

2. Gold, H. S.; Moellering, R. C., Jr., Antimicrobial-drug resistance. *N Engl J Med* 1996, 335, 1445-53.

3. Levy, S. B.; Marshall, B., Antibacterial Resistance Worldwide: Causes, Challenges and Responses. *Nat Med* 2004, 10, S122-S129.

4. Boucher, H. W.; Talbot, G. H.; Bradley, J. S.; Edwards, J. E., Jr.; Gilbert, D.; Rice, L. B.; Scheld, M.; Spellberg, B.; Bartlett, J., Bad Bugs, No Drugs: No ESKAPE! An Update from the Infectious Diseases Society of America. *Clinical Infectious Diseases* 2009, 48, 1-12.

5. Overbye, K.; Barrett, J., Antibiotics: where did we go wrong. *Drug Discovery Today* 2005, 10, 45-52.

6. Bush, K.; Courvalin, P.; Dantas, G.; Davies, J.; Eisenstein, B.; Huovinen, P.; Jacoby, G. A.; Kishony, R.; Kreiswirth, B. N.; Kutter, E.; Lerner, S. A.; Levy, S.; Lewis, K.; Lomovskaya, O.; Miller, J. H.; Mobashery, S.; Piddock, L. J.; Projan, S.; Thomas, C. M.; Tomasz, A.; Tulkens, P. M.; Walsh, T. R.; Watson, J. D.; Witkowski, J.; Witte, W.; Wright, G.; Yeh, P.; Zgurskaya, H. I., Tackling antibiotic resistance. *Nat Rev Microbiol* 2011, 9, 894-896.

7. Piddock, L., The crisis of no new antibiotics-what is the way forward? *Lancet Infectious Diseases* 2012, 12, 249-253.

8. Fernebro, J., Fighting bacterial infections-Future treatment options. *Drug Resistance Updates* 2011, 14, 125-139.

9. Hancock, R.; Nijnik, A.; Philpott, D., Modulating immunity as a therapy for bacterial infections. *Nature Reviews Microbiology* 2012, 10, 243-254.

10. Barrett, J., Can biotech deliver new antibiotics? *Current Opinion in Microbiology* 2005, 8, 498-503.

11. Zhang, L.; Pornpattananangku, D.; Hu, C. M.; Huang, C. M., Development of Nanoparticles for Antimicrobial Drug Delivery. *Curr Med Chem* 2010, 17, 585-594.

12. Taylor, E.; Webster, T., Reducing infections through nanotechnology and nanoparticles. *International Journal of Nanomedicine* 2011, 6, 1463-1473.

13. Schroeder, A.; Turjeman, K.; Schroeder, J. E.; Leibergall, M.; Barenholz, Y., Using liposomes to target infection and inflammation induced by foreign body injuries or medical implants. *Expert Opin Drug Deliv* 2010, 7, 1175-89.

14. Maeda, H., Tumor-Selective Delivery of Macromolecular Drugs Via the EPR Effect: Background and Future Prospects. *Bioconjug Chem* 2010, 21, 797-802.

15. Radovic-Moreno, A. F.; Lu, T. K.; Puscasu, V. A.; Yoon, C. J.; Langer, R.; Farokhzad, O. C., Surface charge-switching polymeric nanoparticles for bacterial cell wall-targeted delivery of antibiotics. *ACS Nano* 2012, 6, 4279-87.

16. Gref, R.; Luck, M.; Quellec, P.; Marchand, M.; Dellacherie, E.; Harnisch, S.; Blunk, T.; Muller, R., 'Stealth' corona-core nanoparticles surface modified by polyethylene glycol (PEG): influences of the corona (PEG chain length and surface density) and of the core composition on phagocytic uptake and plasma protein adsorption. *Colloids and Surfaces B-Biointerfaces* 2000, 18, 301-313.

17. Gref, R.; Minamitake, Y.; Peracchia, M. T.; Trubetskoy, V.; Torchilin, V.; Langer, R., Biodegradable Long-Circulating Polymeric Nanospheres. *Science* 1994, 263, 1600-1603.

18. Iizaka, S.; Sanada, H.; Minematsu, T.; Oba, M.; Nakagami, G.; Koyanagi, H.; Nagase, T.; Konya, C.; Sugama, J., Do nutritional markers in wound fluid reflect pressure ulcer status? *Wound Repair and Regeneration* 2010, 18, 31-37.

19. Chambers, H.; Deleo, F., Waves of resistance: Staphylococcus aureus in the antibiotic era. *Nature Reviews Microbiology* 2009, 7, 629-641.

20. Hidron, A. I.; Edwards, J. R.; Patel, J.; Horan, T. C.; Sievert, D. M.; Pollock, D. A.; Fridkin, S. K.; Natl Healthcare Safety Network, T.; Participating Natl Healthcare, S., Antimicrobial-Resistant Pathogens Associated With Healthcare-Associated Infections: Annual Summary of Data Reported to the National Healthcare Safety Network at the Centers for Disease Control and Prevention, 2006-2007. *Infection Control and Hospital Epidemiology* 2008, 29, 996-1011.

21. Poon, Z.; Chang, D.; Zhao, X.; Hammond, P. T., Layer-by-layer nanoparticles with a pH-sheddable layer for in vivo targeting of tumor hypoxia. *ACS Nano* 2011, 5, 4284-92.

22. Labhasetwar, V.; Song, C.; Humphrey, W.; Shebuski, R.; Levy, R., Arterial uptake of biodegradable nanoparticles: Effect of surface modifications. *Journal of Pharmaceutical Sciences* 1998, 87, 1229-1234.

23. Lee, A.; Wang, Y.; Ye, W.; Yoon, H.; Chan, S.; Yang, Y., Efficient intracellular delivery of functional proteins using cationic polymer core/shell nanoparticles. *Biomaterials* 2008, 29, 1224-1232.

24. Cheng, J.; Teply, B. A.; Sherifi, I.; Sung, J.; Luther, G.; Gu, F. X.; Levy-Nissenbaum, E.; Radovic-Moreno, A. F.; Langer, R.; Farokhzad, O. C., Formulation of functionalized PLGA-PEG nanoparticles for in vivo targeted drug delivery. *Biomaterials* 2007, 28, 869-76.

25. Gu, F.; Zhang, L.; Teply, B. A.; Mann, N.; Wang, A.; Radovic-Moreno, A. F.; Langer, R.; Farokhzad, O. C., Precise Engineering of Targeted Nanoparticles by Using Self-Assembled Biointegrated Block Copolymers. *Proc Natl Acad Sci U S A* 2008, 105, 2586-2591.

26. Li, C.; Xia, J.; Wei, X.; Yan, H.; Si, Z.; Ju, S., pH-Activated Near-Infrared Fluorescence Nanoprobe Imaging Tumors by Sensing the Acidic Microenvironment. *Advanced Functional Materials* 2010, 20, 2222-2230.

Chapter 5

Polymeric Nanoparticles for Co-Delivery of Silver(I) and Vancomycin

5. 1. Introduction

Drug resistance (DR) to antibiotics is one of the most significant challenges in modern medicine.[1] Every major drug class introduced into clinical practice thus far has been susceptible to DR.[2, 3] Even more troubling, the speed with which DR emerges is remarkable. Resistance can emerge in the laboratory on the order of hours,[4] and despite extensive best practices training and implementation by physicians, DR typically emerges in the clinic within 3-5 years of use.[5] Clearly, there is a need to explore methods that might boost the effectiveness of therapy and reduce the potential for DR emerging.

Various strategies are being explored to reduce the risk and mitigate the impact of DR. In addition to new small molecule-based screening approaches, alternative agents such as antimicrobial peptides,[6] bacteriophages,[7] antivirulence strategies or drug potentiators,[3, 8] nanoparticles (NP),[9-11] and drug combinations have been major areas of interest (see Chapter 2 for further discussion). In particular, drug combinations offer several potential advantages, including more than one mechanism of action and the potential for synergistic effects. These advantages may translate into reduced hospital stays, lower mortality, and potentially reduced risk of DR. Drug combinations can also be used to increase the spectrum of coverage, particularly during empiric treatment of an infection. Several drug combinations are already successfully used in the clinic. For example, β-lactamase inhibitors such as clavulanate, sulbactam, or tazobactam are routinely

combined with β-lactams such as ampicillin, amoxicillin, or piperacillin to broaden their spectrum of activity and improve their effectiveness.[12] Trimethoprim-sulfamethoxazole (TMP-SMX) is a widely used combination that potentiates the effect of each drug in isolation by sequentially inhibiting bacterial enzymes that lead to synthesis of tetrahydrofolic acid.[13] Other notable antibiotic combinations are listed in Table 5.1.

Table 5.1. Selected drug combinations and their advantages

Combination	**Mechanisms**	**Spectrum**	**Advantages of combination**
Trimethoprim (TMP) Sulfamethoxazole (SMX)	The combination inhibit synthesis of tetrahydrofolic acid sequentially	Gram-positive, Gram-negative	Synergy[13]
Daptomycin (DAP) Rifampicin (RIF)	DAP inserts into bacterial membrane, causing leakage; RIF inhibits RNA synthesis	Gram-positive, especially *Enterococci*	Synergy
Metronidazole (MET) Amoxicillin (AMX)	MET produces toxic free radicals inside bacteria; AMX targets the cell wall	Gram-positive, Anaerobes, especially *Helicobacter pylori*	Greater efficacy[14]
Quinupristin Dalfopristin (a.k.a. Synercid)	The combination inhibits bacterial protein synthesis	Gram-positive (drug resistant)	Synergy[15]

The full potential of drug combination therapy is often difficult to realize *in vivo*. Drugs tend to demonstrate synergy within a narrow range of drug concentrations and ratios. This "window of synergy" can be complex to achieve in patients, particularly if the pharmacokinetics of the single agents are significantly different from one another. Another challenge of drug combination therapy is toxicity, especially in patients with

comorbidities or on other medications. Consequently, there is a need to develop strategies that can achieve synergistic combination ratios more readily while simultaneously reducing drug toxicity. A method to achieve these aims might be to encapsulate the two drugs to be combined inside of a single NP carrier, then targeting the carrier to the infection site. By combining the two drugs inside of a single NP, synergistic drug ratios can be controlled more tightly in a spatiotemporal manner. By targeting the NP to the infection, less drug can be released systemically and more can reach the site, which might be able to reduce drug toxicity while boosting the effectiveness of therapy. In a step towards improving antibiotic drug targeting and therapy, we previously developed a NP drug delivery system based on the triblock copolymer poly(lactic-co-glycolic acid)-*block*-poly(L-histidine)-*block*-poly(ethylene glycol) (PLGA-PLH-PEG).[16] These NPs were demonstrated to encapsulate and deliver vancomycin, a glycopeptide commonly used to treat drug-resistant Gram-positive infections.

The goal of the present work was to develop a method of co-delivering two agents in a single NP to take a step towards potentially improving the efficacy of drug therapy, broaden the spectrum of activity, and reduce the risk of DR emerging. Of the various agents that could be co-delivered with vancomycin, silver has potential because it: (1) demonstrates synergistic effects with vancomycin *in vitro* (private communication, Timothy Lu),[17] (2) has multiple mechanisms of action, making it intrinsically more resistant to DR,[18] (3) has a separate mechanism of action from vancomycin, which reduces the risk of cross DR emerging, and (4) has broad spectrum activity. Silver has been used as an antimicrobial since antiquity, though the rise of the antibiotic era in the 1940s saw its use and development decline significantly. However, the spread of

antibiotic resistant organisms has led to a renaissance both in its use and development as an antimicrobial. Currently, two silver products are used with some degree of regularity in the clinic. Silver sulfadiazine, a combination of silver(I) and the sulfonamide antibiotic sulfadiazine, is used as a topical antibiotic to treat or prevent second or third degree burns.[19] Applied topically as a thick 1% cream, it is favored for its wide spectrum of activity against both Gram-positive and Gram-negative bacteria as well as certain fungi. Silver nitrate (0.5%) is used as an antimicrobial solution, typically to clear topical infections or remove warts. In addition, several experimental approaches are in development that might broaden the clinical utility of this antimicrobial. Recent work has shown its advantages when incorporated into wound dressings or implant materials, where it is favored for its broad spectrum activity.[20-25]

A significant obstacle to using silver as antimicrobial for treating systemic infections has been challenges in devising methods to increase its stability in the body, since silver ions tend to interact with many biological components (particularly proteins and chloride ions). Other broad challenges include toxicity and off-target effects. Various types of NPs have been explored to address these issues, particularly silver(0) NPs, which are usually formed by the controlled reduction of silver nitrate.[26] These NPs demonstrate several desirable properties including controlled release of silver(I) and efficient microbial growth control.[27-29] However, the systemic delivery potential of silver(0) NPs is still complicated by potential for non-specific interactions, challenges in targeting infection sites, and toxicity.[28, 30-32] Alternative approaches for silver delivery have been explored, involving a wide variety of nanoscale structures. In particular, dendrimers have been favored due to their well-defined structure, intrinsic toxicity to bacteria, and potential for

systemic application.[33] Silver(I) is typically coordinated to the dendrimer structure by incubation with silver nitrate followed by reduction step to yield a defined nano-scale structure.[34-36] There has been broad interest in designing polymer/silver composite nanomaterials. For example, a composite of small (~10 nm) silver NPs encapsulated in poly(divinylbenzene) NP (~100 nm) was formed.[37] In another interesting example, the controlled polymerization of benzylthiocyanate on silver NPs led to a core-shell structure, with a 40 nm silver NP being encased in an 8 nm thick polymeric shell.[38] While these and many other polymer/silver composites are very interesting, use of known biocompatible and biodegradable polymers is preferred for biomedical applications due to the difficulties in predicting toxicity in humans. Accordingly, several biocompatible materials have been used to create polymer/silver nanocomposites, including nanofibers 420-590 nm in diameter made of PLGA with silver NP dispersed, which were shown to have antibacterial effects against *S. aureus* and *Klebsiella pneumoniae*.[39] In a striking example, PGA-capped silver NPs encapsulated in PLGA were shown to have both extended release of silver over 85 days and remarkable *in vitro* potency.[40] Further demonstrating the broad potential of silver nanomaterials, silver-coated magnetic nanoparticles were designed to penetrate biofilms and kill bacteria.[30] Despite these promising advances, there is still a need to explore methods for the targeted, systemic delivery of silver, including methods that might enable co-delivery of silver with an antibiotic. Of the various structures that could be used to achieve these aims, biodegradable polymeric NPs, as a class of nanomaterials, have generally shown excellent potential in drug delivery with demonstrated examples of disease targeting, drug encapsulation, and low toxicity or immunogenicity.[41-43] However, encapsulation of

silver ions in polymeric NP is a challenge due to their intrinsic hydrophilicity and size. Therefore, a method for achieving a reasonable loading of silver (greater than ~1% w/w) in a polymeric NP capable of encapsulating another drug would be beneficial.

Herein, we describe a method for loading silver onto drug-encapsulated polymeric NPs, demonstrating the potential of this system to inhibit the growth of the clinically relevant pathogens *Staphylococcus aureus* and vancomycin-resistant *Enterococcus faecalis* (VRE). More specifically, the results show the formation of silver-containing, vancomycin-encapsulated PLGA-PLH-PEG NPs. We characterize the NPs using light scattering, TEM, XPS, FT-IR, TGA, DSC, and UV-Vis. Further, we show through *in vitro* studies that NPs containing both silver and vancomycin are more effective at inhibiting the growth of *S. aureus* than NPs containing either agent alone. We also show that in *S. aureus* bacteria, for a given level of NP-delivered vancomycin, greater activity was obtained by increasing the amount of silver loaded. Against VRE, we show that silver-containing NPs demonstrate enhanced activity as compared to free silver. We also show that vancomycin either in free, NP-encapsulated, or NP-silver-co-encapsulated form did not demonstrate any significant activity, suggesting that silver incorporation was crucial to antibacterial efficacy against VRE. All NPs had low cytotoxicity to cultured human cells *in vitro* at a concentration above the minimum inhibitory concentration (MIC). In all, these results may inform future work aimed at achieving improved drug combination therapy against bacterial infectious diseases, particularly drug combinations seeking to co-deliver an agent with silver(I).

5. 2. Results and Discussion

5. 2. 1. NP Formulation and Drug Loading. Given our previous studies demonstrating the ability to encapsulate vancomycin in PLGA-PLH-PEG NPs using a modified double emulsion protocol,[16] our primary focus was to devise a method to incorporate silver onto the PLGA-PLH-PEG NPs. Poly-L-histidine (PLH) is known to provide sites for binding of silver ions,[44] and block copolymers containing PLH have been shown to be able to successfully bind silver(I) following incubation in a silver nitrate solution.[45] Consequently, we reasoned that silver- and vancomycin-containing NPs could be formulated using a two step procedure, whereby a double emulsion process could encapsulate the vancomycin (as described previously, see Chapter 3), followed by washing steps to remove unencapsulated vancomycin and excess salts, then an incubation in silver nitrate solution to incorporate the silver (Figure 5.1A). The binding of silver onto histidine-containing materials is known to be relatively rapid, with optimal reaction time being reported as approximately 90 minutes at room temperature.[46] This relatively short reaction time under mild conditions is important, since drug-loaded NPs begin to release their payload immediately in aqueous solution, so a reaction time on the order of several hours or at high temperature might greatly reduce the encapsulated drug (vancomycin) payload.

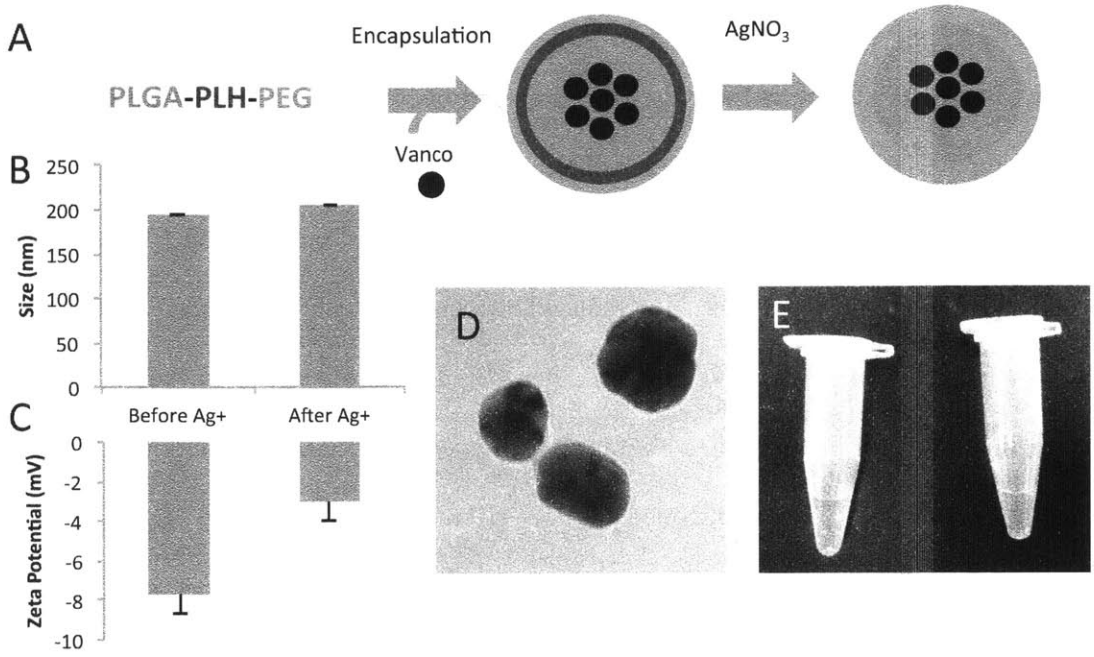

Figure 5. 1. Silver/Vanco Co-Delivery Nanoparticle Formulation and Characterization. (A) Schematic of nanoparticle (NP) formulation strategy. PLGA-PLH-PEG polymer was formulated into NPs using a double emulsion protocol to encapsulate vancomycin. This was followed by incubation of the NP suspension in a silver nitrate solution to lead to silver incorporation. (B) Effect of silver addition on NP size and (C) zeta potential. (D) Transmission electron micrograph (TEM) of NPs following reduction of silver at 68,000x, (E) NP formulation prior to (left) and after (right) addition of reduced silver.

5. 2. 2. NP Characterization. ***Physicochemical properties.*** NPs were formulated using a modified double emulsion process and purified. A silver nitrate solution was added to NPs, and they were incubated for ~90 minutes in the dark at room temperature. Free silver was removed by repeated washing using Amicon Ultra-4 100,000 NMWL filters, then the NPs were characterized in terms of their size and zeta potential by quasi-elastic laser light scattering and transmission electron microscopy (TEM) (Figure 5.1B, C, D). Similar to previous reports,[16] the PLGA-PLH-PEG NPs demonstrated nano-size (195.2±6.7 nm) and slightly anionic zeta potential (-11.9±1.6 mV) at pH 7.4. The addition of silver to the NPs increased the zeta potential, consistent with the adsorption of

the cationic silver(I) on the surface, and increased the NP size. To observe the NP morphology and structure, the NPs were analyzed by TEM, without the addition of any contrast material. The bound silver ions on the NPs were reduced by a short incubation in sodium borohydride, washed, concentrated, and then loaded onto carbon film-supported copper grids. If the silver was not reduced, no contrast could be observed (data not shown). The images (Figure 5.1D) show that the silver is reduced onto the NPs, giving enough contrast for imaging. In addition, a suspension of the reduced silver NPs gave the solution a brownish tint at high concentration (~10 mg/mL NP) (Figure 5.1E).

X-ray Photoelectron Spectroscopy (XPS). To quantify the amount of silver on the PLGA-PLH-PEG NPs, we evaluated their surface composition using XPS. PLGA-PLH-PEG and PLGA-PLH-PEG-Ag NPs were prepared, purified, and lyophilized without a cryoprotectant and taken for XPS analysis (MIT CMSE). PLGA-PEG NPs were prepared in similar fashion to provide an additional control for NP composition. The silver-loaded PLGA-PLH-PEG NPs had 0.6 mol% elemental silver (Table 5.1) in the top ~10 nm, corresponding to approximately ~4.6% (w/w) loading in this region. In contrast, no silver could be detected in the PLGA-PLH-PEG or PLGA-PEG NPs. This is in good agreement with the expected loading from theoretical arguments, which suggest a loading ~4-5% (w/w) throughout the entire NP structure, if one assumes a 1:1 binding of silver(I) per histidine monomer. Since the PLH is relatively enriched on the surface due to its hydrophilicity, this suggests that the silver loading is more towards the NP surface and that less silver is likely to be found towards the NP core. This is consistent with the relatively short incubation time under which silver could be loaded onto the NPs (~90 min), which is only enough time for silver ion diffusion to occur through the top layers. It

is interesting to note also that these data suggest that significant PLH is present in the top layers, as evidenced by the increase in nitrogen (0.0 to 2.2 mol%) and reduction in oxygen (40.9 to 36.3 mol%) content. It may be that during the NP formulation procedure, the cationic PLH polymer competes for the NP surface with the hydrophilic PEG polymer. This is consistent with observations of protein binding and zeta potential explored in greater detail in Chapter 4. These numbers for silver loading are also consistent with quantification using a selective silver ion electrode, which showed an approximate loading of silver of 2.6±0.7% (w/w).

Table 5.2. X-ray Photoelectron Spectroscopy Analysis of Nanoparticles (some data taken from Table 4.1)

	Mol % (Top ~10 nm of NP surface)			
Nanoparticle	**C (C 1s)**	**O (O 1s)**	**N (N 1s)**	**Ag (Ag 3d)**
PLGA-PLH-PEG + Ag	57.9	40.4	1.1	0.6
PLGA-PLH-PEG	61.4	36.3	2.2	0.0
PLGA-PEG	59.1	40.9	0.0	0.0

Fourier Transform Infrared Spectroscopy (FT-IR). We used FT-IR to investigate the potential interaction site of silver with the PLGA-PLH-PEG. Relative to pure PLGA-PLH-PEG, we observed a marked enhancement of transmittance (reduction in absorbance) in the region corresponding to the ring CN stretch, imidazole ring bend, and ring CH bend (peak at 1374 cm^{-1}), as well as a general blueshift of 9-14 cm^{-1} in that region (1385 to 1394; 1360 to 1374) (Table 5.2). Consistent with previous observations,[47] this suggests that a potential interaction site with silver may be through imidazole group. However, it should be noted that establishing this with great precision is very difficult in a mixed species as is the case with the PLGA-PLH-PEG polymer, where interactions

between the PLH chains, with the PLGA or PEG regions, the polydispersity of the NPs or interference from salts during preparation may make interpretation of the highly convoluted FT-IR spectra difficult.

Table 5.3. Fourier Transform Infrared Spectroscopy Analysis of Nanoparticles

PLGA-PLH-PEG	PLGA-PLH-PEG + Ag
1751 s	1750 s
1455 w	
1422 w	1418 w
1385 w	1394 w
1360 w	1374 s
1342 w	
1273 w	1274 w
1163 m	1170 m
1089 s	1090 s
957 w	957 w
843 w	835 w

Thermogravimetric Analysis (TGA). The thermal properties of the silver-containing and untreated PLGA-PLH-PEG NPs were compared to assess the impact of silver loading (Table 5.3). The incorporation of silver into the NPs leads to a 9°C increase in the decomposition temperature and 15°C increase in the first derivative peak. These are indicative of greater thermal stability of the silver-containing NPs. It may be that the addition of inter-chain bonding or due to the formation of more endothermic bonds mediated by the silver ion mediate the higher decomposition temperature.

Table 5.4. Differential Scanning Calorimetry Analysis of Nanoparticles

Nanoparticle	Onset T (°C)	First Derivative Peak (°C)
PLGA-PLH-PEG + Ag	338	365
PLGA-PLH-PEG	329	350

Differential Scanning Calorimetry (DSC). To obtain greater insight into the properties of the silver-incorporated PLGA-PLH-PEG NPs, we performed DSC to determine the

glass transition temperature (Table 5.4). It appears that the incorporation of silver has a plasticizing effect on the PLGA-PLH-PEG NPs. It may be that the silver ions, while increasing the number of bonds leading to an increase in the decomposition temperature per gram, actually increase the free volume of the polymer chains. This is consistent with the observation of increased NP size on addition of silver ions (Figure 5.1B). These observations could potentially be explained by noting that the addition of a hydrophilic ion on the surface might increase the overall hydrophilicity of the NP, leading to greater water incorporation. These changes may therefore lead to an easier transition from a melt to a glass, slightly reducing the glass transition temperature.

Table 5.5. Glass Transition Temperature Determined by Differential Scanning Calorimetry

Nanoparticle	**Glass Transition Temperature (°C)**
PLGA-PLH-PEG + Ag	37
PLGA-PLH-PEG	44

UV-Vis Absorption. PLGA-PLH-PEG NPs were formulated and incubated with or without silver reduced then analyzed by a UV-vis spectrophotometer (Figure 5.2). The data show that the silver-containing PLGA-PLH-PEG NPs demonstrate significantly greater UV-vis absorption in the range 200-450 nm than plain PLGA-PLH-PEG. In addition, notable features include a shoulder region at 250-300 nm and a broad peak centered at ~380 nm. Both of these features are consistent with a previous report of histidine-silver complex formation.[46]

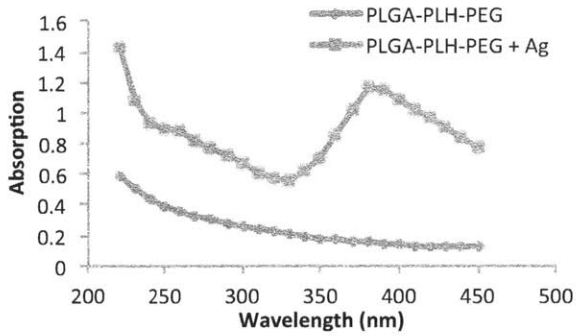

Figure 5. 2. UV-Vis Analysis of PLGA-PLH-PEG and silver-containing PLGA-PLH-PEG NPs. PLGA-PLH-PEG NPs with or without silver were suspended in water and their UV-vis absorption in the range 200-450 nm determined. Most notably, addition of silver results in a shoulder region in the ~250-300 nm range and a peak ~380 nm, similar to previous reports of histidine-silver complexes.[46]

5. 2. 3. Antibacterial Studies. Next, we sought to evaluate the antibacterial properties of silver and vancomycin as free drugs against *Staphylococcus aureus*. After establishing the minimum inhibitory concentration (MIC) of free silver (4 ug/mL) and vancomycin (1.6 ug/mL), we performed a checkerboard analysis to evaluate the combination drug properties (Figure 5.3A). We observed synergistic inhibition of bacterial growth of the two drugs (Figure 5.3B).

A

% Growth	Frac. MIC Silver							
Frac. MIC Vanco	0	0.031	0.063	0.125	0.25	0.5	1	2
0	97%	94%	92%	84%	76%	65%	1%	1%
0.016	90%	88%	95%	91%	84%	66%	5%	1%
0.031	94%	99%	103%	90%	83%	67%	1%	1%
0.063	88%	100%	99%	90%	82%	66%	3%	1%
0.125	88%	81%	81%	79%	83%	59%	1%	1%
0.25	88%	83%	79%	84%	75%	3%	1%	1%
0.5	57%	68%	66%	51%	15%	1%	1%	1%
1	10%	3%	3%	3%	1%	1%	1%	1%

B

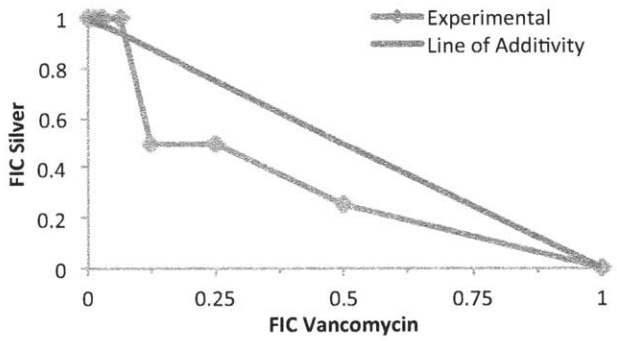

Figure 5. 3. Free silver and vancomycin are synergistic against *Staphylococcus aureus*. (A) Heat map demonstrating the growth inhibitory effects using the checkerboard method. Numbers represent the average growth compared to untreated bacteria. Colors correspond to ranges of growth inhibition, with high inhibition corresponding to green, intermediate corresponding to yellow, and low corresponding to red. (B) Isobologram demonstrating synergy between free vancomycin and silver. FIC is the fractional inhibitory concentration of the indicated drug, defined as $FIC_x = C_x/MIC_x$ where C_x is the lowest concentration where no visible growth occurs.

To evaluate the antibacterial properties of silver and vancomycin loaded NPs, we performed growth inhibition studies using the broth microplate dilution method. The NPs containing both silver and vancomycin, T(Vanco, Silver), were found to have the most potent growth inhibitory effects (Figure 5.4). The greatest impact was seen in terms of the vancomycin content, where T(Vanco, Silver) NPs had significantly improved growth inhibition than T(Vanco) and were more potent than free vancomycin, though they had the same MIC (1.56 ug/mL vancomycin for both T(Vanco, Silver) and free vanco)

(Figure 5.4A). Interestingly, the shape of the inhibitory curves is approximately the same in the case of the T(Vanco) and the free vanco, but exhibited a lower slope with the T(Vanco, Silver) NPs. In terms of the silver content, the addition of vancomycin led to a more subtle effect on growth inhibition (Figure 5.4B). The MIC for T(Vanco, Silver), T(Silver) and free silver were not significantly different (4 ug/mL silver), though the slope of the inhibition curve was the smallest with the T(Vanco, Silver), indicating slightly more potent antibacterial activity of this formulation. Similar to our previous work (see Chapter 3), we sought to determine the pH-dependence of the activity of the co-delivered agents. However, the NPs demonstrated a lack of stability at pH ~6.0 in the presence of proteins and bacteria (data not shown). It may be that the cationic charge produced by the histidine region at this pH leads to destabilization.

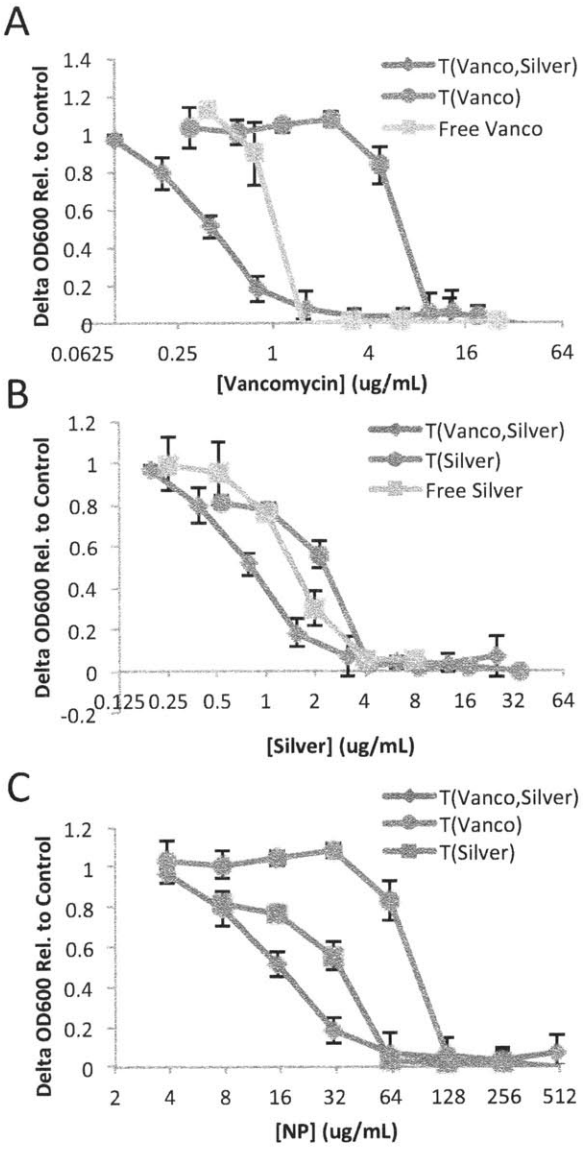

Figure 5. 4. Bacterial Growth Inhibition of Silver- and/or Vancomycin-containing Nanoparticles. PLGA-PLH-PEG NPs containing vancomycin only (T(Vanco)), silver only (T(Silver)), or both (T(Vanco, Silver)) were assessed for their ability to inhibit the growth of *Staphylococcus aureus* using the broth microplate dilution method. Growth inhibition based on the (A) vancomycin, (B) silver, or (C) NP concentration.

To explore the impact of increasing the total drug loaded onto the NPs, we prepared NPs containing various vancomycin-to-silver (V:S) ratios (Figure 5.5). At a given concentration of vancomycin, incorporation of an increasing amount of silver led to

greater growth inhibition of *S. aureus*, meaning that a lower V:S ratio led to greater amount of activity in terms of the total vancomycin level. This can be understood by noting that a greater amount of total drug was incorporated into the NPs as the V:S ratio decreased. This suggests that maximizing the amount of total drug that is loaded onto the NPs yields the most potent effect against *S. aureus* bacteria.

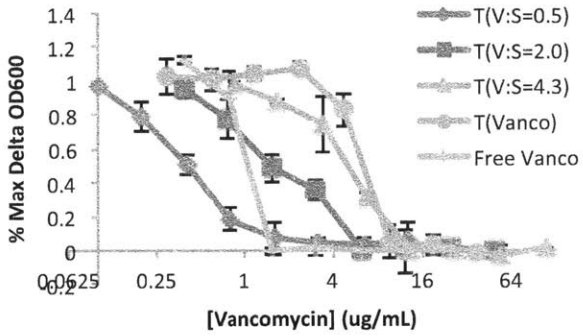

Figure 5. 5. Effect of Vancomycin-to-Silver Drug Loading Ratio on Bacterial Growth Inhibition. PLGA-PLH-PEG NPs were loaded at different ratios of vancomycin-to-silver (V:S) ranging from 0.5-4.3. Increasing the silver content inside of the PLGA-PLH-PEG NPs increases the growth inhibitory effect of the NPs. This can be explained by the greater potency of silver than vancomycin.

We were also interested in understanding the impact of drug co-delivery on bacteria that had developed resistance to vancomycin. This is important since the spontaneous formation of DR during treatment with vancomycin is known to occur. Having the ability to inhibit the growth of the spontaneously-generated vancomycin-resistant mutants with silver would be a significant advantage of a vancomycin and silver co-delivering system. For this purpose, we selected a strain of vancomycin-resistant *Enterococcus faecalis* (VRE) as a model organism to study this phenomenon due to its increasing clinical relevance as well as the increasing concern for its potential to pass vancomycin resistance to other pathogens.[48] We explored the potential of T(Vanco, Silver), T(Vanco), T(Silver), D(Vanco), and free drug formulations to inhibit the growth of VRE using the broth

microplate dilution method. The data show that vancomycin, in any form, did not appear to have any growth inhibitory activity against VRE (Figure 5.6A). Interestingly, the PLGA-PLH-PEG NP formulations of silver demonstrated slightly improved activity against VRE as compared to free silver, though this was quite modest (MICs: T(Vanco, Silver) ~1.6 ug/mL, T(Silver) ~1.6 ug/mL, free silver ~3.1 ug/mL) (Figure 5.6B). In terms of the total mass, there did not appear to be any difference in activity between the T(Vanco, Silver) and the T(Silver) (MICs ~32 ug/mL NP for both) (Figure 5.6C). These data suggest that for treating vancomycin-resistant bacteria, the incorporation of vancomycin is unnecessary. Further, they show that silver-containing NPs are capable of inhibiting the growth of vancomycin-resistant bacteria, which is an attractive property due to the known risk of emergence of vancomycin resistance.

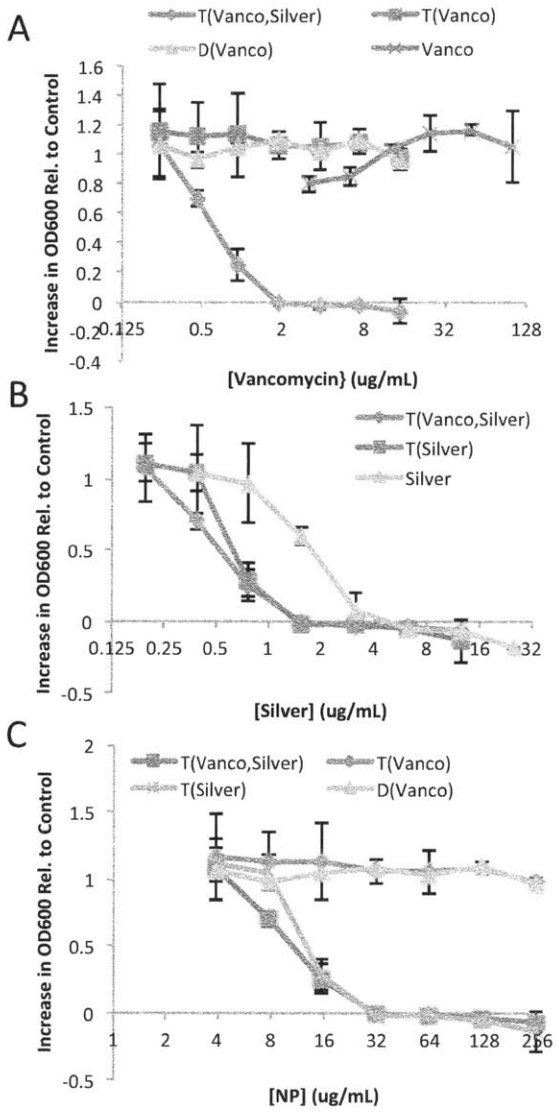

Figure 5. 6. Growth Inhibition Study against Vancomycin-Resistant *Enterococcus faecalis* (VRE). PLGA-PLH-PEG NPs containing silver (T(Silver)), vancomycin (T(Vanco)), or both T(Vanco, Silver) were measured for their growth inhibitory activity against VRE. PLGA-PEG containing vancomycin (D(Vanco)) were used as a control. Data expressed as increase in optical density at 600 nm relative to untreated control.

5. 2. 4. Cytotoxicity. Finally, we sought to examine the cytotoxicity of the different NP formulations, given that low toxicity is a crucial prerequisite for systemic delivery. We incubated ~150 ug/mL NPs (or the corresponding quantity of free silver or vancomycin, in the case of the free drugs) with a model human cell line, LNCaP prostate

adenocarcinoma cells, for 30 min, washed, added complete growth medium, then assessed cell viability using the AlamarBlue assay. We did not observe any significant cytotoxicity from any of the formulations tested (Figure 5.7). We also explored the cytotoxicity of NPs after the silver had been reduced onto the NPs after a short incubation in sodium borohydride. The rationale was to enhance the stability of the silver on the NP surface by forming a silver(0) shell. However, we observed high cytotoxicity of silver reduced NPs, with obvious cell death occurring rapidly on addition to the cells (data not shown), consistent with previous reports of the cytotoxicity of reduced silver NPs.[30] These data suggest that for silver(I)-bound NPs have potential for systemic delivery, methods to reduce the cytotoxicity of reduced silver-PLGA-PLH-PEG NPs are needed.

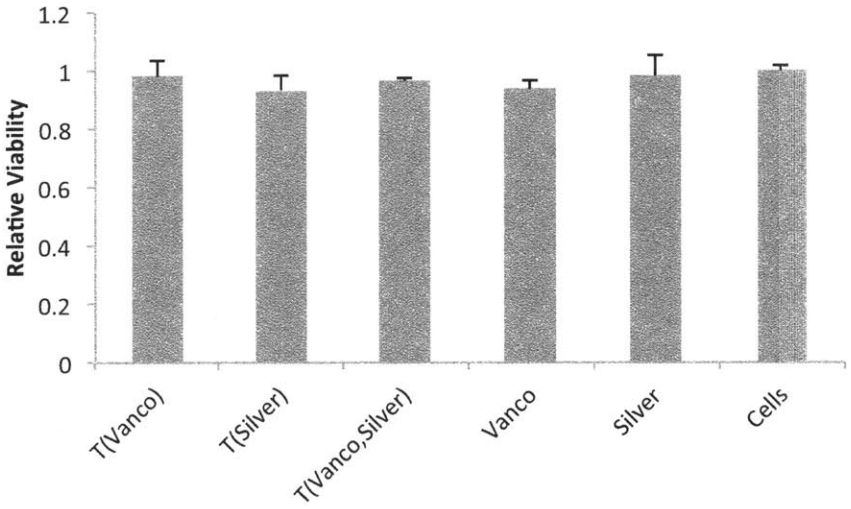

Figure 5. 7. Nanoparticle Cytotoxicity Study. PLGA-PLH-PEG NPs containing vancomycin only, T(Vanco), silver only, T(Silver), both vancomycin and silver, T(Vanco, Silver), and free vancomycin (Vanco) or silver (Silver) were incubated at ~150 ug/mL NP, ~10 ug/mL vancomycin, or 7.5 ug/mL silver with a model human cell line (LNCaP prostate adenocarcinoma) for 30 min, washed, replaced with complete growth medium, then relative viability assayed by AlamarBlue (Invitrogen). At these concentrations, the NP did not demonstrate any significant cytotoxicity.

5. 2. 5. Summary. In summary, we have developed a method for co-delivering silver(I) and vancomycin together using a polymeric PLGA-PLH-PEG NP and explored its potential applicability through *in vitro* bacterial growth inhibition studies as well as model human cell line cytotoxicity studies. We explored the effect of silver loading on NP properties using a variety of analytical techniques, including light scattering, TEM, XPS, FT-IR, TGA, DSC, and UV-Vis. We achieved reasonably good loading of both silver (~2-5 wt%) and vancomycin (~7-8 wt%) by silver/histidine interactions and encapsulation, respectively. In growth inhibition studies against *Staphylococcus aureus*, the NPs containing both vancomycin and silver, T(Vanco, Silver), had improved activity over NPs containing only one or the other drug (T(Vanco) and T(Silver)). Against vancomycin-resistant *Enterococcus faecalis*, T(Vanco, Silver) performed equal to T(Silver), whereas T(Vanco) and free vancomycin had no discernible growth inhibitory effect, suggesting no benefit from delivering vancomycin against this strain of VRE. In cytotoxicity studies, the NPs were non-toxic to human LNCaP cells at concentrations above the MIC, though NPs with reduced silver demonstrated significant toxicity. Taken together, these results suggest that the PLGA-PLH-PEG NPs described herein may have potential for co-delivering silver(I) and vancomycin to treat vancomycin- and silver-sensitive infections. However, more work is needed to continue developing these NPs. In particular, the longer-term stability of silver on the NP surface in complex media needs to be evaluated to ensure that silver remains present on the NP surface. Methods to improve the stability of the NPs under low pH conditions are also needed. In addition, the ability of these NPs to circulate for extended periods of time in the body needs to be evaluated. Finally, the efficacy of these NPs in treating vancomycin- and silver-sensitive infections

needs to be evaluated in a mouse model of infection to confirm the systemic delivery potential of this system.

5. 3. Materials and Methods

5. 3. 1. Chemicals. All chemicals were obtained from Sigma Aldrich and used as received unless otherwise specified.

5. 3. 2. Polymer Synthesis and Characterization. We synthesized the triblock copolymer poly(D, L-lactic-co-glycolic acid)-*b*-poly(L-histidine)-*b*-poly(ethylene glycol) (PLGA-PLH-PEG) using a polymer end grafting strategy as detailed in Chapter 2. PLGA-PEG was synthesized in a similar manner and both polymers were characterized as detailed in Chapter 3.

5. 3. 3. NP Formulation. To form vancomycin-encapsulated NPs, 1 mg of polymer (PLGA-PLH-PEG or PLGA-PEG) dissolved in 15/85 v/v DMSO/ethyl acetate solution was diluted into a final volume of 500 uL of ethyl acetate (with trace DMSO) to form the organic phase. The drug-containing aqueous phase would typically consist of 50 uL of a 4 g/L solution of vancomycin (Sigma Aldrich, St. Louis, MO) dissolved in pure water. The aqueous phase was sonicated into the polymer-containing organic phase for 15 sec at 40% amplitude using a probe tip sonicator (Misonix Sonicator S-4000, Farmingdale, NY). This primary emulsion was then emulsified into 2 mL of a 10% w/v NaCl solution at 40% amplitude for 30 sec. This concentrated double emulsion was diluted into 8 mL of a 5% w/v NaCl solution under magnetic stirring. The NPs were allowed to harden by allowing slow organic solvent evaporation for 4 hours in the hood. NPs were purified by triple filtration using Amicon Ultra-4 100,000 NMWL centrifugal filter units (Millipore,

Billerica, MA) using sterile water to remove unencapsulated drug and residual salts from the emulsion process. NPs without vancomycin were prepared in the same manner, only 50 uL of pure water were used instead of the vancomycin solution, as mentioned above. To load silver, the freshly prepared and purified NPs were resuspended at ~10 mg/mL in pure water, at which point 100-500 ug of silver nitrate were added. The NPs were incubated in the dark at room temperature for approximately 90 minutes, then washed in Amicon Ultra-4 100,000 NMWL centrifugal filter units to remove any excess silver nitrate salts.

5. 3. 4. Quantification of Drug Encapsulation. 2.0 mg of PLGA-PEG or PLGA-PLH-PEG NPs were formulated with 0.4 mg initial vancomycin. Vancomycin encapsulation was determined by quantifying the amount of unencapsulated vancomycin relative to the initial amount of drug by UV absorbance at 220 nm relative to a standard curve. The amount of silver encapsulated was estimated by quantifying the amount of free silver in solution following incubation relative to the initial amount of silver. Free silver quantification was performed using a selective silver ion electrode (Cole-Parmer Silver/Sulfide Electrode, Vernon Hills, IL) relative to a free silver standard curve, as recommended by the manufacturer.

5. 3. 5. Nanoparticle Characterization. ***ZetaPALS Analysis.*** PLGA-PLH-PEG NPs were freshly prepared with or without silver, purified, and resuspended in pH 7.4 salt solution at approximately 0.1 mg/mL. Size and zeta potential were measured for each solution by quasi-elastic laser light scattering using a ZetaPALS dynamic light scattering detector (15 mW laser, incident beam 676 nm, Brookhaven Instrument Corporation).

Transmission Electron Microscopy. PLGA-PLH-PEG NPs were prepared containing silver, washed to remove unbound silver, silver was reduced following a brief (< 5 min) incubation in an excess sodium borohydride solution, washed again, resuspended at ~5 mg/mL in a pure water solution, deposited onto carbon supported copper TEM grids for 5 min, dried, then imaged on a JEOL 200 CX TEM (MIT CMSE) at an accelerating voltage of 200 kV.

X-ray Photoelectron Spectroscopy (XPS). NPs were prepared, purified, then lyophilized to yield 1-3 mg of powder per sample. The NP powder was then analyzed on a PH1 VersaProbe II XPS (MIT CMSE) with the expert technical help of Elisabeth Shaw using 3 sweeps with PE 187.85, 50W, and 200 um.

Fourier Transform Infrared Spectroscopy (FT-IR). 2 mg of NPs without vancomycin were prepared and purified, and split into two 1 mg samples. One sample was treated with 1 mg of silver nitrate in water (PLGA-PLH-EG-Ag), the other was diluted in an equal volume of water with no silver nitrate (PLGA-PLH-PEG). Both were purified by triple filtration, snap frozen in liquid nitrogen, then lyophilized for 4 days without any cryoprotectants. The solid NP powder was analyzed by FT-IR using a Bruker Alpha-E FT-IR Spectrometer (Billerica, MA).

Thermogravimetric Analysis (TGA). 4 mg of NPs without vancomycin were prepared, loaded with 500 ug of silver (if appropriate), washed, then lyophilized without any cryoprotectants. The resulting powders were then loaded onto the TGA analyzer (PerkinElmer Thermogravimetric Analyzer Pyris 1 TGA (Waltham, MA)) and analyzed as directed by the manufacturer.

Differential Scanning Calorimetry (DSC). 4 mg of NP without vancomycin were prepared, loaded with 500 ug of silver (if appropriate), washed, then lyophilized without any cryoprotectants. The resulting powders were analyzed on a Perkin Elmer Pyris 1 Differential Scanning Calorimeter with the expert assistance of Tim McClure (MIT CMSE).

UV-Vis Absorption. 2 mg of NP were prepared and split into two batches. One was treated with 100 ug of silver, the other was left as an untreated control. The two NP batches were washed using Amicon Ultra-4 100,000 NMWL filters, then resuspended at approximately 5 mg/mL in pure water. The UV absorption in the range 250-500 nm was then recorded using a plate reader.

5. 3. 6. Antibacterial Studies. ***Bacterial culture.*** *Staphylococcus aureus* (ATCC# 25923) were cultured in tryptic soy broth (BD# 211825). Initially, colonies were streaked on a TSB-agar plate, selected, inoculated into 5 mL of growth medium and allowed to grow overnight in an incubated shaker at 37°C. The resulting suspension was diluted into 80% sterile glycerol solution and frozen at -80°C. For experimentation, a small amount of frozen bacteria were collected using a sterile inoculating loop and transferred to 5 mL of TSB media. This suspension was then allowed to grow overnight prior to experimental manipulation. Vancomycin-resistant (genotype: vanB ant(6)-I aac(6') aph(2"")) *Enterococcus faecalis* (ATCC#5299) were cultured in the same manner except using brain heart infusion (ATCC# 2174) supplemented with 4 ug/mL vancomycin.

Antibacterial assays. Bacteria from overnight cultures were inoculated into 5 mL media and allowed to enter log phase (OD_{600} ~0.3) after approximately 2 hours of incubation. NPs (PLGA-PLH-PEG or PLGA-PEG) encapsulating vancomycin with or without silver

as appropriate were freshly prepared, purified, and serially diluted into a final volume of 100 uL of sterile water in triplicate at a 2x concentration in clear, flat bottom 96 well plates. Bacteria in log phase were diluted to a theoretical OD_{600} of 0.001 in media and seeded onto the microplates to produce a final volume per well of 200 uL. The OD_{600} was measured immediately before placing into an incubated shaker at 37°C, then ~18-24 hours later. The drug concentration is the total drug concentration present inside the nanoparticles, as determined by loading studies. The MIC was reported as the lowest concentration yielding no obvious bacterial growth.

5. 3. 7. Cytotoxicity Studies. ***Cell culture.*** LNCaP prostate adenocarcinoma cells (ATCC# CRL-1740) were cultured in phenol red-free RPMI-1640 medium supplemented with 10% FBS and 1% penicillin/streptomycin at 37°C and 5% CO_2. LNCaPs were subcultured by using 0.05-0.25% trypsin/EDTA-based methods at a passage ratio of 1:3 with no more than ~15 passages.

Cytotoxicity assay. The toxicity of the NPs was determined using the AlamarBlue assay (Invitrogen Corporation). In brief, the day before experiments, LNCaP cells were seeded onto 24-well plates at a density yielding 70% confluence (~40,000 cm^2). NPs containing vancomycin + silver, vancomycin only, or silver only were prepared, purified, resuspended, then diluted into a PBS solution to yield ~150 ug/mL NP, incubated for 30 minutes, washed, then complete growth medium was added to the cells. The cells were allowed to recover for 48 hours, at which point the AlamarBlue cytotoxicity assay was performed according to the manufacturer's instructions. The data was expressed as viability relative to untreated control on the basis of the colorimetric assay. No significant difference in the trend was observed when the fluorescent data was used for comparison.

5. 3. 8. Statistics. All data are expressed as mean ± SD. Differences between groups were assessed using one-way ANOVA. Post hoc group comparisons were done using Fisher's LSD method. A significance level of $p < 0.05$ was used for all comparisons.

5. 4. Acknowledgments. I would like to thank Vlad Puscasu for help in performing the antibacterial growth studies and for many helpful discussions. I would also like to acknowledge the expert technical assistance of Tim McClure (MIT CMSE) in performing the DSC analysis and data collection, Dr. Ana Jaklenec (MIT Langer Lab) in performing the TGA data collection, and Elisabeth Shaw (MIT CMSE) in collecting the data for the XPS.

5. 5. References

1. Levy, S. B.; Marshall, B., Antibacterial Resistance Worldwide: Causes, Challenges and Responses. *Nat Med* 2004, 10, S122-S129.

2. Payne, D.; Gwynn, M.; Holmes, D.; Pompliano, D., Drugs for bad bugs: confronting the challenges of antibacterial discovery. *Nature Reviews Drug Discovery* 2007, 6, 29-40.

3. Fernebro, J., Fighting bacterial infections-Future treatment options. *Drug Resistance Updates* 2011, 14, 125-139.

4. Kohanski, M. A.; DePristo, M. A.; Collins, J. J., Sublethal antibiotic treatment leads to multidrug resistance via radical-induced mutagenesis. *Mol Cell* 2010, 37, 311-20.

5. Huh, A. J.; Kwon, Y. J., "Nanoantibiotics": A New Paradigm for Treating Infectious Diseases Using Nanomaterials in the Antibiotics Resistant Era. *J Control Release* 2011, 156, 128-145.

6. Zasloff, M., Antimicrobial peptides of multicellular organisms. *Nature* 2002, 415, 389-95.

7. Lu, T. K.; Koeris, M. S., The next generation of bacteriophage therapy. *Current Opinion in Microbiology* 2011, 14, 524-531.

8. Park, B.; Liu, G. Y., Targeting the host-pathogen interface for treatment of Staphylococcus aureus infection. *Seminars in Immunopathology* 2012, 34, 299-315.

9. Abeylath, S. C.; Turos, E., Drug delivery approaches to overcome bacterial resistance to beta-lactam antibiotics. *Expert Opin Drug Deliv* 2008, 5, 931-49.

10. Abeylath, S. C.; Turos, E., Nanobiotics to combat bacterial drug resistance. In *Antibiotic resistance: causes and risk factors, mechanisms and alternatives*, Bonilla, A. R.; Muniz, K. P., Eds. Nova Science Publishers: New York, 2009; pp 425-465.

11. Zhang, L.; Pornpattananangku, D.; Hu, C. M.; Huang, C. M., Development of Nanoparticles for Antimicrobial Drug Delivery. *Curr Med Chem* 2010, 17, 585-594.

12. Calderwood, S. B., Combination beta-lactamase inhibitors, carbapenems, and monobactams. In *UpToDate*, Basow, D. S., Ed. UpToDate: Waltham, MA, 2012.

13. May, D. B., Trimethoprim-sulfamethoxazole: An overview. In *UpToDate*, Basow, D. S., Ed. UpToDate: Waltham, MA, 2012.

14. CHIBA, N.; RAO, B.; RADEMAKER, J.; HUNT, R., METAANALYSIS OF THE EFFICACY OF ANTIBIOTIC-THERAPY IN ERADICATING HELICOBACTER-PYLORI. *American Journal of Gastroenterology* 1992, 87, 1716-1727.

15. Delgado, G.; Neuhauser, M.; Bearden, D.; Danziger, L., Quinupristin-dalfopristin: An overview. *Pharmacotherapy* 2000, 20, 1469-1485.

16. Radovic-Moreno, A. F.; Lu, T. K.; Puscasu, V. A.; Yoon, C. J.; Langer, R.; Farokhzad, O. C., Surface charge-switching polymeric nanoparticles for bacterial cell wall-targeted delivery of antibiotics. *ACS Nano* 2012, 6, 4279-87.

17. Ghosh, S.; Patil, S.; Ahire, M.; Kitture, R.; Kale, S.; Pardesi, K.; Cameotra, S.; Bellare, J.; Dhavale, D.; Jabgunde, A.; Chopade, B., Synthesis of silver nanoparticles using Dioscorea bulbifera tuber extract and evaluation of its synergistic potential in combination with antimicrobial agents. *International Journal of Nanomedicine* 2012, 7, 483-496.

18. Lok, C. N.; Ho, C. M.; Chen, R.; He, Q. Y.; Yu, W. Y.; Sun, H. Z.; Tam, P. K. H.; Chiu, J. F.; Che, C. M., Proteomic analysis of the mode of antibacterial action of silver nanoparticles. *Journal of Proteome Research* 2006, 5, 916-924.

19. Rennekampf, H.; Tenenhaus, M., Local treatment of burns: Topical antimicrobial agents and dressings. In *UpToDate*, Basow, D. S., Ed. UpToDate: Waltham, MA, 2012.

20. Chen, W.; Liu, Y.; Courtney, H.; Bettenga, M.; Agrawal, C.; Bumgardner, J.; Ong, J., In vitro anti-bacterial and biological properties of magnetron co-sputtered silver-containing hydroxyapatite coating. *Biomaterials* 2006, 27, 5512-5517.

21. Podsiadlo, P.; Paternel, S.; Rouillard, J.; Zhang, Z.; Lee, J.; Lee, J.; Gulari, L.; Kotov, N., Layer-by-layer assembly of nacre-like nanostructured composites with antimicrobial properties. *Langmuir* 2005, 21, 11915-11921.

22. Li, Z.; Lee, D.; Sheng, X. X.; Cohen, R. E.; Rubner, M. F., Two-level antibacterial coating with both release-killing and contact-killing capabilities. *Langmuir* 2006, 22, 9820-9823.

23. Fu, J.; Ji, J.; Fan, D.; Shen, J., Construction of antibacterial multilayer films containing nanosilver via layer-by-layer assembly of heparin and chitosan-silver ions complex. *Journal of Biomedical Materials Research Part a* 2006, 79A, 665-674.

24. Sambhy, V.; MacBride, M. M.; Peterson, B. R.; Sen, A., Silver bromide nanoparticle/polymer composites: dual action tunable antimicrobial materials. *J Am Chem Soc* 2006, 128, 9798-808.

25. Dallas, P.; Sharma, V.; Zboril, R., Silver polymeric nanocomposites as advanced antimicrobial agents: Classification, synthetic paths, applications, and perspectives. *Advances in Colloid and Interface Science* 2011, 166, 119-135.

26. Sharma, V.; Yngard, R.; Lin, Y., Silver nanoparticles: Green synthesis and their antimicrobial activities. *Advances in Colloid and Interface Science* 2009, 145, 83-96.

27. Pal, S.; Tak, Y. K.; Song, J. M., Does the antibacterial activity of silver nanoparticles depend on the shape of the nanoparticle? A study of the gram-negative bacterium Escherichia coli. *Applied and Environmental Microbiology* 2007, 73, 1712-1720.

28. Marambio-Jones, C.; Hoek, E. M. V., A review of the antibacterial effects of silver nanomaterials and potential implications for human health and the environment. *Journal of Nanoparticle Research* 2010, 12, 1531-1551.

29. Lara, H.; Ayala-Nunez, N.; Turrent, L.; Padilla, C., Bactericidal effect of silver nanoparticles against multidrug-resistant bacteria. *World Journal of Microbiology & Biotechnology* 2010, 26, 615-621.

30. Mahmoudi, M.; Serpooshan, V., Silver-coated engineered magnetic nanoparticles are promising for the success in the fight against antibacterial resistance threat. *ACS Nano* 2012, 6, 2656-64.

31. Choi, O.; Yu, C.; Fernandez, G.; Hu, Z., Interactions of nanosilver with Escherichia coli cells in planktonic and biofilm cultures. *Water Research* 2010, 44, 6095-6103.

32. AshaRani, P. V.; Mun, G. L. K.; Hande, M. P.; Valiyaveettil, S., Cytotoxicity and Genotoxicity of Silver Nanoparticles in Human Cells. *ACS Nano* 2009, 3, 279-290.

33. Mintzer, M. A.; Dane, E. L.; O'Toole, G. A.; Grinstaff, M. W., Exploiting Dendrimer Multivalency To Combat Emerging and Re-Emerging Infectious Diseases. *Molecular Pharmaceutics* 2012, 9, 342-354.

34. Mahapatra, S.; Karak, N., Silver nanoparticle in hyperbranched polyamine: Synthesis, characterization and antibacterial activity. *Materials Chemistry and Physics* 2008, 112, 1114-1119.

35. Balogh, L.; Swanson, D. R.; Tomalia, D. A.; Hagnauer, G. L.; McManus, A. T., Dendrimer-silver complexes and nanocomposites as antimicrobial agents. *Nano Letters* 2001, 1, 18-21.

36. Esumi, K.; Suzuki, A.; Yamahira, A.; Torigoe, K., Role of poly(amidoamine) dendrimers for preparing nanoparticles of gold, platinum, and silver. *Langmuir* 2000, 16, 2604-2608.

37. van Berkel, K.; Hawker, C., Tailored Composite Polymer-Metal Nanoparticles by Miniemulsion Polymerization and Thiol-ene Functionalization. *Journal of Polymer Science Part a-Polymer Chemistry* 2010, 48, 1594-1606.

38. Kumar, V.; Pradeep, T., Polymerization of benzylthiocyanate on silver nanoparticles and the formation of polymer coated nanoparticles. *Journal of Materials Chemistry* 2006, 16, 837-841.

39. Xing, Z.; Chae, W.; Huh, M.; Park, L.; Park, S.; Kwak, G.; Yoon, K.; Kang, I., In Vitro Anti-Bacterial and Cytotoxic Properties of Silver-Containing Poly(L-lactide-co-glycolide) Nanofibrous Scaffolds. *Journal of Nanoscience and Nanotechnology* 2011, 11, 61-65.

40. Stevanovic, M.; Skapin, S.; Bracko, I.; Milenkovic, M.; Petkovic, J.; Filipic, M.; Uskokovic, D., Poly(lactide-co-glycolide)/silver nanoparticles: Synthesis, characterization, antimicrobial activity, cytotoxicity assessment and ROS-inducing potential. *Polymer* 2012, 53, 2818-2828.

41. Kamaly, N.; Xiao, Z.; Valencia, P. M.; Radovic-Moreno, A. F.; Farokhzad, O. C., Targeted polymeric therapeutic nanoparticles: design, development and clinical translation. *Chem Soc Rev* 2012, 41, 2971-3010.

42. Alexis, F.; Pridgen, E.; Molnar, L. K.; Farokhzad, O. C., Factors affecting the clearance and biodistribution of polymeric nanoparticles. *Molecular Pharmaceutics* 2008, 5, 505-515.

43. Farokhzad, O. C.; Langer, R., Nanomedicine: Developing smarter therapeutic and diagnostic modalities. *Advanced Drug Delivery Reviews* 2006, 58, 1456-1459.

44. Nomiya, K.; Takahashi, S.; Noguchi, R.; Nemoto, S.; Takayama, T.; Oda, M., Synthesis and characterization of water-soluble silver(I) complexes with L-histidine (H(2)his) and (S)-(-)-2-pyrrolidone-5-carboxylic acid (H(2)pyrrld) showing a wide spectrum of effective antibacterial and antifungal activities. Crystal structures of chiral helical polymers [Ag(Hhis)](n) and {[Ag(Hpyrrld)](2)}(n) in the solid state. *Inorganic Chemistry* 2000, 39, 3301-3311.

45. Shin, N.; Lee, J.; Li, H.; Ha, C.; Shchipunov, Y.; Kim, I., Synthesis of Poly(methyl methacrylate)-Block-Poly(L-histidine) and Its Use as a Hybrid Silver Nanoparticle Conjugate. *Journal of Nanoscience and Nanotechnology* 2010, 10, 6948-6953.

46. Yu-hua, Y.; Chao-ping, Z., Interaction between silver ions and histidine. *Journal of Clinical Rehabilitation and Tissue Engineering Research* 2010, 14, 5498-5504.

47. LIU, C., HISTIDINE AS THE FUNCTIONAL-GROUP FOR A CHELATING ION-EXCHANGER. *Analytica Chimica Acta* 1987, 192, 85-93.

48. Boucher, H. W.; Talbot, G. H.; Bradley, J. S.; Edwards, J. E., Jr.; Gilbert, D.; Rice, L. B.; Scheld, M.; Spellberg, B.; Bartlett, J., Bad Bugs, No Drugs: No ESKAPE! An Update from the Infectious Diseases Society of America. *Clinical Infectious Diseases* 2009, 48, 1-12.

Chapter 6

Nanoparticles for Vaccination Against *Chlamydia Trachomatis*

Work contained in this chapter was done as a collaboration led by Prof. Ulrich von Andrian, MD, PhD and Dr. Georg Stary, MD of the Department of Microbiology and Immunobiology at Harvard Medical School.

6. 1. Introduction

Chlamydia trachomatis, a small (0.3-1 um), Gram-negative, obligate intracellular pathogen, is the most common cause of bacterial sexually transmitted disease (STD) in the world.[1] It is responsible for approximately 90 million of all 500 million new cases of STD each year globally. In the US, 4 million new cases a year lead to healthcare expenditures of approximately $3 billion.[2] Treatment with azithromycin or doxycycline results in clearance of genital infections in 97-98% of cases, but identifying infected individuals is difficult.[3] Over 60% of infections in women are asymptomatic, leading to continued disease transmission and delaying appropriate therapy. If left untreated, as high as 40% of genital infections lead to severe or irreversible complications including pelvic inflammatory disease, ectopic pregnancy, and infertility.[4] With prevalence rates as high as 3-4% in young adults aged 18-26, periodic screening of at-risk individuals and antibiotic therapy add a significant burden to already strained healthcare systems.[5] These effects are still significant, despite extensive disease control and public education programs.[1, 6] A highly desirable alternative is the development of a safe and effective prophylactic vaccine.

Despite decades of development, no vaccine is currently available for preventing *Chlamydia* infections in humans. Early attempts at vaccination used whole inactivated

pathogens, but these did not lead to safe and effective protection in humans.[7] Many subunit vaccine strategies have been explored as alternatives, mostly focusing on the major outer membrane protein (MOMP) as the antigen.[2, 7, 8] However, safely boosting the immunogenicity of these preparations has been hampered by unacceptable side effects, suboptimal immune responses, or both. For example, aluminum salt adjuvants, which have a proven track record of safety in the clinic, are biased towards producing Th2-weighted and primarily humoral responses[9] that do not yield optimal protective immunity against intracellular *Chlamydia* infections. Several other adjuvants exist, but these have generally been complicated by excessive toxicity and side effects when administered in free form.[10] A method to reduce the toxicity of these formulations while retaining the immune-potentiating effects is to more precisely deliver the required signals to the subset of cells responsible for immune activation. Highly specific delivery of adjuvant and antigen to antigen presenting cells (APCs) can also reduce the dose delivered to off-target cells and to the rest of the body, thereby limiting the potential for toxicity.[11]

Nanoparticles (NPs) have seen increasing use as delivery systems for vaccines due to their ability to load proteins, polysaccharides, or small molecules by surface adsorption or encapsulation, leading to greater antigen stability and targeted delivery to APCs.[12] Within the context of anti-*Chlamydia* immunity, a number of promising submicron structures have been explored (reviewed by Igietseme et al[2, 8]). Examples include vault NPs ~40-70 nm in diameter, which were loaded with MOMP from *Chlamydia muridarum* in their internal cavity and surface-modified with IgG for targeting the FC-γ receptor on dendritic cells (DCs).[13] Intranasal immunization of the NPs was shown to elicit anti-*Chlamydia* Th1 cell responses, leading to secretion of interferon-gamma (IFN-γ), production of anti-

Chlamydia antibodies, and reductions in bacterial burden following intravaginal challenge. Protection against bacterial challenge was also observed in a cationic liposome formulation encapsulating *C. muridarum* MOMP with synthetic mycobacterial cord factor as an adjuvant.[14] These liposomes were administered subcutaneously, leading to high levels of IFN-γ, systemic IgG2b, and protection against vaginal challenge. One of the most potent vaccines reporting protective immunity to *Chlamydia* is an IL-10 deficient DC pulsed with *Chlamydia ex vivo* then delivered to mice.[15] This report suggested that targeting vaccines to DCs is a highly effective strategy for eliciting anti-*Chlamydia* immunity. While many of these early results are promising, a major pitfall historically has been translating results from animal models to humans. Consequently, there is a continuing need to develop alternative methods that have high potential for clinical translation. For a vaccine formulation to be clinically viable, the formulation must induce potent immunity with a limited number of immunizations and yield side effects only in very rare numbers. Consequently, seeking to use biocompatible, biodegradable, and non-toxic materials is highly desirable.

Herein, we report the design of a novel nontoxic, nanoparticle (NP)-based prophylactic vaccine formulation to immunize against *Chlamydia trachomatis*. It consists of R848-poly(lactic acid) conjugate encapsulated in a cationic PLGA-based NP administered together with UV-inactivated *C. trachomatis*. The NPs are rendered cationic via incorporation of poly-L-histidine (PLH) into the formulation. The R848-encapsulated NP-*Chlamydia* vaccine formulation is shown to induce proliferation of *Chlamydia*-specific TCR transgenic T cells at a level comparable to immunization with live pathogenic *C. trachomatis* 6 days post-vaccination. One month post-vaccination, the

cationic NP-*Chlamydia* formulation demonstrates protection from infection with contagious *C. trachomatis* delivered directly into the uterus, mimicking a natural route of infection. Further, we show that the cationic NPs elicit more effective immunity than control anionic NPs lacking PLH, and that NP formulation of R848 adjuvant results in more potent responses than free adjuvant co-administered with the UV-inactivated bacteria. The results contained herein may inform the future development of vaccines for *C. trachomatis*.

6. 2. Results and Discussion

6. 2. 1. Vaccine Design. Current understanding of the basic immunobiology and design of anti-*Chlamydia* vaccines has begun to define the key elements in the proper stimulation of immunity (for review, see Brunham and Rey-Ladino[1] and Igietseme et al, [16]). Several effectors are believed to play a role, including CD4+ and CD8+ T cells, dendritic cells, macrophages, B cells, NK cells, as well as several cytokines and chemokines. The most prominent effector is the CD4+ T cell which, when activated, homes to the site of infection and releases Th1 cytokines including IFN-γ, TNF-α, and IL-2.[8] IFN-γ plays a highly prominent role, as IFN-γ-R knockout mice (IFN-γ-$R^{-/-}$) were unable to control *C. trachomatis* infections as compared to control mice.[17] It appears that IFN-γ functions at least in part by activating the expression of indoleamine-2,3-dioxygenase (IDO) in cells, an enzyme that degrades tryptophan leading to tryptophan starvation and cell death.[1] In addition, ICAM-1 has been shown to play a major role in the rapid activation, early recruitment, and proper response of T cells to *Chlamydia* infections.[18] Dendritic cells and macrophages play an essential role as APCs, sources of

cytokines (such as IL-12 and IL-1), costimulation (B7, CD40), phagocytosis, and antibody-dependent cellular cytotoxicity (ADCC). Other parts of the immune system play a less significant and ancillary role. B cells can be activated to secrete IgG or IgA, which can help neutralize *Chlamydia* or facilitate ADCC.[15] In addition, NK cells are believed to secrete Th1 cytokines (particularly IFN-γ) and participate in ADCC to aid in bacterial clearance. Finally, CD8+ T cells are believed to play a role, though it is currently suggested to be primarily via secretion of Th1 cytokines and not through direct cytotoxic activity as is more canonical for this cell type.[8]

Key elements of a successful vaccine include: (1) antigenic stimulus, which defines the immunologic specificity, (2) adjuvant, which can both boost and guide the type of immune response, and (3) a delivery vehicle, which can be used to protect and control presentation of the vaccine components to the immune system. All of these components must work in concert to elicit the most potent and safe immunity possible.

The first signal required for an immune response comes from the antigen and drives the exquisite specificity of the immune system. Given the requirement of robust cell-mediated immunity (CMI) for effective anti-*Chlamydia* responses, at least part of the formulation must contain a peptide antigen. This arises since T cells can only recognize antigen in the context of MHC-I (CD8+) or MHC-II (CD4+)-peptide complexes, which are designed to load and present short peptides. Selection of the proper antigenic stimulus is not straightforward, and significant effort has gone towards identifying antigens or combinations of antigens that can lead to protective anti-*Chlamydia* immunity. If a suitable antigen can be identified, subunit vaccines offer several potential advantages, including reduced risk of toxicity, a more focused immune response, avoidance of

"distracting" immunodominant epitopes that do not lead to protective immunity if this is a problem for the pathogen of interest, and potentially greater ease in manufacturing and purification, particularly if only a few components are needed. However, recombinant proteins tend to have much lower immunogenicity and can be susceptible to degradation, particularly in inhospitable environments like the acidic genital mucosa. An alternative is to use the entire pathogen in attenuated or inactivated form. Whole organisms are often favored due to the fact that they present antigens in a form more closely mimicking the infectious body and because of the long history of clinical success in eliciting protective immunity to a range of organisms. In addition, whole organisms contain many candidate antigens. These might lead to combined or synergistic immunologic responses. Because of these advantages, we selected a whole pathogen approach to deliver the antigenic stimulus in our vaccine. To reduce the potential for toxicity of a live pathogen, we chose to utilize a UV-inactivated version. UV inactivation is a common method to reduce bacterial infectivity and can be considered a four $\log_{10}$ reduction in bacterial viability on treatment with UV light.[19]

Selection of a proper adjuvant is critical to formation of a robust immune response. Adjuvants facilitate the maturation of APCs and induce upregulation of costimulatory signals including CD80 and/or CD86, which are needed for proper immune activation. Whole pathogens typically contain or produce elements such as peptidoglycan (PG), unmethylated cytosine-guanine dinucleotides (CpG), lipopolysaccharides (LPS), N-acetyl muramyl-L-alanyl-D-isoglutamine (MDP) or other components that can boost immunity. However, these do not provide sufficient adjuvanticity in *Chlamydia*. The commonly used aluminum salt adjuvants (alum) tend to favor secretion of Th2 over Th1 cytokines,[9,

[10] leading to relatively weak induction of cell-mediated immunity. In the case of *Chlamydia* infection, this is highly important, as preskewing cells toward Th2 was shown to cause disease exacerbation in mice.[20] Today, there are literally hundreds of alternatives to alum, though remarkably few have potential for use in humans due to unacceptable toxicities. A short list of these alternatives include tensoactive agents such as Quil A,[21] purified bacteria-derived adjuvants such as PG,[22] CpG,[23-25] LPS,[26] or MDP,[27] oil-based emulsions such as Montanide or Lipovant,[28] liposomes,[29] polymeric microspheres,[30] inulin-derived compounds,[31] DNA vaccines,[32] and NPs.[10, 33-35]

Commonly used adjuvants include agonists of toll-like receptors (TLR), such as triacyl lipopeptides (TLR1), lipoteichoic acid (TLR2), dsRNA (TLR3), LPS (TLR4), flagellin (TLR5), diacyl lipopeptides (TLR6), guanosine analogs (TLR7), ssRNA (TLR8), and unmethylated CpG (TLR9), among others, though alternatives involving retinoic acid-inducible gene (RIG)-like receptors, nucleotide oligomerization domain (NOD) receptors and others exist.[36] Notably, FDA approved vaccines against HPV (Cervarix®, GlaxoSmithKline) and hepatitis B (Fendrix®, GlaxoSmithKline) include in their formulation monophosphoryl lipid A, a potent agonist of TLR4.[37] Of the various TLR agonists, there has been an interest in using resiquimod (also known as R848) due to its ability to stimulate both TLR7 and TLR8 in humans. R848 has been shown to activate APCs, stimulate Th1 cytokines, and elicit both humoral and CMI effectively across a range of animal disease models, including non-human primates.[38] However, challenges to effective use include its relatively low molecular weight and high aqueous solubility, which lead to a short half-life and rapid distribution throughout the body's tissues. The combination of these factors leads to lower quantities of R848 per mg injected being

delivered to APCs as well as higher systemic cytokine levels, which translate into lower potency and higher side effects. To reverse these, it is necessary to create a depot of R848 then target it more effectively to APCs. Targeting has the potential to reduce the total dose administered while simultaneously increasing the dose delivered precisely to APCs. NPs offer excellent potential as delivery vehicles for R848 as well as other adjuvants due to their ability to encapsulate or adsorb a wide variety of materials including proteins, small molecules, carbohydrates, or lipids, as well as their ability to be engulfed by phagocytic cells. Of the various types of structures that can be used, NPs based on poly(lactic-co-glycolic acid) (PLGA) are attractive because of high biocompatibility and history of safety in humans. However, encapsulating and delivering unmodified R848 in a PLGA matrix is challenging due to the high aqueous solubility and low molecular weight of R848. In fact, when we performed pilot studies evaluating the encapsulation of R848 in poly(lactic-co-glycolic acid)-*block*-poly(ethylene glycol) (PLGA-PEG) copolymer, we observed little encapsulation (data not shown). In addition, release of R848 encapsulated in this manner is expected to be rather rapid, due to most encapsulation occurring at or near the NP surface. A strategy that has previously been used to increase encapsulation of active agents and reduce their release rate is conjugation to a polyester polymer, followed by blending of the drug-polymer conjugate together with other PLGA-containing polymers to yield mixed NPs.[39-41] This method leads to high encapsulation efficiencies and can release the active agent in unmodified form as the polymer degrades by hydrolysis. Consequently, we sought to incorporate the TLR7/8 agonist R848 by forming poly(lactic acid) (PLA)-R848 conjugates and blending them to yield mixed R848-encapsulated NPs.

The final core element of a vaccine is the delivery system. The delivery system must incorporate both the antigen(s) and the adjuvant, as well as effectively deliver them together to APCs in the necessary quantity and with the correct timing to prime immunity. Given our use of a whole pathogen as the source of antigen(s), it was necessary to devise a method to deliver adjuvant together with the inactivated bacterium. We reasoned that one method to achieve this was to use cationic NPs. Cationic NPs tend to promote interactions with biological surfaces, which are typically negatively charged. To achieve this, we turned to a widely used method to target bacterial surfaces using NPs, which involves targeting the negative charges on the surface of bacteria using cationic charges (see discussion in Chapter 1). We used poly-L-histidine (PLH), a cationic polymer to yield a positive surface charge on PLGA-based NPs. Use of a PLGA-based polymer was important, since this could facilitate incorporation of PLA-R848 conjugates into NPs using established protocols.[39] These R848-encapsulated NP-UV inactivated *Chlamydia* constructs might then be able to deliver the needed combination of signals in a delivery system to enable induction of protective anti-*Chlamydia* immunity (Figure 6.1).

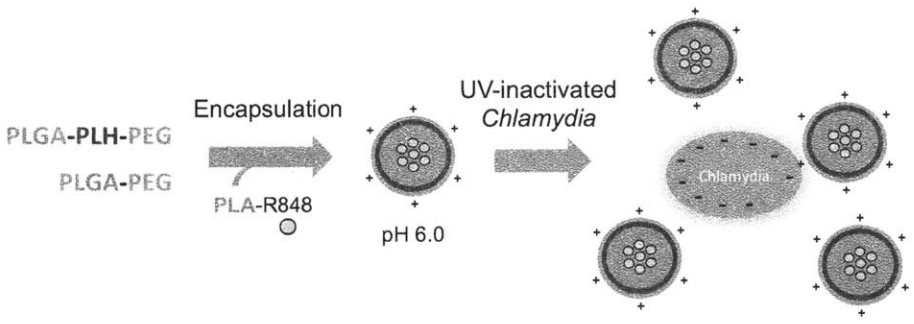

Figure 6. 1. Schematic representation of the *Chlamydia* vaccine design. A combination of PLGA-PLH-PEG and PLGA-PEG (optimized for cationic charge generation and stability, see text) are used to encapsulate the TLR7/8 agonist R848 conjugated to PLA (PLA-R848). In slightly acidic conditions, the PLH becomes cationically charged, enabling interactions with the UV-inactivated *Chlamydia*.

To confirm the applicability of this approach to *Chlamydia* bacteria, we measured the zeta potential of *Chlamydia trachomatis* over a range of pH values and found them to be anionic (zeta potential -12.7±1.2 mV at pH 5.5 to -25.8±1.7 mV at pH 7.4) over physiologically meaningful range (Figure 6.2).

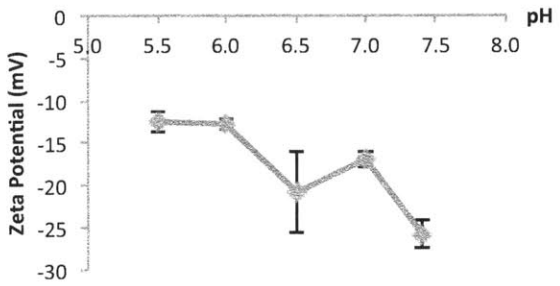

Figure 6. 2. Zeta potential of *Chlamydia trachomatis* at different pH. 1.5 uL of a 1.5e7 IFU/mL solution was diluted in 1.5 mL pH-adjusted buffer and measured using quasi-elastic laser light scattering. The bacteria are negatively charged over the entire measured pH range.

6. 2. 2. NP and Vaccine Formulation and Characterization. We formulated R848-encapsulated NPs using a modified single emulsion/solvent evaporation procedure. A combination of PLA-R848 polymer, PLH-containing polymer (PLGA-PLH-PEG), and PLGA-PEG were co-dissolved in the organic phase, emulsified into water using a probe tip sonicator, allowed to harden by solvent evaporation, then purified by ultrafiltration. In order to maximize the potency of the adjuvant-containing NPs while retaining sufficient cationic charge to potentially enable interactions with *Chlamydia*, we first sought to understand how different ratios of polymers would affect the mixed NP properties. Using unmodified PLGA as a proxy for PLA-R848, we varied the composition of NPs and studied the impact on the size, zeta potential, and NP stability (Figure 6.3). The data show that increasing the content of PLH-containing polymer mixture in the NPs led to

increases in the cationic charge in slight acidity (pH 6.0), and that there is a significant leap in charge as the weight fraction of PLH-containing polymer mixture reaches 0.4 (zeta potential from +2-7 to +23-25 mV) (Figure 6.3B). We reasoned that this higher cationic charge density would be preferred in the vaccine design, as this would lead to a greater driving force for interacting with the anionic *Chlamydia*. We then sought to identify conditions that would incorporate higher quantities of PLGA while also demonstrating acceptable NP size and stability. NPs that contained a weight fraction of PLGA of 0.4 demonstrated a good trade-off between higher incorporation of PLGA and good NP stability post processing and purification (Figure 6.3C).

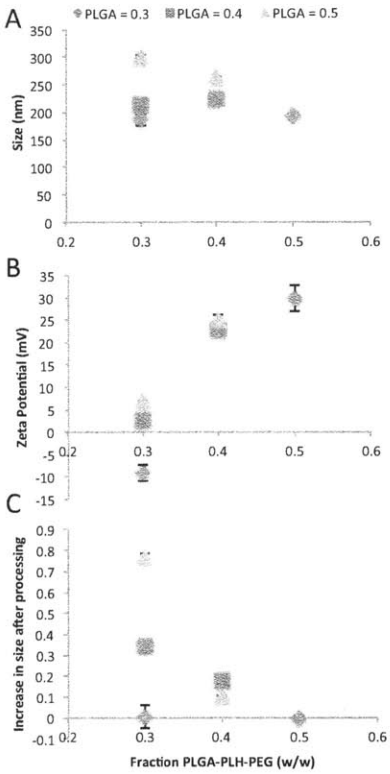

Figure 6. 3. Effect of Polymer Blending on Nanoparticle Size, Zeta Potential, and Stability. PLGA-PLH-PEG NPs were blended with PLGA-PEG and the model polymer PLGA to assess the impact of polymer blending on NP properties. A composition containing 40% PLGA-PLH-PEG (w/w) was selected due to the balance of colloidal stability following processing with generation of sufficient cationic charge to enable binding to *Chlamydia trachomatis*. (A) NP size, (B) zeta potential at pH 6.0, (C) fraction increase in size following NP purification.

We then sought to explore the ability of these NPs to bind to *C. trachomatis*. NPs were formulated (40% w/w PLH-containing polymer, 40% w/w PLA-R848, 20% PLGA-PEG), purified, and then incubated with 10^7 inclusion forming units (IFU) per milligram of NPs in a pH 6.0 solution, incubated for ~2 hr at 37°C, added to high grade mica to allow for adhesion, washed, then taken for AFM imaging. The images show formation of aggregate

structures containing both *Chlamydia* bacteria and NPs (Figure 6.4A, B), indicative of interactions occurring between the bacteria and the NPs.

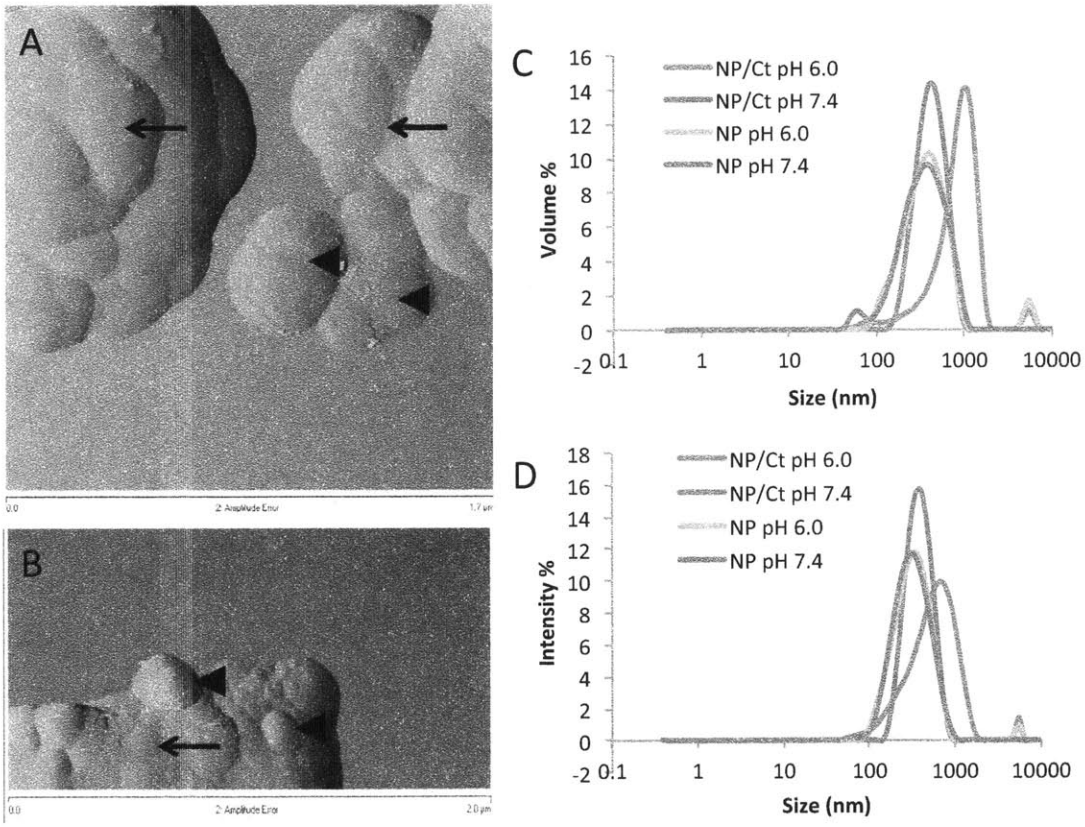

Figure 6. 4. Nanoparticle-*Chlamydia* Vaccine Characterization. PLH-containing nanoparticles (NP) were incubated with *Chlamydia trachomatis*, adsorbed onto prepared mica slides, washed, then imaged using atomic force microscopy (AFM). (A) AFM micrograph of *C. trachomatis* bacteria alone. Width of image corresponds to 1.7 um. (B) *C. trachomatis* bacteria following incubation with NPs, demonstrating attractive forces between the two. Width of image corresponds to 2 um . Size distributions by volume (C) and intensity (D) of NPs alone and *C. trachomatis* + NP mixed together by dynamic light scattering, showing a shift in the size distribution towards larger sizes of the mixed species relative to the pure species after incubation in pH 6.0.

To further investigate the properties of NP solutions incubated with *Chlamydia*, we evaluated the size distribution by dynamic light scattering (Figure 6.4C, D). We observed a shift to the right in the size distribution by volume of the NP-*Chlamydia* mixture solution as compared to the NPs or *Chlamydia* alone, suggesting the possible formation

of aggregates in at least a subset of species in the mixture. We note that neutralization of the pH following an incubation of the NPs with the *Chlamydia* leads to a reduction in the size of the formulation, perhaps suggesting that an acidic buffer solution is required to achieve formation and rotation of the construct. We additionally performed some pilot studies to see if it might be possible to view the formation of NP-*Chlamydia* constructs using fluorescently labeled NPs and *Chlamydia* by flow cytometry. We prepared and purified NPs modified with Alexa-488-modified PLGA (NP-488) and labeled *Chlamydia* using *Bac*Light Red, incubated them together in slight acidity then ran on a flow cytometer. We observed an increase in the fluorescence in both the green (FL1-H) and red (FL3-H) channel in samples where both the NPs and bacteria were labeled, which also scaled based on the amount of NPs added (Figure 6.5, 6.6). However, we also observed that the *Bac*Light Red dye appeared to bind nonspecifically to the NPs as well (data not shown), confounding the interpretation of whether this shift in fluorescence in both channels can be attributed to the formation of a NP-*Chlamydia* construct.

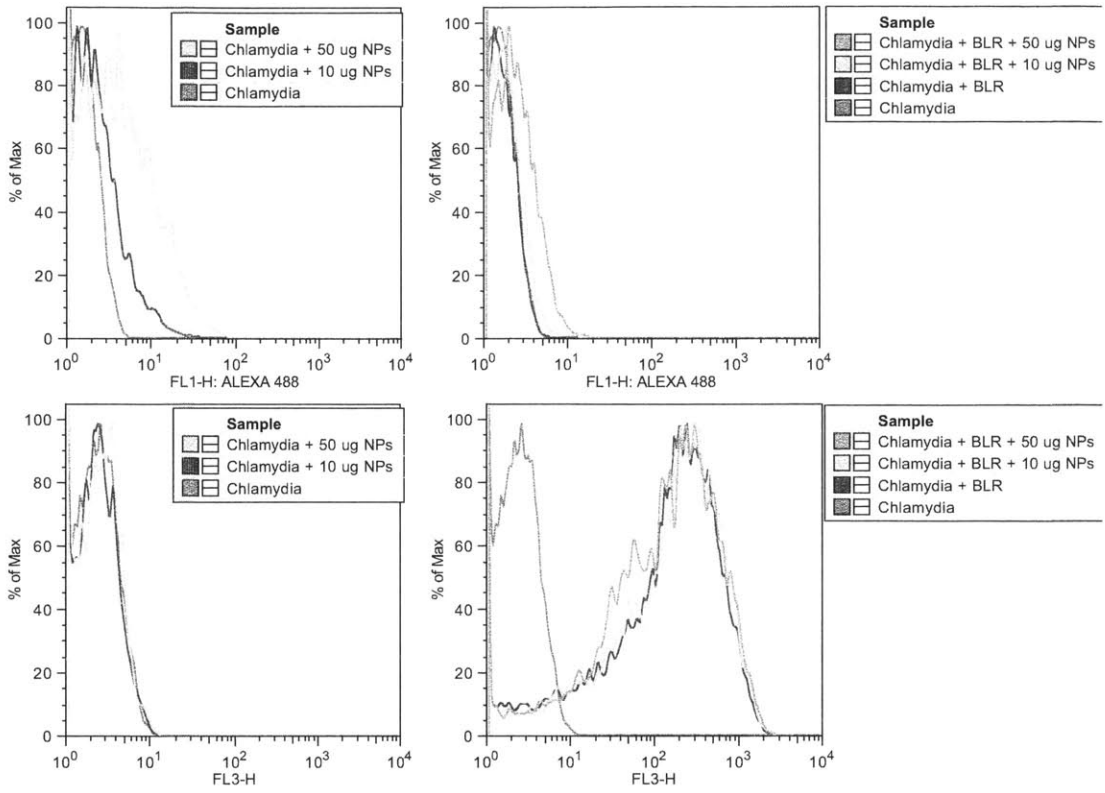

Figure 6. 5. Flow Cytometry Analysis of NP-*Chlamydia* Vaccine. Alexa-488 modified-PLGA incorporated into PLGA-PLH-PEG NPs were incubated with (or without) BacLight Red® (BLR)-labeled *Chlamydia trachomatis* then run on a flow cytometer. The data suggests formation of double-labeled constructs (*Chlamydia* + BLR + 50 ug NPs). FL1-H fluorescence corresponds to Alexa-488, FL3-H corresponds to BLR fluorescence (see also Figure 6.6).

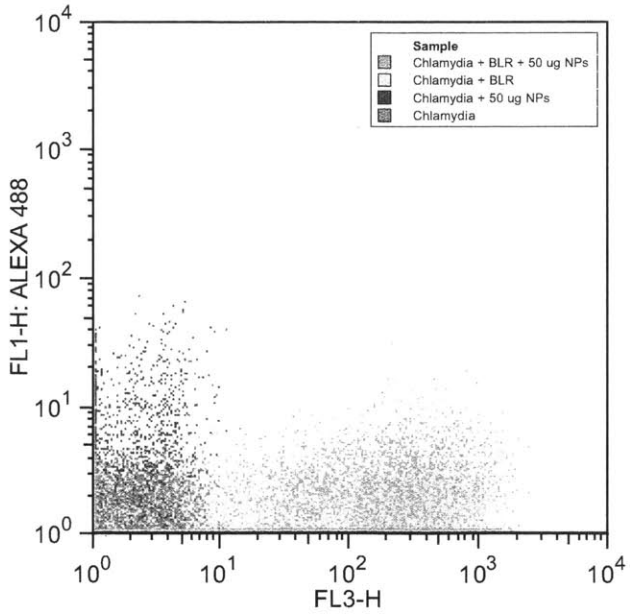

Figure 6. 6. Flow Cytometry Analysis of NP-*Chlamydia* Vaccine (II). The data from Figure 5.5 shown on different axes to suggest the possible formation of double-positive, that is, Alexa-488-PLGA and BacLight Red (BLR)-labeled constructs (see also Figure 6.5).

6. 2. 3. *Chlamydia*-Specific T Cell Expansion *In Vivo*. Next, we sought to determine whether the cationic NP-*Chlamydia* vaccine formulation could induce expansion of *Chlamydia*-specific, T cell receptor (TCR)-transgenic T cells adoptively transferred into mice. Mice were inoculated transcervically with a vaccine formulation containing 0.67 mg R848-encapsulated NP/mouse and $1.3x10^7$ IFU UV-inactivated *Chlamydia* vaccine, together with controls including live pathogenic *Chlamydia*, UV-inactivated *Chlamydia* alone, and anionic NPs mixed with *Chlamydia*. This latter group was formed by creating a NP formulation containing 60% (w/w) PLGA-PEG and 40% PLA-R848. Since no PLH-containing polymer mixture is incorporated, the NP do not elicit a cationic charge at the incubation conditions and consequently no interactions with *Chlamydia* could be observed by AFM, despite repeated attempts. On day 5 post vaccination, *Chlamydia*-specific, TCR-transgenic, CFSE-labeled T cells were adoptively transferred into mice and given approximately 24 hours to traffic to lymphoid organs and expand if they encounter properly activated APCs. T cells were then collected and analyzed by FACS for expansion of *Chlamydia*-specific T cells (Figure 6.7).

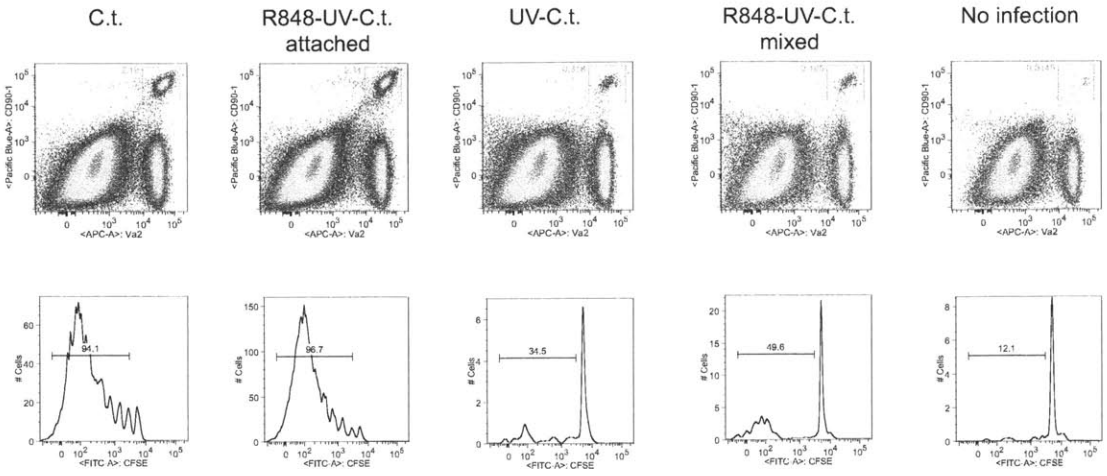

Figure 6. 7. Induction of *Chlamydia*-specific T cells. *Chlamydia*-specific, CFSE-labeled, TCR transgenic T cells were transferred to mice the day prior to immunization. On day 0, mice were immunized transcervically with either infectious *Chlamydia trachomatis* (C.t., positive control), R848 encapsulated in PLGA-PLH-PEG nanoparticles (NP) that were treated with UV-inactivated *Chlamydia* (R848-UV-C.t. attached), UV-inactivated *Chlamydia* (UV-C.t., negative control), R848 encapsulated in PLGA-PEG NPs that were treated with UV-inactivated *Chlamydia* (R848-UV-C.t. mixed), or untreated control (no infection). On day 6, the T cell response was measured by collecting cells from the draining lymph node and analyzing by FACS. Top row: gating on total leukocytes. One can appreciate expansion of the Chlamydia-specific T cells particularly in the C.t. and R848-UV-C.t. attached groups. Bottom row: CFSE cell proliferation assay, showing enhanced CFSE dilution (indicative of cell proliferation) particularly in the C.t. and R848-UV-C.t. attached groups, noting that it is greater than the UV-inactivated pathogen alone or mixed NPs groups.

The data show that vaccination with R848-encapsulated cationic NP-*Chlamydia* formulation leads to expansion of *Chlamydia*-specific T cells at levels comparable to live pathogenic *Chlamydia*. This can be observed by the increased quantity of specific T cells (Figure 6.7, top row) as well as the greater amount of CFSE dilution (Figure 6.7, bottom row). NPs that were mixed with the *Chlamydia* demonstrate an attenuated response that appeared similar to inoculation with UV-inactivated *Chlamydia* alone. This suggests that R848-encapsulated PLH-containing NPs appear to more effectively expand *Chlamydia*-specific T cells *in vivo* as compared to controls.

6. 2. 4. Protection Against *Chlamydia* Challenge. We then sought to determine whether the expansion of specific T cells that was observed could translate into protection from infection. Immunologically naïve mice were vaccinated transcervically with R848-encapsulated NP-*Chlamydia* formulation or with controls which included the live infectious pathogen, UV-inactivated *Chlamydia*, UV-inactivated *Chlamydia* co-administered with free R848, and UV-inactivated *Chlamydia* treated with NP-*Chlamydia* that did not contain any R848 (Figure 6.8). The mice were then given 4 weeks to mount a *Chlamydia*-specific immune response, at which point they were inoculated transcervically with live and infectious *C. trachomatis*, mimicking the typical mode of sexual transmission. Six days later, the bacterial loads in the uterus were evaluated by quantitative PCR (qPCR) and by counting the number of IFU. The results show that immunization with the R848-encapsulated cationic NP-*Chlamydia* constructs led to significantly lower levels of *Chlamydia*-specific 16S DNA relative to total host DNA extracted as compared to negative controls containing only the UV-inactivated bacteria or UV-inactivated bacteria attached to non-R848-containing NPs and at levels equivalent to that in the group immunized with the infectious organism (Figure 6.8). In addition, the UV-inactivated bacteria co-administered with free R848 demonstrated only a partial effect. It is likely that the free R848 was not present at sufficiently high concentration, perhaps due to rapid diffusion throughout the tissue and more rapid elimination from the uterus than the R848-encapsulated NP treated group.

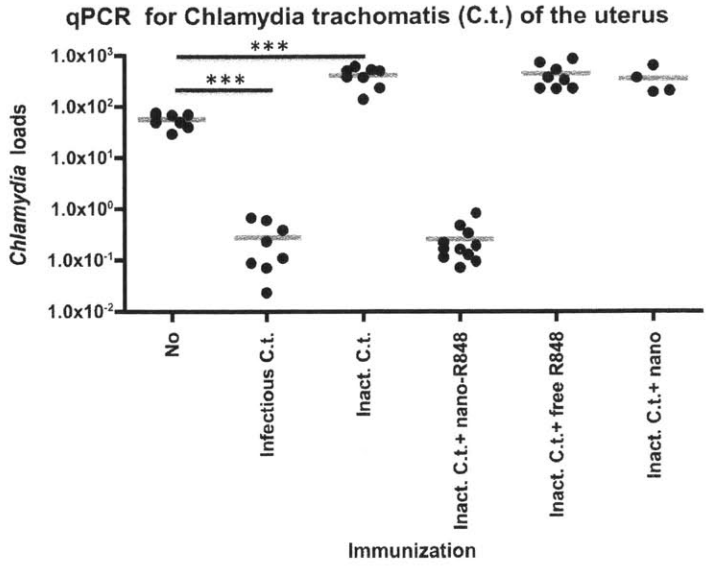

Figure 6. 8. Quantitative PCR Analysis of *Chlamydia trachomatis* burden in the uterus following transcervical immunization. Mice were immunized transcervically with infectious *Chlamydia trachomatis* (Infectious C.t., positive control), UV-inactivated C.t. (Inact. C.t., negative control), UV-inactivated C.t. treated with R848-encapsulated PLH-containing NPs (Inact. C.t. + nano-R848), UV-inactivated C.t. + free R848, and UV-inactivated C.t. with PLH-containing NPs that did not contain any R848 (inactivated C.t. + nano). Four weeks later, all mice were challenged with live *C. trachomatis* transcervically. Six days later, the amount of *Chlamydia* in the uterus was quantified by measuring the quantity of *Chlamydia*-specific 16S DNA and normalizing by the quantity of host DNA collected using quantitative PCR. The data show that the R848-encapsulated NP-*Chlamydia* constructs protect mice from bacterial challenge similar to pre-exposure with infectious *C. trachomatis*, and that the response is superior to free R848. No significant protection was observed with empty NP conjugated to *Chlamydia*, indicating that the effect depends on incorporation of R848.

To gain greater understanding of the methods by which the vaccine constructs can be administered, we explored intranasal (a mucosal surface) and subcutaneous (a non-mucosal surface) routes using the same experimental design. The data show that the R848-encapsulated NP-*Chlamydia* formulation led to reduced levels of *Chlamydia*-specific 16S DNA relative to host DNA as compared to negative controls via intranasal but not subcutaneous vaccination (Figure 6.9, 6.10). It is possible that when the vaccine is injected into non-mucosal tissue, the resulting T cells lack the appropriate chemokine

receptors needed for entry into the inflamed uterus. The resulting lower level of T cells in the uterus would then result in an inability to protect the host from infection. In fact, the importance of expressing the appropriate chemokine receptors was recently elucidated in a study that showed that both CXCR3 and CCR5 are required for T cell-mediated protection against *Chlamydia* infection.[42]

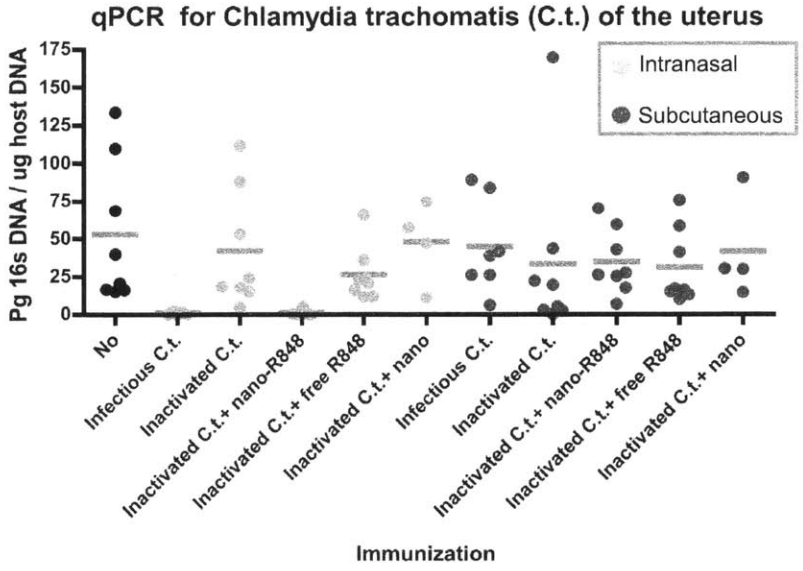

Figure 6. 9. Quantitative PCR Analysis of *Chlamydia trachomatis* burden in the uterus following intranasal or subcutaneous immunization. Mice were immunized with infectious *C. trachomatis* (infectious C.t.), UV-inactivated C.t., UV-inactivated C.t. with R848-encapsulated PLGA-PLH-PEG NPs (inactivated C.t. + nano-R848), UV-inactivated C.t. with free R848, and UV-inactivated C.t. with PLGA-PLH-PEG NPs that did not contain R848 (inactivated C.t. + nano) either intranasally (green dots) or subcutaneously (blue dots). Four weeks later, all mice were challenged with infectious *C. trachomatis* transcervically. Six days later, the quantity of *Chlamydia*-specific 16S DNA relative to host DNA was quantified using quantitative PCR. The data show that the R848-encapsulated NP-*Chlamydia* constructs protect mice from challenge with infectious *Chlamydia* when the constructs are delivered into mucosal (in this case nasal, and in Figure 5.8, uterine) tissue but not when injected subcutaneously.

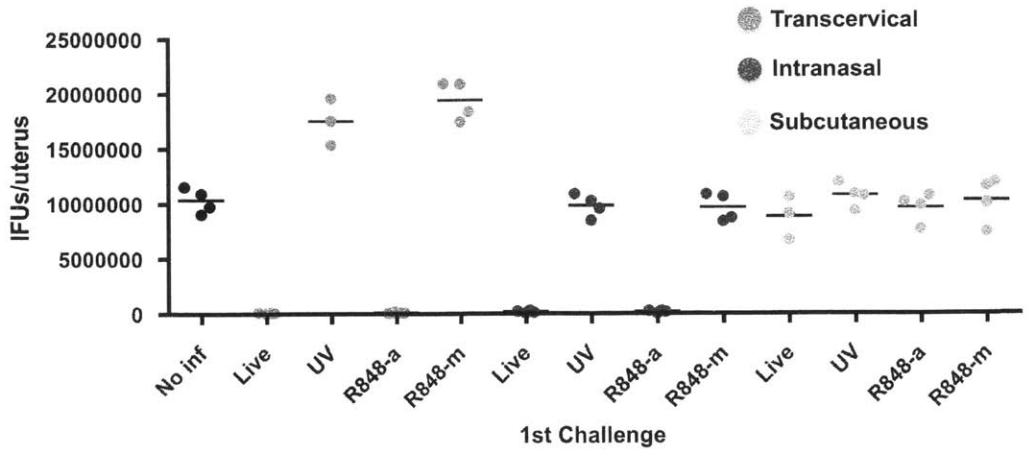

Figure 6. 10. Inclusion Forming Unit (IFU) Analysis of *Chlamydia trachomatis* burden in the uterus following immunization. Mice were immunized with live *C. trachomatis* (Live), UV-inactivated *C. trachomatis* (UV), R848-encapsulated PLGA-PLH-PEG NPs with UV-inactivated *C. trachomatis* (R848-a), or R848-encapsulated PLGA-PEG NPs with UV-inactivated *C. trachomatis* (R848-m) using either a transcervical, intranasal, or subcutaneous route. Four weeks later, all mice were challenged with 10^7 IFU of *C. trachomatis* transcervically. Six days later, the quantity of *C. trachomatis* in the uterus were determined by counting the IFUs. The data show that mucosal immunization is necessary to elicit a protective immune response and that use of PLH-containing NP appears to be an important precondition for protective immunization.

Next, we sought to study how *Chlamydia*-specific T cells distribute themselves in immunized mice four weeks after immunization. The data show that the number and anatomical distribution of T cells depended on the type of immunization (Figure 6.11).

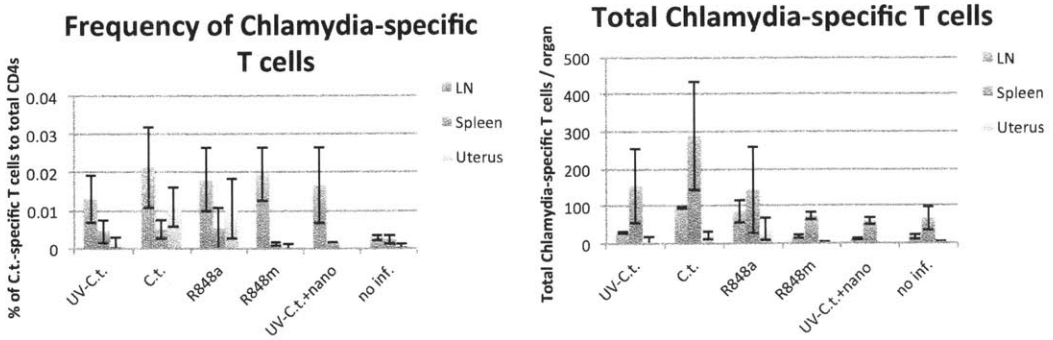

Figure 6. 11. Analysis of *Chlamydia*-specific T cell levels in the uterus and lymphoid organs following immunization. Mice were immunized with infectious *Chlamydia trachomatis* (C.t.), UV-inactivated C.t. (UV-C.t.), R848-encapsulated PLGA-PLH-PEG NPs with UV-inactivated C.t. (R848a), R848-encapsulated PLGA-PEG NPs with UV-

inactivated C.t. (R848m), UV-inactivated C.t. with empty PLGA-PLH-PEG NPs (UV-C.t. + nano) and uninfected control (no inf.) transcervically. Four weeks later, mice were sacked and the draining lymph node (LN), spleen, and uterus were collected. The organs were then analyzed for counts of total and *Chlamydia*-specific T cells by flow cytometry. The data show that immunization with R848-encapsulated UV-inactivated *Chlamydia*-specific T cells leads to greater trafficking of *Chlamydia*-specific T cells to the uterus, correlating with the protective immunity of this and the C.t. control. Other groups did not demonstrate significant levels of *Chlamydia*-specific T cells in the uterus.

Mice immunized with the live pathogen or the R848-encapsulated NP-*Chlamydia* formulation showed a higher frequency of *Chlamydia*-specific T cells, particularly in the uterus. This higher T cell frequency in the uterus correlated well with the observation of protection against challenge with infectious *Chlamydia* in these but not any of the other groups. This is consistent with many findings demonstrating a prominent role played by CD4+ T cells in anti-*Chlamydia* immunity and also suggests that these cells are playing a significant role in controlling the infection in the vaccinated groups. To further explore the mechanism behind the observed protection, we immunized a variety of immunodeficient mice transcervically with R848-encapsulated NP-*Chlamydia* formulations as well as controls, waited 4 weeks for immunity to develop, then, as before, challenged mice with infectious *Chlamydia* (Figure 6.12). To explore whether antibodies were playing a prominent role, we used D_HLMP2A mice. These mice are genetically engineered to have B cells that do not express the B cell receptor but retain other B cell functions.[43, 44] D_HLMP2A mice immunized with R848-encapsulated NP-*Chlamydia* constructs demonstrated very low levels of *Chlamydia*-specific 16S RNA relative to host DNA as compared to controls, suggesting that the mechanism of protection did not depend highly on antibodies, though it is unclear whether there is an antibody-independent protective effect by B cells. To clarify this point, we performed the same

experiment on B cell-deficient (uMT) mice, finding that the R848-encapsulated NP-*Chlamydia* formulation, similar to live pathogen, are leading to protection in a manner that appears to be B cell-independent and driven mostly by T cells though other cell types, particularly NK cells, may also be playing an ancillary role.

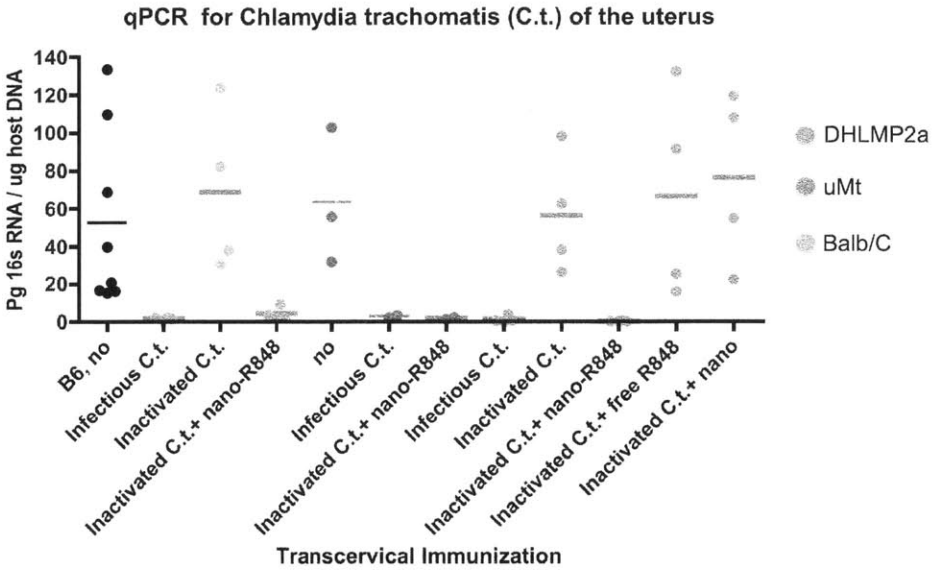

Figure 6. 12. Quantitative PCR analysis of *Chlamydia trachomatis* burden in the uterus following transcervical immunization in various immunodeficient mice. Three different mouse strains were immunized to explore the mechanism behind the protective immunity. Antibody deficient mice (D_HLMP2a, orange dots), B cell deficient mice (uMT), and Balb/C mice were immunized transcervically with infectious *C. trachomatis* (C.t.), UV-inactivated C.t. (inactivated C.t.), UV-inactivated C.t. treated with R848-encapsulated PLGA-PLH-PEG NPs (inactivated C.t. + nano-R848), with additional controls including untreated Black-6 mice (B6, no), untreated uMT mice (no), UV-inactivated C.t. with free R848, or UV-inactivated C.t. with empty PLGA-PLH-PEG NPs (inactivated C.t. + nano). Four weeks later, all mice were challenged with live, pathogenic *C. trachomatis* transcervically. Six days later, the bacterial load in the uterus was assessed by quantitative PCR. The data suggest that the protective effect of immunization with either live pathogen or UV-inactivated *Chlamydia*-R848-encapsulated NPs does not depend on functional B cells or antibodies.

To further explore the potential immunologic mechanism, we sought to confirm that activation of the immune system requires the presence of intact MHC-II complexes. MHC-II complexes are present on APCs and are involved in presenting antigen to CD4+

T cells via the T cell receptor. We inoculated MHC-II knockout (KO) mice as described previously and found that no protective effect could be observed either with infectious *Chlamydia* or R848 encapsulated NP-*Chlamydia* formulations, consistent with the mechanism involving activation of CD4+ T cells (Figure 6.13).

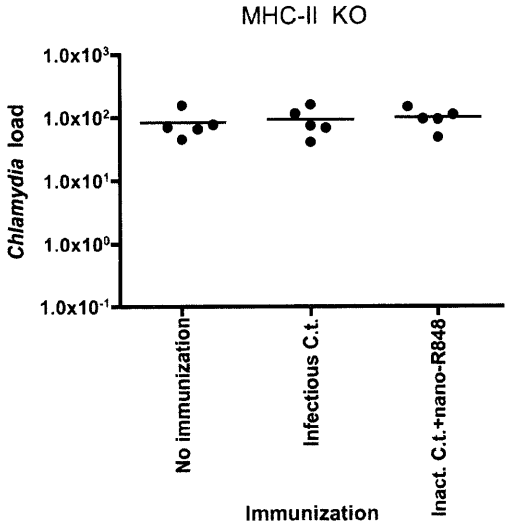

Figure 6. 13. Protection is MHC-II Dependent. MHC-II knockout (KO) mice were immunized as described and challenged with infectious *Chlamydia trachomatis*, showing no protection. This indicates that MHC-II complexes are required for proper induction of immunity.

We next sought to determine if protection could be observed in mice with no mature T cells, using RAG-2 knockout (KO) mice. As expected, the RAG-2 KO mice did not have any protection from re-challenge with *Chlamydia* bacteria (Figure 6.14).

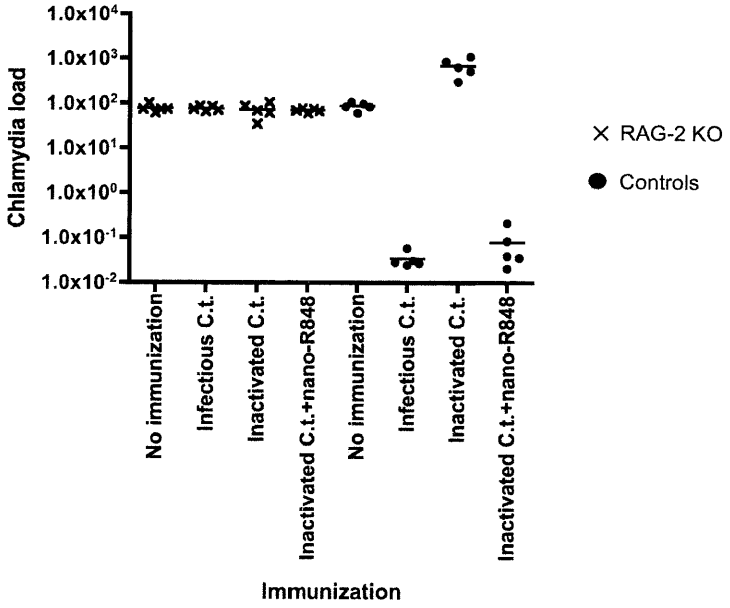

Figure 6. 14. Protection requires functional RAG-2. RAG-2 knockout (KO) mice were immunized as described and challenged with infectious *Chlamydia trachomatis*, showing no protection. This indicates that RAG-2 (and mature T cells) are required for proper induction of immunity.

Given the previous data, it appears likely that CD4+ T cells are the major cell type involved in eliciting protective immunity against rechallenge with *Chlamydia trachomatis* delivered into the uterus. To further confirm this, we adoptively transferred CD4+ and CD8+ T cells isolated from immunized mice to uninfected mice then challenged these mice with *Chlamydia* as before. We found that transfer of CD4+ T cells into naïve mice led to protective immunity (Figure 6.15), and interestingly, that some small but statistically significant effect could be observed by adoptively transferring CD8+ T cells. However, it is clear that the CD4+ T cell subset are the major cell type involved in inducing protective immunity.

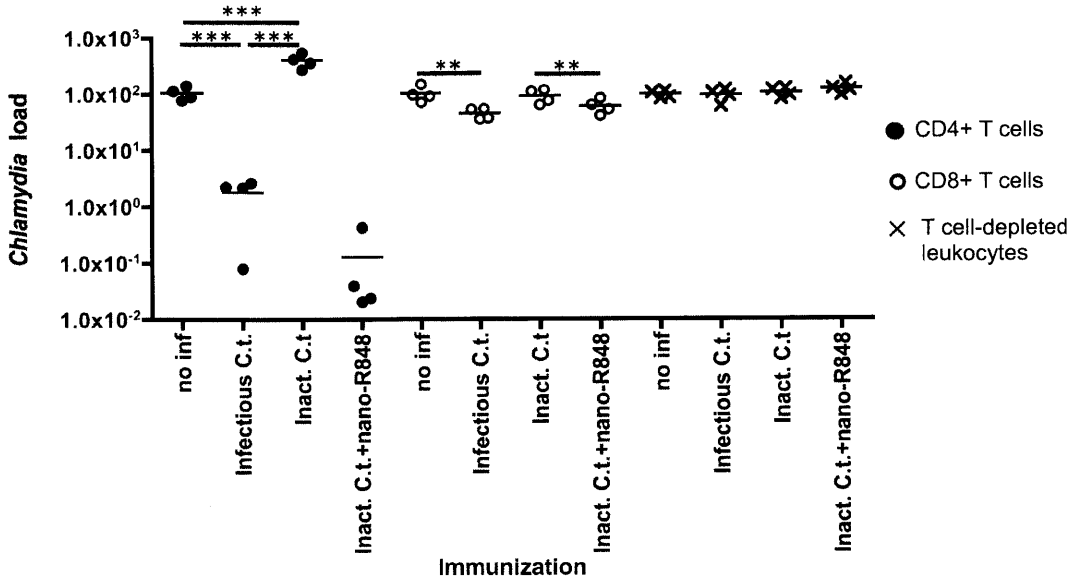

Figure 6. 15. Adoptive transfer of CD4+ T cells induces protection. Mice were immunized with the given condition and then allowed one month to develop immunity. CD4+ and CD8+ T cells were isolated from the immunized mice then adoptively transferred into naïve mice. The naïve mice were then infected with *Chlamydia trachomatis* bacteria and their *Chlamydia* loads evaluated. The data show that CD4+ T cells play the most significant role in controlling the *Chlamydia* infection. There is also evidence for CD8+ T cells playing a very minor role.

6. 2. 5. Summary. In summary, we have taken steps towards developing a novel prophylactic vaccine formulation for immunizing against genital infections involving *Chlamydia trachomatis*, a common bacterial sexually transmitted disease. The vaccine consists of a combination of (1) PLH-containing NPs that encapsulate the TLR7/8 agonist R848 and (2) UV-inactivated *C. trachomatis*. Encapsulation of the highly water soluble R848 was achieved by using R848-PLA polymer conjugates and blending them into the oil-in-water emulsion during the NP preparation step. The R848-encapsulated NP-*Chlamydia* formulation was achieved by incubating the R848-encapsulated NPs with *C. trachomatis* under conditions in which the NPs would have a positive surface charge, which might enable binding to the negatively charged *C. trachomatis*. Evidence for

binding to *Chlamydia* was observed by AFM and dynamic light scattering. The constructs were shown to induce the proliferation of adoptively transferred *Chlamydia*-specific TCR transgenic T cells on day 6 post vaccination, whereas controls including R848-encapsulated anionic NPs did not. Further study showed that vaccination with PLH-containing NPs demonstrated protection against challenge with live pathogenic *Chlamydia* 4 weeks post vaccination, as measured 6 days following infection. This protection correlated with high levels of *Chlamydia*-specific CD4+ T cells present in the uterus and did not depend on antibodies or on B cells, based on retained protection in genetically engineered mice lacking these (D_HLMP2A and uMT mice, respectively). Further, we show using knockout mouse studies that protective immunity required MHC-II complexes and functional RAG-2, suggesting the need for intact elements of adaptive immunity. Finally, we show that adoptive transfer of CD4+ T cells from immunized mice into immunologically naïve mice leads to protection in the naïve mouse. Taken together, these results suggest the induction of protective immunity using a novel vaccine formulation and may have implications in the further development of NP-based vaccines against *Chlamydia trachomatis*.

6. 3. Materials and Methods

6. 3. 1. Polymer Synthesis. Poly(L-histidine) (PLH) was custom synthesized by GenScript (Piscataway, NJ) to contain an N-terminal lysine and C-terminal cysteine with 20 histidine residues in between (N- to C-terminus sequence: $KH_{20}C$). This PLH peptide (0.01 mmol) was mixed with orthopyridyl-modified methoxy PEG, (mPEG-OPSS, 0.01 mmol, Laysan Bio, Arab, AL) in water, followed by purification by dialysis using Slide-

A-Lyzer 2,000 MWCO dialysis cassettes (Thermo Scientific) and lyophilization to dry the product. Separately, PLGA-COOH (5 umol) (inherent viscosity 0.67, LACTEL Absorbables) was activated using EDC (0.246 mmol) and NHS (0.295 mmol) in 2 mL dichloromethane, precipitated in -20°C methanol, then dried *in vacuo* at 50°C. 104.9 mg of PLGA-NHS was then coupled to 24.8 mg PLH-PEG copolymer and stored in DMSO until use. PLGA-PEG copolymer was purchased from Boehringer Ingelheim GmbH. R848-PLA synthesized by ring opening polymerization was a generous gift by Ms. Pamela Basto.

6. 3. 2. NP Formulation. All NPs were formulated using a modified emulsion/solvent evaporation technique. In a typical formulation, NPs designed to attach to *Chlamydia* were prepared by mixing 5.33 mg of PLH-containing polymer with 2.66 mg of PLGA-PEG and 5.33 mg of R848-PLA conjugate together in 400 uL of a 15/85 DMSO/ethyl acetate solution. Control NPs that were not positively charged were formulated in a similar manner, only using 8.0 mg of PLGA-PEG and 5.33 mg of R848-PLA. For NPs that did not contain R848-PLA, an equal amount of PLGA was used (inherent viscosity 0.67, LACTEL absorbables). The polymer-containing organic solution was sonicated into 2 mL of pure water using a probe tip sonicator (Misonix Sonicator S-4000, Farmingdale, NY) for 30 sec in continuous mode at 40% amplitude then diluted into 8 mL of pure water under magnetic stirring in a fume hood. The solvent was allowed to evaporate for at least 2 hours, at which point the NPs were collected and purified by repeated ultrafiltration using Amicon Ultra-4 100,000 NMWL cutoff filters (Millipore, Billerica, MA).

6. 3. 3. Physicochemical Property Characterization. NPs were prepared, purified, then resuspended at ~100 ug/mL. *Chlamydia trachomatis* were diluted to ~10^7 IFU/mL. The size and zeta potential were measured for each solution by quasi-elastic laser light scattering using a ZetaPALS dynamic light scattering detector (15 mW laser, incident beam 676 nm, Brookhaven Instrument Corporation).

6. 3. 4. Nanoparticle-*Chlamydia* Vaccine Formation. In a typical formulation designed to yield sufficient material for 20 mice, 13.3 mg of cationic or anionic NPs were prepared, purified, then resuspended in a dilute pH 6.0 solution. To this was added $2.8x10^8$ *Chlamydia trachomatis* and solution added to yield a total volume of 400 uL, taking care to ensure that the pH of the resulting solution remained at pH 6.0. This mixture was then incubated at 37°C for at least 30 minutes in the dark under gentle shaking. Controls were prepared in the same manner, only with an appropriate buffer solution in place of a NP suspension.

6. 3. 5. Nanoparticle-*Chlamydia* Vaccine Characterization. ***Atomic Force Microscopy.*** AFM samples were prepared as described, with slight modifications.[45] Cells with or without nanoparticles were deposited on a freshly cleaved mica surface. Samples were air-dried 4–8 h before imaging with a Dimension V 3100 atomic force microscope (Veeco Instruments Inc., Plainview, NY). The instrument has a 100-μm multi-purpose large scanner and was operated in tapping mode with speeds ranging from 0.5 to 1.0 Hz and 512 pixels per line scan. A Veeco MLCT-E cantilever with a nominal spring constant of 0.5 N m^{-1} and a resonant frequency ranging from 26 to 50 kHz was used for imaging. For all samples, first-order flattened topography and deflection scans were acquired with sizes ranging from 1 to 75 μm.

Dynamic Light Scattering. NP-*Chlamydia* vaccines were formed as described and measured on a Zetasizer Nano ZS (Malvern, UK) using a He-Ne laser at 633 nm with a max 5mW of power.

Flow cytometry. 2 mg of NPs were prepared and purified. Cationic NP-*Chlamydia* formulations were formed as described in section 5. 3. 4, with the following modifications: 10^8 IFU/mL *Chlamydia* were preincubated with 5 uL of a working solution of *Bac*Light Red (Invitrogen) for 15 minutes before adding to the Alexa-488 modified NPs in the indicated quantities in a total volume of ~600 uL. These were incubated for 1 hr then run on a flow cytometer (FACSCalibur, BD Biosciences, Koch Institute Flow Cytometry Core). Forward scatter (FSC), side scatter (SSC), green fluorescence (ex: 488, filter: 530/30), and red fluorescence (ex: 488, filter: 650 LP) data were collected on a minimum of 1,000 events per sample. Bacteria were gated for live using FSC vs. SSC plots using an untreated negative control for reference.

6. 3. 6. Vaccination. The indicated vaccine formulations and controls were administered on day 0 via various routes of infection. Each mouse received 0.67 mg of NP and $1.3x10^7$ IFU. Transcervical inoculation was performed using the Non-Surgical Embryo Transfer Device (NSET). Essentially, the mice were briefly restrained while a single small plastic speculum was inserted into the vagina. This allowed a special micropipet tip (on a regular pipetter) to be positioned for precise delivery of 10-20 ul of the vaccine formulation across the cervix. For intranasal challenge, mice were anesthetized and a drop of the vaccine formulation was placed on its nostril until it was inhaled. For subcutaneous inoculation, the conjugate was be administered under the skin at the base of the tail or flank.

6. 4. References

1. Brunham, R. C.; Rey-Ladino, J., Immunology of Chlamydia infection: Implications for a Chlamydia trachomatis vaccine. *Nature Reviews Immunology* 2005, 5, 149-161.

2. Igietseme, J. U.; Eko, F. O.; Black, C. M., Chlamydia vaccines: recent developments and the role of adjuvants in future formulations. *Expert Review of Vaccines* 2011, 10, 1585-1596.

3. Marrazzo, J., Treatment of Chlamydia trachomatis infection. In *UpToDate*, Basow, D. S., Ed. UpToDate: Waltham, MA, 2012.

4. Marrazzo, J., Clinical manifestations and diagnosis of Chlamydia trachomatis infections. In *UpToDate*, Basow, D. S., Ed. UpToDate: Waltham, MA, 2012.

5. Miller, W.; Ford, C.; Morris, M.; Handcock, M.; Schmitz, J.; Hobbs, M.; Cohen, M.; Harris, K.; Udry, J., Prevalence of chlamydial and gonococcal infections among young adults in the United States. *Jama-Journal of the American Medical Association* 2004, 291, 2229-2236.

6. Gotz, H.; Lindback, J.; Ripa, T.; Arneborn, M.; Ramstedt, K.; Ekdahl, K., Is the increase in notifications of Chlamydia trachomatis infections in Sweden the result of changes in prevalence, sampling frequency or diagnostic methods? *Scandinavian Journal of Infectious Diseases* 2002, 34, 28-34.

7. Rockey, D. D.; Wang, J.; Lei, L.; Zhong, G. M., Chlamydia vaccine candidates and tools for chlamydial antigen discovery. *Expert Review of Vaccines* 2009, 8, 1365-1377.

8. Igietseme, J. U.; Eko, F. O.; Black, C. M., Contemporary approaches to designing and evaluating vaccines against Chlamydia. *Expert Review of Vaccines* 2003, 2, 129-146.

9. Davis, H. L.; Weeranta, R.; Waldschmidt, T. J.; Tygrett, L.; Schorr, J.; Krieg, A. M., CpG DNA is a potent enhancer of specific immunity in mice immunized with recombinant hepatitis B surface antigen. *Journal of Immunology* 1998, 160, 870-876.

10. Petrovsky, N.; Aguilar, J. C., Vaccine adjuvants: Current state and future trends. *Immunology and Cell Biology* 2004, 82, 488-496.

11. Swartz, M. A.; Hirosue, S.; Hubbell, J. A., Engineering Approaches to Immunotherapy. *Science Translational Medicine* 2012, 4.

12. Peek, L. J.; Middaugh, C. R.; Berkland, C., Nanotechnology in vaccine delivery. *Advanced Drug Delivery Reviews* 2008, 60, 915-928.

13. Champion, C. I.; Kickhoefer, V. A.; Liu, G. C.; Moniz, R. J.; Freed, A. S.; Bergmann, L. L.; Vaccari, D.; Raval-Fernandes, S.; Chan, A. M.; Rome, L. H.; Kelly, K. A., A Vault Nanoparticle Vaccine Induces Protective Mucosal Immunity. *Plos One* 2009, 4, 12.

14. Hansen, J.; Jensen, K.; Follmann, F.; Agger, E.; Theisen, M.; Andersen, P., Liposome delivery of Chlamydia muridarum major outer membrane protein primes a Th1 response that protects against genital chlamydial infection in a mouse model. *Journal of Infectious Diseases* 2008, 198, 758-767.

15. Igietseme, J.; Ananaba, G.; Bolier, J.; Bowers, S.; Moore, T.; Belay, T.; Eko, F.; Lyn, D.; Black, C., Suppression of endogenous IL-10 gene expression in dendritic cells enhances antigen presentation for specific Th1 induction: Potential for cellular vaccine development. *Journal of Immunology* 2000, 164, 4212-4219.

16. Igietseme, J. U.; Black, C. M.; Caldwell, H. D., Chlamydia vaccines - Strategies and status. *Biodrugs* 2002, 16, 19-35.

17. Ito, J.; Lyons, J., Role of gamma interferon in controlling murine chlamydial genital tract infection. *Infection and Immunity* 1999, 67, 5518-5521.

18. Igietseme, J.; Ananaba, G.; Bolier, J.; Bowers, S.; Moore, T.; Belay, T.; Lyn, D.; Black, C., The intercellular adhesion molecule type-1 is required for rapid activation of T helper type 1 lymphocytes that control early acute phase of genital chlamydial infection in mice. *Immunology* 1999, 98, 510-518.

19. Rose, L. J.; O'Connell, H., UV Light Inactivation of Bacterial Biothreat Agents. *Applied and Environmental Microbiology* 2009, 75, 2987-2990.

20. Gondek, D. C.; Roan, N. R.; Starnbach, M. N., T Cell Responses in the Absence of IFN-gamma Exacerbate Uterine Infection with Chlamydia trachomatis. *Journal of Immunology* 2009, 183, 1313-1319.

21. Barr, I. G.; Sjolander, A.; Cox, J. C., ISCOMs and other saponin based adjuvants. *Advanced Drug Delivery Reviews* 1998, 32, 247-271.

22. Ellouz, F.; Adam, A.; Ciorbaru, R.; Lederer, E., MINIMAL STRUCTURAL REQUIREMENTS FOR ADJUVANT ACTIVITY OF BACTERIAL PEPTIDOGLYCAN DERIVATIVES. *Biochemical and Biophysical Research Communications* 1974, 59, 1317-1325.

23. Chu, R. S.; Targoni, O. S.; Krieg, A. M.; Lehmann, P. V.; Harding, C. V., CpG oligodeoxynucleotides act as adjuvants that switch on T helper 1 (Th1) immunity. *Journal of Experimental Medicine* 1997, 186, 1623-1631.

24. Hartmann, G.; Weiner, G. J.; Krieg, A. M., CpG DNA: A potent signal for growth, activation, and maturation of human dendritic cells. *Proceedings of the National Academy of Sciences of the United States of America* 1999, 96, 9305-9310.

25. Esumi, K.; Suzuki, A.; Yamahira, A.; Torigoe, K., Role of poly(amidoamine) dendrimers for preparing nanoparticles of gold, platinum, and silver. *Langmuir* 2000, 16, 2604-2608.

26. DeSmedt, T.; Pajak, B.; Muraille, E.; Lespagnard, L.; Heinen, E.; DeBaetselier, P.; Urbain, J.; Leo, O.; Moser, M., Regulation of dendritic cell numbers and maturation by lipopolysaccharide in vivo. *Journal of Experimental Medicine* 1996, 184, 1413-1424.

27. Parant, M., BIOLOGIC PROPERTIES OF A NEW SYNTHETIC ADJUVANT, MURAMYL DIPEPTIDE (MDP). *Springer Seminars in Immunopathology* 1979, 2, 101-118.

28. Lawrence, G. W.; Saul, A.; Giddy, A. J.; Kemp, R.; Pye, D., Phase I trial in humans of an oil-based adjuvant SEPPIC MONTANIDE ISA 720. *Vaccine* 1997, 15, 176-178.

29. Suzuki, Y.; Wakita, D.; Chamoto, K.; Narita, Y.; Tsuji, T.; Takeshima, T.; Gyobu, H.; Kawarada, Y.; Kondo, S.; Akira, S.; Katoh, H.; Ikeda, H.; Nishimura, T., Liposome-encapsulated CpG oligodeoxynucleotides as a potent adjuvant for inducing type 1 innate immunity. *Cancer Research* 2004, 64, 8754-8760.

30. Jiang, W. L.; Gupta, R. K.; Deshpande, M. C.; Schwendeman, S. P., Biodegradable poly(lactic-co-glycolic acid) microparticles for injectable delivery of vaccine antigens. *Advanced Drug Delivery Reviews* 2005, 57, 391-410.

31. Silva, D. G.; Cooper, P. D.; Petrovsky, N., Inulin-derived adjuvants efficiently promote both Th1 and Th2 immune responses. *Immunology and Cell Biology* 2004, 82, 611-616.

32. Donnelly, J. J.; Ulmer, J. B.; Shiver, J. W.; Liu, M. A., DNA vaccines. *Annual Review of Immunology* 1997, 15, 617-648.

33. Couvreur, P.; Vauthier, C., Nanotechnology: Intelligent design to treat complex disease. *Pharmaceutical Research* 2006, 23, 1417-1450.

34. Singh, M.; Chakrapani, A.; O'Hagon, D., Nanoparticles and microparticles as vaccine-delivery systems. *Expert Review of Vaccines* 2007, 6, 797-808.

35. Moon, J.; Huang, B.; Irvine, D., Engineering Nano- and Microparticles to Tune Immunity. *Advanced Materials* 2012, 24, 3724-3746.

36. Ishii, K. J.; Akira, S., Toll or toll-free adjuvant path toward the optimal vaccine development. *Journal of Clinical Immunology* 2007, 27, 363-371.

37. Tomai, M. A.; Miller, R. L.; Lipson, K. E.; Kieper, W. C.; Zarraga, I. E.; Vosilakos, J. P., Resiquimod and other immune response modifiers as vaccine adjuvants. *Expert Review of Vaccines* 2007, 6, 835-847.

38. Tomai, M.; Vasilakos, J., TLR-7 and-8 agonists as vaccine adjuvants. *Expert Review of Vaccines* 2011, 10, 405-407.

39. Kamaly, N.; Xiao, Z.; Valencia, P. M.; Radovic-Moreno, A. F.; Farokhzad, O. C., Targeted polymeric therapeutic nanoparticles: design, development and clinical translation. *Chem Soc Rev* 2012, 41, 2971-3010.

40. Kolishetti, N.; Dhar, S.; Valencia, P. M.; Lin, L. Q.; Karnik, R.; Lippard, S. J.; Langer, R.; Farokhzad, O. C., Engineering of self-assembled nanoparticle platform for precisely controlled combination drug therapy. *Proceedings of the National Academy of Sciences of the United States of America* 2010, 107, 17939-17944.

41. Tong, R.; Cheng, J. J., Drug-Initiated, Controlled Ring-Opening Polymerization for the Synthesis of Polymer-Drug Conjugates. *Macromolecules* 2012, 45, 2225-2232.

42. Olive, A. J.; Gondek, D. C.; Starnbach, M. N., CXCR3 and CCR5 are both required for T cell-mediated protection against C. trachomatis infection in the murine genital mucosa. *Mucosal Immunology* 2011, 4, 208-216.

43. Moseman, E. A.; Iannacone, M.; Bosurgi, L.; Tonti, E.; Chevrier, N.; Tumanov, A.; Fu, Y. X.; Hacohen, N.; von Andrian, U. H., B Cell Maintenance of Subcapsular Sinus Macrophages Protects against a Fatal Viral Infection Independent of Adaptive Immunity. *Immunity* 2012, 36, 415-426.

44. Casola, S.; Otipoby, K. L.; Alimzhanov, M.; Humme, S.; Uyttersprot, N.; Kutok, J. L.; Carroll, M. C.; Rajewsky, K., B cell receptor signal strength determines B cell fate. *Nature Immunology* 2004, 5, 317-327.

45. Siuti, P.; Green, C.; Edwards, A. N.; Doktycz, M. J.; Alexandre, G., The chemotaxis-like Che1 pathway has an indirect role in adhesive cell properties of Azospirillum brasilense. *Fems Microbiology Letters* 2011, 323, 105-112.

Chapter 7

Summary, Conclusions, and Suggestions for Future Work

7. 1. Summary and Conclusions

This thesis sought to contribute towards the development of technologies that might improve the management of bacterial infections and is organized into two major thrust areas: (1) *treatment:* using NPs for antibacterial drug delivery, and (2) *prevention:* developing a vaccine formulation for the model bacterial pathogen *Chlamydia trachomatis*. Work in the first part was motivated by observing that currently, there is a significant need for new technologies that can be applied for the treatment of bacterial infections. Existing drugs are slowly succumbing to drug resistance and may lose potency *in vivo* due to biofilms, abscesses, or acidity in some cases. Compounding this concern is the observation that the pipeline for new antibiotics is thin. In addition to strategies aimed at developing new drugs, there is a need to explore new methods that might make existing drugs more effective. More effective delivery is one method to improve the effectiveness of a drug by increasing the local concentration while reducing the systemic dose, which also has the benefit of reducing toxicity, a prevalent feature of drugs designed to treat drug resistant organisms. The second part was motivated by the observation that there is currently no prophylactic vaccine available for *Chlamydia trachomatis* in humans, despite it being the most common bacterial sexually transmitted disease in the world.

This work involved the use of polymers containing poly-L-histidine, a polymer that demonstrates pH sensitivity particularly in the range 5.5-8.0.[1-3] In the first part, we used a

triblock copolymer poly(D, L-lactic-co-glycolic acid)-*block*-poly(L-histidine)-*block*-poly(ethylene glycol) (PLGA-PLH-PEG). Each segment within this polymer structure was designed to serve a particular function. The PLGA block is the most hydrophobic and forms an anchor point and core for the NP self-assembly process. PLGA is known to precipitate into a matrix-like structure that can encapsulate active agents, such as drugs or polymer-drug conjugates.[4] PLGA is also attractive for biomaterial development because it has been used for years in the clinic in controlled release microparticle formulations and resorbable sutures, providing some validation of its safety. The PLH segment is a polymer of the amino acid L-histidine, characterized by its imidazole group with a side chain pKa ~6.0-6.5. At pH values < ~6.0-6.5, the polymer will have a net positive charge. This net positive charge may be used to bind to negatively charged biological components, such as bacteria, protein, or human cells. It should be noted that under conditions where there is a change in environmental pH from above to below pH ~6.0, these NPs will demonstrate an increase in the cationic charge density. Increased cationic charge density can be used to bind to target biological components, such as bacteria, which tend to be negatively charged. The PEG segment was incorporated to improve the circulation time of the NPs in the blood at physiologic pH 7.4, as has been widely reported.[5]

The basis for our work focused on *treating* established infections is documented in Chapters 3-5. Here we begin developing PLH-containing NPs, with the goal of taking a step towards improving drug targeting to infections. Improved drug targeting might allow for higher local but lower systemic concentration, a combination that can potentially make therapeutics more effective and less toxic. This is worthwhile for two reasons: (1)

methods of improving drug therapy are needed to reduce the impact of drug resistance (DR), even if the effect is only to delay the onset of DR thanks to improved properties like delivery, and (2) drugs used to treat DR infections tend to be more toxic, particularly in patient populations that have significant comorbidities. Given the potential demonstrated by NPs in bacterial infectious disease, cancer, and cardiovascular disease in previous work,[6-11] we used a NP delivery system as a starting point. We pursued an infection-targeting strategy relying first on the phenomenon of "passive" accumulation of NPs at sites of infection, since bacteria can trigger an inflammatory response with release of vascular mediators.[12-14] Second, we explored the potential of further increasing targeting potential by adding an element of "active" targeting to bacteria, in the form of acid-sensitive cationic surface charge generation. Inflammation has been associated with acidity since at least the 1950s.[15] The precise mechanism is not completely understood, but likely involves production of acids during phagocytosis and release of acidic mediators of inflammation. Further, aggressive growth or expansion tends to bring with it high oxygen consumption (if applicable for the bacterium), and if this occurs in an environment where there is low oxygen tension at baseline, an acidic microenvironment can be created by the liberation of acidic metabolic products. This decreased acidity can sometimes impact the efficacy of therapy, as some antibiotics may lose potency under these conditions (while some gain potency). Of interest to us in this application, acidity acts as an indicator of the presence inflammation, which may be more pronounced in patients with an aggressive bacterial infection, as well as a potential marker of places where a boost in drug potency is needed.

Our initial efforts to design and test antibiotic NPs are documented in Chapter 3. We began by evaluating the physicochemical properties of the NPs, finding that there is a pH-dependent change in the zeta potential from slightly anionic to cationic as the pH declines from pH 7.4 to 5.5. This correlated well with an increase in binding to both Gram-positive (*Staphylococcus aureus*) and Gram-negative (*Escherichia coli*) bacteria at the lower pH range (pH < 6.5). We demonstrated the ability to encapsulate the model antibiotic vancomycin, which is used to treat Gram-positive infections, using a double emulsion / solvent evaporation strategy, then showed the ability to deliver it via NP form to inhibit the growth of *S. aureus* with a release kinetic on the order of ~50 hours. The major conclusion from the studies in Chapter 3 that the NP formulations explored may be better than free drug only if they are able to achieve high sustained local drug concentrations at the infection site, since the free drug formulations are nearly 4x more effective at the same total concentration of vancomycin. It is likely that this difference is because much of the vancomycin loaded in the NPs is unable to interact with the bacteria, and that the impact of the PLH-containing NPs interacting with the bacteria was quite modest. Given this observation, work continued in two major directions: (1) further evaluation of the NP's ability to target bacteria under more complex biological conditions (Chapter 4), and (2) exploration of methods to enhance activity (Chapter 5).

In Chapter 4, we sought to continue exploring the potential of this system for antibiotic delivery by gaining a greater understanding of the interactions of PLH-containing NPs with selected biological components. These biological components were selected based on ones one might expect to impact the ability to target bacteria, particularly under conditions found at a site of infection: (1) mammalian cells, and (2) soluble protein.

Mammalian cells are particularly significant, since they are present in high numbers at a typical infection site, and are widely known to internalize NPs, particularly if they are cationically charged.[16, 17] We began by evaluating the binding of PLH-containing NPs to two model mammalian cells: RAW 264.7 murine macrophages, a model phagocytic cell, and LNCaP prostate adenocarcinomas, a model tissue resident cell. We found that the NPs demonstrated binding/internalization to both of these cell types, particularly at low pH using a combination of flow cytometry and fluorescent microscopy techniques. To further understand NP-mammalian cell interactions, we explored the kinetics of binding and compared it to that of binding to bacteria. We observed that binding saturation in mammalian cells was slower than the saturation in binding to bacteria, suggesting the possibility of differential targeting based on kinetic arguments under a narrow set of conditions. Of course, this observation needed to be explored further. To do so, we used a simple model, in which NPs would be co-incubated with bacteria and a monolayer of mammalian cells (LNCaP). We found that there was retained binding to bacteria, but that this was attenuated by the presence of the monolayer. However, this simple model was not a complete picture, since there are negatively charged proteins at a site of infection which might compete with the NPs for binding to the bacteria. Therefore, we sought to explore the effect of a model negatively charged protein, albumin (from bovine serum, BSA), and studied the NP binding properties at different concentrations of this protein. Albumin has been shown to passively extravasate from the vasculature at sites of inflammation[12] and is present in abundant quantities, making it a good model protein for our purposes. The results show that there is a logarithmic reduction in the amount of binding to bacteria in the presence of BSA. This reduction in binding is significant, with

a ~83% reduction in the fluorescence associated with bacteria at 4 g/dL, a conservative estimate of the albumin concentration one might observe at a site of infection. We hypothesized that this reduction was due to reduced PEG density on the NP surface, since we observed evidence of significant PLH presence on the surface by virtue of cationic charge by quasi-elastic laser light scattering as well as XPS measurements. We therefore sought to explore the effect of adding an increasing quantity of PLGA-PEG to the formulation. We hypothesized that this might impact the binding properties In various ways, including potentially increasing the PEG density on the NP surface. We expected this on the basis that PEG is preferentially exposed on the NP surface during NP formulation and would compete with PLH for sites on the surface, thereby reducing the PEG density. Given the extensive previous work on reducing non-specific protein binding by PEG, we hypothesized that this might reduce some of the non-specific protein binding while potentially still enabling binding to the bacteria. The mixed PLGA-PLH-PEG / PLGA-PEG NPs (20-60%; 80% represents PLGA-PLH-PEG with Alexa-488-PLGA) tend to demonstrate a reduction in the amount of binding to bacteria as compared to what was observed for the 80% PLGA-PLH-PEG at 0 g/dL when there is BSA present. As the BSA level is increased, the mixed NPs demonstrate comparable or improved binding relative to the 80% PLGA-PLH-PEG, except for 20% PLGA-PLH-PEG, which demonstrated low bacteria-associated fluorescence at all BSA concentrations. Importantly, we also noted that the mixed NPs demonstrated improved stability both over time and during the stresses of NP purification and processing. Consequently, we chose 40-60% PLGA-PLH-PEG mixed NPs for further evaluation. Next, we sought to evaluate whether these NPs could demonstrate extended circulation time *in vivo*. Following a tail

vein injection into healthy mice, we determined distribution half-lives of these NPs to be between 1.8-2.0 hours, consistent with an extended circulation time and comparable to a PLGA-PEG control. The NPs distribute primarily to the spleen and liver, suggesting clearance by the mononuclear phagocytic system. We conclude from the results in Chapter 4 that targeting bacteria based on cationic charge using PLH-containing NPs is likely to be complicated, at the very least, by the presence of both infection-resident mammalian cells and proteins. We expect that *in vivo*, the NPs will be taken up by mammalian cells and covered by protein, though the precise impact of this on the overall targeting strategy is likely to be different based on the specific microenvironmental factors of each infection, which are also going to vary with time within a given infection. These results have significant implications for the use and design of these NPs for delivery of antibacterials. In particular, these results suggest that one should select drugs to load inside of the NPs that are able to diffuse through the mammalian cell membrane, since it is likely that mammalian cells will endocytose these NPs and sequester them in subcellular compartments, in addition to being covered, at least in part, by protein. In addition, these results suggest new avenues to pursue should seek to either take advantage of the subcellular targeting potential of this delivery system, such as for treating tuberculosis (TB), or other intracellular bacterial pathogens.

Chapter 5 documents our efforts to improve the potency of the NP formulation by co-delivering a synergistic drug combination. Initial studies allowed us to confirm previous reports (Timothy K. Lu, personal communication) that vancomycin works synergistically with silver, as determined using the fractional inhibitory concentration (FIC) and checkerboard methods. Extensive previous work has shown that silver(I) can form

complexes with various histidine-containing materials. We therefore sought to incorporate silver(I) into our NP structure. Following an established protocol for silver(I) incorporation onto histidine, we show using a variety of techniques such as zeta potential, TEM, XPS, FT-IR, TGA, DSC, and UV-Vis the loading of ~2-5 wt% silver. Growth inhibition studies against *Staphylococcus aureus* show that the NPs containing both silver(I) and vancomycin are more potent than NPs containing only vancomycin or only silver(I). We also tested the growth inhibitory potential in a vancomycin-resistant strain of *Enterococcus faecalis* (VRE), finding that the presence of vancomycin in the NPs had a negligible effect on growth inhibition, but that co-delivery still had an improved effect on growth inhibition in this DR strain. We conclude that co-delivery of silver(I) and vancomycin improves the potency of PLH-containing NPs in strains where the bacteria are sensitive to both drugs, but that there is future work needed to continue developing this system. In particular, methods are needed to establish greater stability of silver(I) on the NP surface. Initial efforts were made in this regard by exploring the potential to reduce the silver(I) to silver(0) using sodium borohydride, but we found that the reduced silver NPs demonstrated unacceptable acute toxicity to a model human cell line (LNCaP). Chapter 6 documents our efforts to use PLH-containing polymeric NPs to formulate a vaccine against *Chlamydia trachomatis*, the most common bacterial sexually transmitted disease in the world. Currently, there is no effective prophylactic vaccine against *Chlamydia* for in-human use despite decades of development, in part due to the poor immunogenicity of inactivated *Chlamydia* but also due to how challenging it has been to develop suitable adjuvants or delivery systems for use with this pathogen. This is often attributed to toxicity, something that can be tolerated only in very rare cases in a

prophylactic vaccine due to the target patient population being healthy young adults. The most commonly used adjuvant, the FDA-approved adjuvant alum, tends to promote Th2-weighted cytokine responses and humoral immunity, which are not optimal in *Chlamydia* vaccines. *Chlamydia* is an intracellular pathogen that is cleared primarily by action of IFN-γ secreting CD4+ T cells, though other components of the immune system are believed to play an ancillary role, including NK cells and antibody-secreting B cells.

Consequently, we sought to develop a prophylactic vaccine formulation against *Chlamydia trachomatis* designed to contain the necessary components to elicit protective immunity via CD4+ T cell and Th1-weighted immune responses. The necessary components include (1) the antigenic stimulus, for which we chose whole UV-inactivated *Chlamydia* due to the more native presentation of epitopes as well as potential for synergistic effects between multiple epitopes, (2) the adjuvant, for which we chose the TLR7/8 (in humans) agonist R848, which is known to induce Th1-weighted immunity, and (3) the delivery system for the vaccine, for which we used cationic polymeric NPs. These NPs were formulated by encapsulating an R848-poly(lactic acid) (R848-PLA) conjugate in a poly-L-histidine (PLH)-containing PLGA-based NP, then co-administering them with the UV-inactivated *C. trachomatis*. Following studies to define conditions under which the NPs will yield a balance of positive charge with sufficient input of R848-PLA, we show that this cationic NP-*Chlamydia* formulation is able to induce the expansion of *Chlamydia*-specific, TCR-transgenic, CFSE-labeled, adoptively transferred CD4+ T cells on day 6 post-vaccination. Further, we show the ability to induce protective immunity against *C. trachomatis* at 1 month post-vaccination, which we show to be a CD4+ T cell dependent process and independent of antibodies and B cells. We conclude

from these studies that R848-encapsulated PLH-containing NP-UV-inactivated *Chlamydia* formulation shows promise as a prophylactic vaccine formulation, though more work is needed to optimize the precise molecular structure of the polymer and macromolecular structure of the vaccine to yield maximal anti-*Chlamydia* immunity.

7. 2. Summary of Suggestions for Future Work

This thesis was concerned with the development of technologies for improving the management of bacterial infections and was divided into efforts aimed at: (1) *treatment* of established infections, and (2) *prevention* of infections through prophylactic vaccination.

Further work in *treatment* of established infections can be summarized as follows:

1) *Increasing the specificity of targeting bacteria.* Our efforts here have shown that selective production of cationic charge at a site of infection, while potentially improving specificity as compared to perpetually cationic NPs, still faces significant non-specific binding at a site of infection as a major challenge. Work is needed that might lead to greater specificity for bacteria from a systemic injection if the concept of improved targeting is to be achieved. If one is to continue the idea of selectively producing a cationic charge in the vicinity of bacteria triggered by acidity, it will be necessary to precisely define conditions under which NPs will achieve selective targeting of bacteria in the presence of high protein concentration and mammalian cells. Because of the complexity and time dependence of these conditions in an actual infection, any *in vitro* studies will likely need to be confirmed in a predictive *in vivo* model. Exploring the impact of charge magnitude on targeting ability is likely to be a very important

factor. Previously, it has been shown that a very high cationic charge (+47 to +65 mV) is capable of achieving this.[18] To yield this magnitude of charge, it might be necessary to identify a pH-sensitive material with a larger density of protonable groups, since the linear PLH polymers explored in this thesis do not achieve such high zeta potentials. In addition, greater pH-sensitivity leading to a shorter dynamic range might broaden the applicability of the targeting strategy presented here, especially if sufficient cationic charge can be generated by pH ~6.8. Another potential strategy to achieve improved bacterial targeting specificity is to use targeting ligands conjugated to the surface of NPs. These might enable binding to bacteria independent of the presence of factors such as high protein concentrations. A wide variety of targeting ligands have been explored in the literature already for this purpose (for a detailed discussion, see Chapter 2), though more work is needed to evaluate their potential to improve the activity of NPs. A potential pitfall of this strategy is that bacteria may develop resistance to highly specific targeting ligands. Therefore, it will be necessary to select a targeting ligand that targets bacterial components that are more essential to survival, such as is the case with some antimicrobial peptides.

2) *Increasing potency.* Another major hurdle to using NPs for antibiotic delivery is that it will be necessary to significantly improve efficacy. This can best be appreciated by noting how much drug needs to be delivered to achieve an effect. A typical dose of an antibiotic is on the order of grams per day on a daily basis for a week to two weeks in some cases, sometimes even longer. Given the drug loading and potency achieved in this thesis, this suggests that there will be

hundreds of grams of polymer delivered a day, which is very high. By increasing the potency of a drug via NP formulation, the quantity of polymer delivered can be reduced, particularly if the NP can also effectively target the antibiotic to the infection site. Strategies to improve drug potency often involve a synergistic effect between the NP and the drug, such as using a NP to enhance membrane permeability or produce hyper local drug concentrations.[19] Cationic NPs have successfully been shown to achieve toxicity independent of any antibiotic delivery,[18, 20] it might be interesting to identify drugs that might interact synergistically with these NPs and explore methods to achieve high drug loading. In Chapter 5, we explored the potential to co-deliver the synergistic combination of silver(I) and vancomycin. This method was shown to improve the potency of the NP formulation, but further work was needed to make this a more clinically viable drug delivery method. In particular, increasing the stability of the silver(I) loaded onto the NPs was needed. We tried a method involving reducing the silver(I) onto the NP using sodium borohydride, but we observed unacceptable acute toxicity in model human cells. Further work might involve understanding the mechanism of this toxicity. Following an understanding of the mechanism of toxicity, it may be possible to design a strategy that may overcome this particular hurdle. In addition, it will be necessary to understand whether these reduced silver NPs may continue to demonstrate extended circulation *in vivo* as well as bacteria targeting potential.

3) *Establishment of predictive in vivo models of infection.* The work contained in this thesis focused on *treatment* of established infections used acidity as a method to

identify sites of infection in the body. Acidity has been documented in human patients under various conditions, but requires further exploration to find a suitable *in vivo* model that mimics the formation of acidity as observed in humans. To continue exploring the pH-sensitive targeting mechanism as developed in this thesis, it will be necessary to characterize the formation of acidity both in terms of the anatomical spread of the acidity as well as the magnitude of the pH depression in candidate animal models. Potential examples include pneumonia models, subcutaneous abscess models or models of bacterial vaginosis.

4) *Evaluation of infection targeting potential by NPs and efficacy in predictive in vivo infection models.* Once an appropriate *in vivo* model of infection is established and characterized, it will be possible to evaluate the potential to target sites of infection from a systemic injection on the basis of a selective cationic charge-based targeting strategy. This can be achieved, for example, by using Alexa-647-labeled 40-60 wt% mixed PLGA-PLH-PEG / PLGA-PEG NPs, injecting them intravenously by the tail vein, and then using an *in vivo* imaging technique to explore the co-localization of fluorescence over time with fluorescently tagged bacteria. Following confirmation of targeting potential, one can envision testing the comparative efficacy of the delivery systems.

Further work in development of prophylactic anti-*Chlamydia* vaccines is summarized as follows:

1) *Further exploration of the precise mechanism of action.* The results contained in this thesis begin to offer an explanation for the mechanism of action, but more

work is needed to explore this in greater depth. We have shown here that the formulation containing PLH (which yield a cationic NP surface charge), leads to a robust immune response. However, greater detail in the precise molecular structure of the vaccine formulation is needed. Questions to be resolved include: what are the structures formed by the mixture of cationic NPs and UV-inactivated *Chlamydia*, and which of these lead to productive activation of the immune system? How exactly do the different substructures formed contribute to the induction of immunity, if more than one is involved? Which cell types are involved in activating the immune response *in vivo*, and how are these being targeted by these key structures? Many of these questions can begin to be resolved using a suite of imaging techniques, such as scanning or transmission electron microscopy, further AFM imaging, confocal fluorescent imaging, and *in vivo* imaging methods. Another interesting question is whether the effect observed here can be broadened to include other cationic NPs. To perform this, one could test the efficacy of other cationic NP formulations. In particular, one could try creating a cationic charge by changing the cationic polymer used, such as trying poly(L-lysine), poly(ethyleneimine), poly(L-arginine), or chitosan, using cationic surfactants, such as dimethyldioctadecylammonium (DDAB), Eudragit, or amine-modified poly(ethyleneglycol), among many others. It is important to select agents that will reduce the likelihood of toxicity, since there is very low tolerance for toxicity in the target population for the vaccine.

2) *Increase loading of R848 adjuvant.* A consistently observed challenge in the development of *Chlamydia* vaccines has been toxicity. This is often due to high

systemic adjuvant exposure, the result of ineffective targeting of the adjuvant precisely to the key antigen presenting cells involved in inducing the immune response. The NPs that we have developed here use R848-poly(lactic acid) (R848-PLA) to load adjuvant, but this approach nevertheless leads to ug of R848 per mg of PLA. Recently applied polymer synthesis techniques have demonstrated the ability to produce polymers with side chains that allow an active agent to be loaded at higher levels than traditional approaches, which often yield only one drug molecule per polymer chain or less.[21] If proper NP targeting to the immune system can be achieved, one can expect that by loading a larger quantity of adjuvant per mg of NP, a potentially lower total dose of adjuvant could be delivered systemically. This lower systemic adjuvant dose, if the same degree of protection could be shown, might reduce the risk for toxicity observed in further studies. In addition, it might be interesting to explore the impact of different R848 release rates on the vaccine efficacy.

3) *Test efficacy of vaccine formulation in higher animal models.* The studies performed here have only explored the ability to protect *mice* from infection with *Chlamydia*. However, the immune systems of mice and humans are quite different, and further evaluation of the potential needs to be performed in higher animal models as this work begins to be translated towards the clinic.

4) *Explore potential to vaccinate against other bacterial infections.* The technique described here has only been explored for vaccination against *Chlamydia*. It may be worthwhile to explore whether cationic NPs can be used to vaccinate against

other bacterial infections, such as tuberculosis, which has so far evaded effective vaccination.

7. 3. References

1. Lee, E. S.; Na, K.; Bae, Y. H., Polymeric micelle for tumor pH and folate-mediated targeting. *J Control Release* 2003, 91, 103-13.

2. Lee, E. S.; Oh, K. T.; Kim, D.; Youn, Y. S.; Bae, Y. H., Tumor pH-responsive flower-like micelles of poly(L-lactic acid)-b-poly (ethylene glycol)-b-poly(L-histidine). *Journal of Controlled Release* 2007, 123, 19-26.

3. Radovic-Moreno, A. F.; Lu, T. K.; Puscasu, V. A.; Yoon, C. J.; Langer, R.; Farokhzad, O. C., Surface charge-switching polymeric nanoparticles for bacterial cell wall-targeted delivery of antibiotics. *ACS Nano* 2012, 6, 4279-87.

4. Kamaly, N.; Xiao, Z.; Valencia, P. M.; Radovic-Moreno, A. F.; Farokhzad, O. C., Targeted polymeric therapeutic nanoparticles: design, development and clinical translation. *Chem Soc Rev* 2012, 41, 2971-3010.

5. Gref, R.; Minamitake, Y.; Peracchia, M. T.; Trubetskoy, V.; Torchilin, V.; Langer, R., Biodegradable long-circulating polymeric nanospheres. *Science* 1994, 263, 1600-3.

6. Huh, A. J.; Kwon, Y. J., "Nanoantibiotics": A new paradigm for treating infectious diseases using nanomaterials in the antibiotics resistant era. *J Control Release* 2011, 156, 128-145.

7. Zhang, L.; Pornpattananangku, D.; Hu, C. M.; Huang, C. M., Development of nanoparticles for antimicrobial drug delivery. *Curr Med Chem* 2010, 17, 585-94.

8. Abeylath, S. C.; Turos, E., Drug delivery approaches to overcome bacterial resistance to beta-lactam antibiotics. *Expert Opin Drug Deliv* 2008, 5, 931-49.

9. Abeylath, S. C.; Turos, E., Nanobiotics to combat bacterial drug resistance. In *Antibiotic resistance: causes and risk factors, mechanisms and alternatives*, Bonilla, A. R.; Muniz, K. P., Eds. Nova Science Publishers: New York, 2009; pp 425-465.

10. Hrkach, J.; Von Hoff, D.; Mukkaram Ali, M.; Andrianova, E.; Auer, J.; Campbell, T.; De Witt, D.; Figa, M.; Figueiredo, M.; Horhota, A.; Low, S.; McDonnell, K.; Peeke, E.; Retnarajan, B.; Sabnis, A.; Schnipper, E.; Song, J. J.; Song, Y. H.; Summa, J.; Tompsett, D.; Troiano, G.; Van Geen Hoven, T.; Wright, J.; LoRusso, P.; Kantoff, P. W.; Bander, N. H.; Sweeney, C.; Farokhzad, O. C.; Langer, R.; Zale, S., Preclinical

development and clinical translation of a PSMA-targeted docetaxel nanoparticle with a differentiated pharmacological profile. *Sci Transl Med* 2012, 4, 128ra39.

11. Chan, J. M.; Zhang, L.; Tong, R.; Ghosh, D.; Gao, W.; Liao, G.; Yuet, K. P.; Gray, D.; Rhee, J. W.; Cheng, J.; Golomb, G.; Libby, P.; Langer, R.; Farokhzad, O. C., Spatiotemporal controlled delivery of nanoparticles to injured vasculature. *Proc Natl Acad Sci U S A* 107, 2213-8.

12. Maeda, H., Tumor-Selective Delivery of Macromolecular Drugs Via the EPR Effect: Background and Future Prospects. *Bioconjug Chem* 2010, 21, 797-802.

13. Maeda, H.; Wu, J.; Okamoto, T.; Maruo, K.; Akaike, T., Kallikrein-kinin in infection and cancer. *Immunopharmacology* 1999, 43, 115-28.

14. Schroeder, A.; Turjeman, K.; Schroeder, J. E.; Leibergall, M.; Barenholz, Y., Using liposomes to target infection and inflammation induced by foreign body injuries or medical implants. *Expert Opin Drug Deliv* 2010, 7, 1175-89.

15. Dubos, R. J., The micro-environment of inflammation of Metchnikoff revisited. *Lancet* 1955, 269, 1-5.

16. Alexis, F.; Pridgen, E.; Molnar, L. K.; Farokhzad, O. C., Factors affecting the clearance and biodistribution of polymeric nanoparticles. *Molecular Pharmaceutics* 2008, 5, 505-515.

17. Allen, T. M.; Cullis, P. R., Drug delivery systems: entering the mainstream. *Science* 2004, 303, 1818-22.

18. Nederberg, F.; Zhang, Y.; Tan, J. P.; Xu, K.; Wang, H.; Yang, C.; Gao, S.; Guo, X. D.; Fukushima, K.; Li, L.; Hedrick, J. L.; Yang, Y. Y., Biodegradable nanostructures with selective lysis of microbial membranes. *Nat Chem* 2011, 3, 409-14.

19. Umamaheshwari, R. B.; Jain, N. K., Receptor mediated targeting of lectin conjugated gliadin nanoparticles in the treatment of Helicobacter pylori. *J Drug Target* 2003, 11, 415-23; discussion 423-4.

20. Liu, L. H.; Xu, K. J.; Wang, H. Y.; Tan, P. K. J.; Fan, W. M.; Venkatraman, S. S.; Li, L. J.; Yang, Y. Y., Self-assembled cationic peptide nanoparticles as an efficient antimicrobial agent. *Nature Nanotechnology* 2009, 4, 457-463.

21. Kolishetti, N.; Dhar, S.; Valencia, P. M.; Lin, L. Q.; Karnik, R.; Lippard, S. J.; Langer, R.; Farokhzad, O. C., Engineering of self-assembled nanoparticle platform for precisely controlled combination drug therapy. *Proceedings of the National Academy of Sciences of the United States of America* 2010, 107, 17939-17944.